Prenylated Bibenzyls from the Chinese Liverwort *Radula constricta* and Their Mitochondria-Derived Paraptotic Cytotoxic Activities

Chunyang Zhang,[†,§] Yun Gao,[†,§] Rongxiu Zhu,[‡] Yanan Qiao,[†] Jinchuan Zhou,[⊥] Jiaozhen Zhang,[†] Yi Li,[†] Siwen Li,[†] Shenghua Fan,[†] and Hongxiang Lou[†,*]

[†]Department of Natural Products Chemistry, Key Lab of Chemical Biology of the Ministry of Education, Shandong University, Jinan 250012, People's Republic of China

[‡]School of Chemistry and Chemical Engineering, Shandong University, Jinan 250010, People's Republic of China

[⊥]School of Pharmacy, Linyi University, Linyi 276000, People's Republic of China

Contents

Figure S17. IR (KBr disc) spectrum of **2**.

Figure S18. UV spectrum of **2**.

Figure S19. Chiral-phase HPLC analysis of **2**.

Figure S20. Experimental ECD spectra of **2a**/**2b** and calculated ECD spectrum of **2a**.

Data for compound 3

Figure S21. ^{1}H NMR spectrum (400 MHz) of **3** in $CDCl_3$.

Figure S22. ^{13}C NMR spectrum (100 MHz) of **3** in $CDCl_3$.

Figure S23. HMQC spectrum (400 MHz) of **3** in $CDCl_3$.

Figure S24. ^{1}H–^{1}H spectrum (400 MHz) of **3** in $CDCl_3$.

Figure S25. HMBC spectrum (400 MHz) of **3** in $CDCl_3$.

Figure S26. HRESIMS Spectrum of **3**.

Figure S27. IR (KBr disc) spectrum of **3**.

Figure S28. UV spectrum of **3**.

Figure S29. Chiral-phase HPLC analysis of **3**.

Figure S30. Experimental ECD spectra of **3a**/**3b** and calculated ECD spectrum of **3a**.

Data for compound 4

Figure S31. ^{1}H NMR spectrum (600 MHz) of **4** in $CDCl_3$.

Figure S32. ^{13}C NMR spectrum (150 MHz) of **4** in $CDCl_3$.

Figure S33. HSQC spectrum (600 MHz) of **4** in $CDCl_3$.

Figure S34. ^{1}H–^{1}H spectrum (600 MHz) of **4** in $CDCl_3$.

Figure S35. HMBC spectrum (600 MHz) of **4** in $CDCl_3$.

Figure S36. HRESIMS spectrum of **4**.

Figure S37. IR (KBr disc) spectrum of **4**.

Data for compound 5

Data for compound 6

Data for compound 7

Data for compound 8

Data for compound 9

Figure S80. ^{1}H NMR spectrum (400 MHz) of **9** in CD_3OD.

Figure S81. ^{13}C NMR spectrum (100 MHz) of **9** in CD_3OD.

Figure S82. HSQC spectrum (400 MHz) of **9** in CD_3OD.

Figure S83. $^{1}H–^{1}H$ spectrum (400 MHz) of **9** in CD_3OD.

Figure S84. HMBC spectrum (400MHz) of **9** in CD_3OD.

Figure S85. HRESIMS spectrum of **9**.

Figure S86. IR (KBr disc) spectrum of **9**.

Figure S87. UV spectrum of **9**.

Figure S88. Compounds Induces Vacuolization.

Figure S89. The Histogram of Annexin V and PI Staining in A549 and NCI-H1299 Cells (A549 and NCI-H1299 Cells were Treated with the 10 μM of Compound **10** for 24 h).

Table S1. Cytotoxicity of Compounds and Adriamycin in Several Human Cancer Cell Llines.

Theory and Calculation Details.

The calculations were performed by the Gaussian 03 program package. The semi-empirical AM1 method[1] and a DFT approach[2] B3LYP/6-31G∗ were employed to scan the potential energy surface (PES). The geometries of all ground-state conformations obtained were further optimized at the B3LYP/6-31G∗ level at 298.15 K, followed by calculations of their harmonic frequency analysis to confirm these minima and thence calculations of room-temperature free energies.

Time-dependent density functional theory (TDDFT) at the same level was used to calculate the electronic excitation energies and rotational strengths in gas phase for the first 30 states. The rotatory strengths were summed and energetically weighted following the Boltzmann statistics and the final ECD spectra were then simulated by overlapping Gaussian functions[3] according to the following equation.

$$\Delta\varepsilon(E) = \frac{1}{2.296\times10^{-39}}\frac{1}{\sigma\sqrt{\pi}}\times\sum_i \Delta E_i R_i e^{-[(E-\Delta E_i)/\sigma]^2}$$

Where σ is the width of the band at 1/e height, while ΔE_i and R_i are the excitation energies and rotatory strengths for transition, respectively. σ = 0.4 eV and R_{vel} were used.

REFERENCES

(1) Dewar, M. J. S.; Zoebisch, E. G.; Healy, E. F.; Stewart, J. J. P. *J. Am. Chem. Soc.* **1985**, *107*, 3902−3909.

(2) Becke, A. D. *J. Chem. Phys.* **1993**, *98*, 5648−5652.

(3) Stephens, P. J.; Harada, N. *Chiral-phaseity* **2009**, *22*, 229−233

Scheme S1. Putative biosynthesis pathways of **1**−**20**.

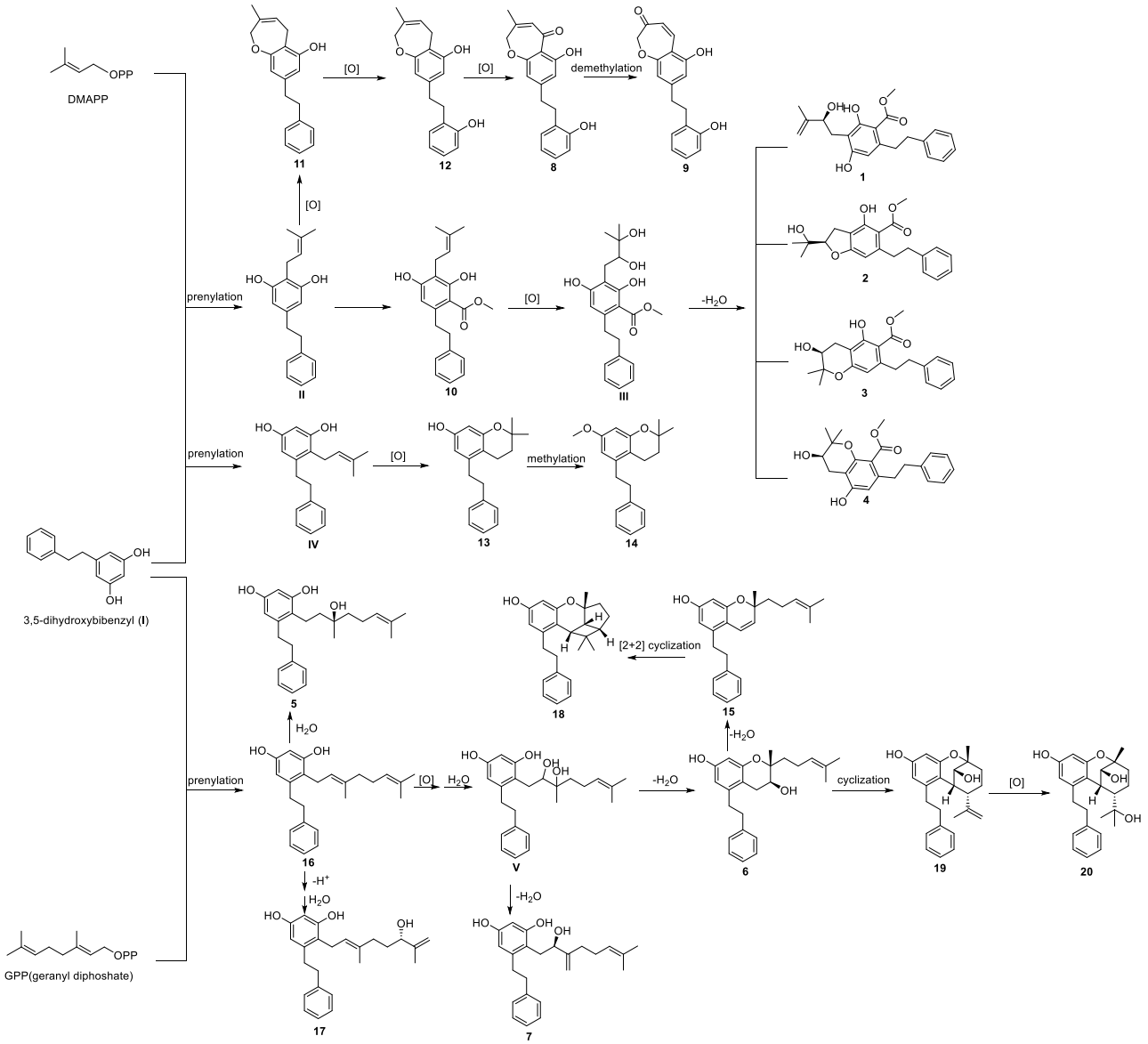

Figure S1. ^{1}H NMR spectrum (600 MHz) of **1** in $CDCl_3$.

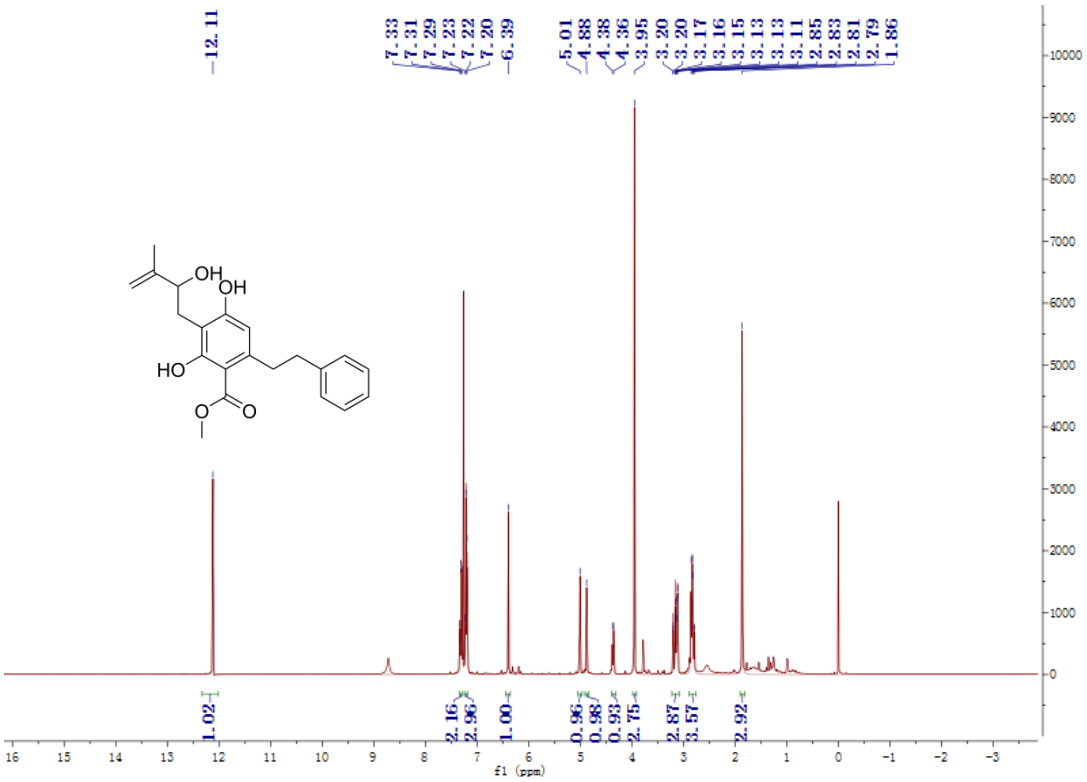

Figure S2. ^{13}C NMR spectrum (150 MHz) of **1** in $CDCl_3$.

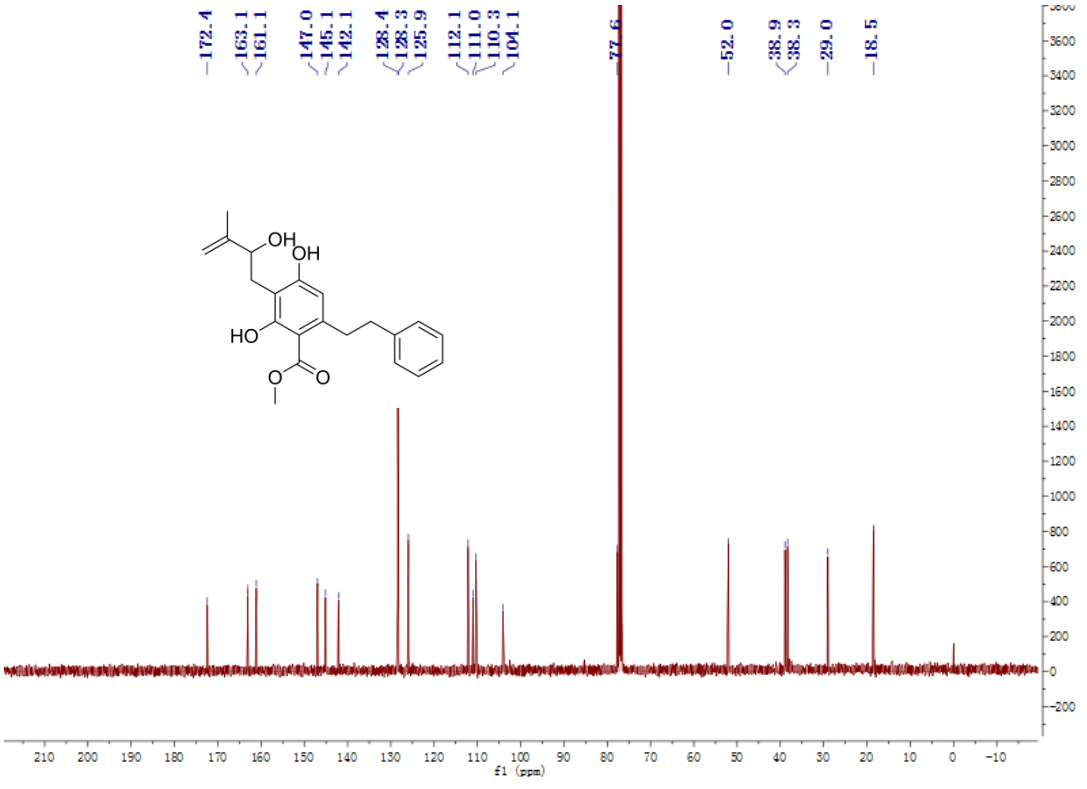

Figure S3. HSQC spectrum (600 MHz) of **1** in $CDCl_3$.

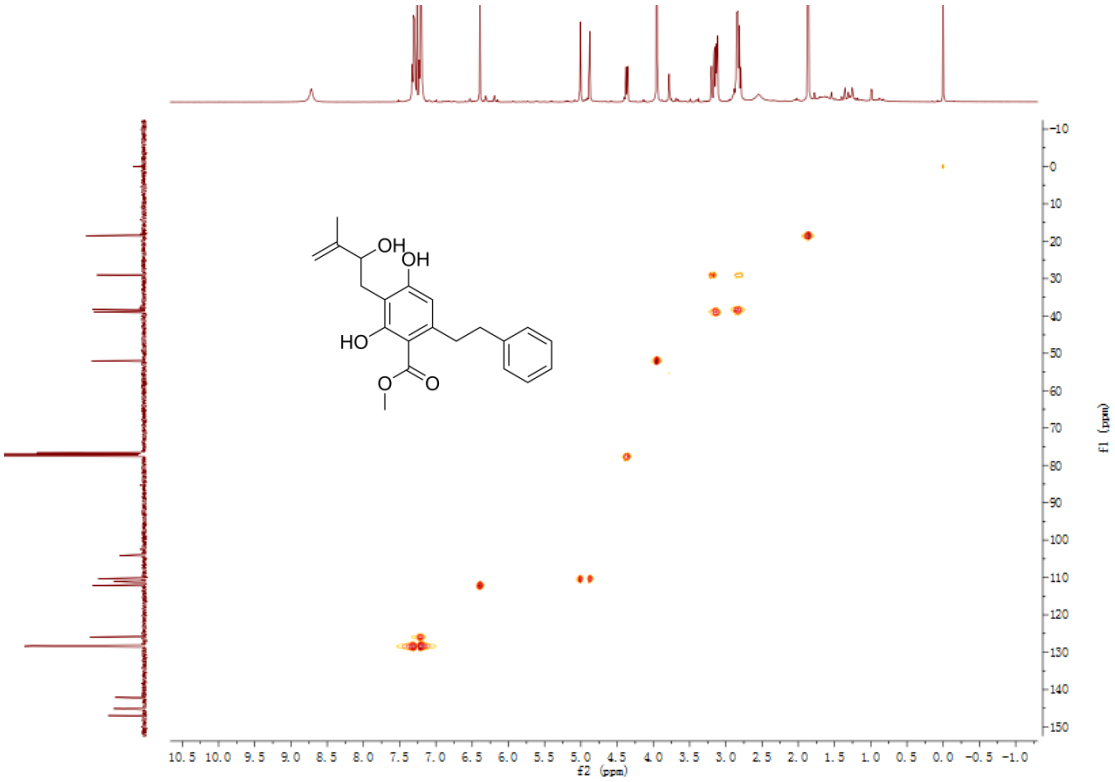

Figure S4. $^{1}H-^{1}H$ spectrum (600 MHz) of **1** in $CDCl_3$.

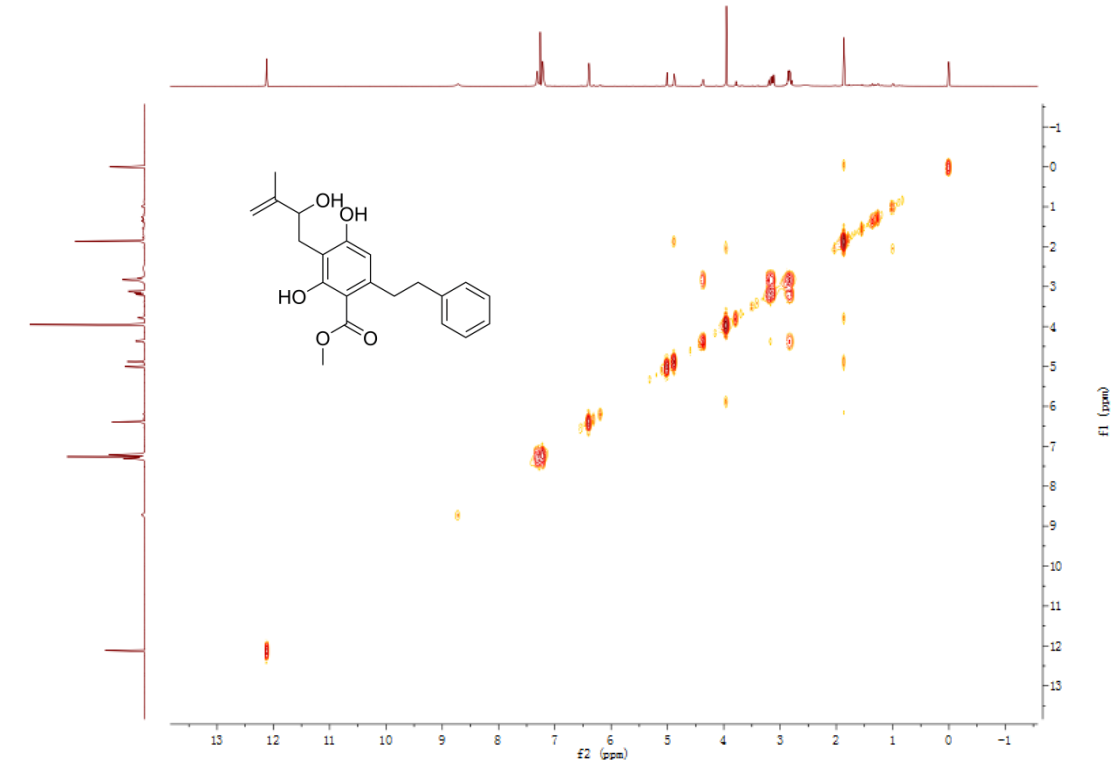

Figure S5. HMBC spectrum (600 MHz) of **1** in $CDCl_3$.

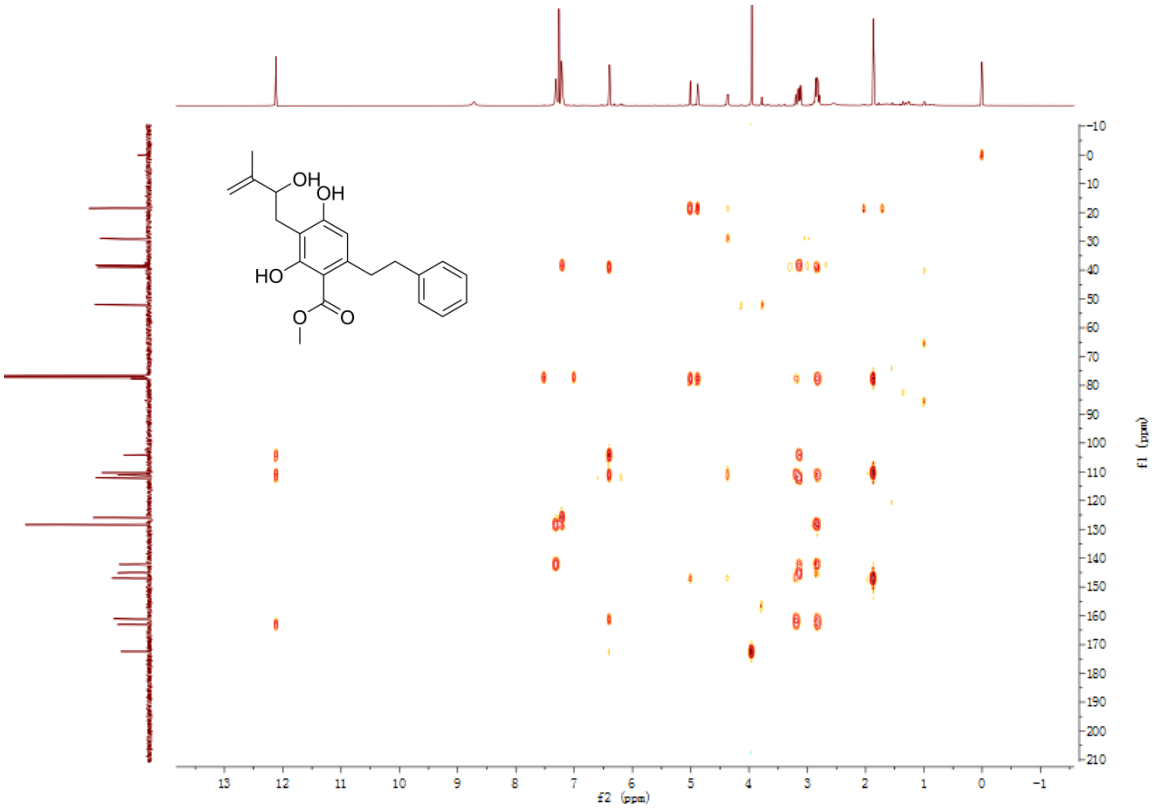

Figure S6. HRESIMS spectrum of **1**.

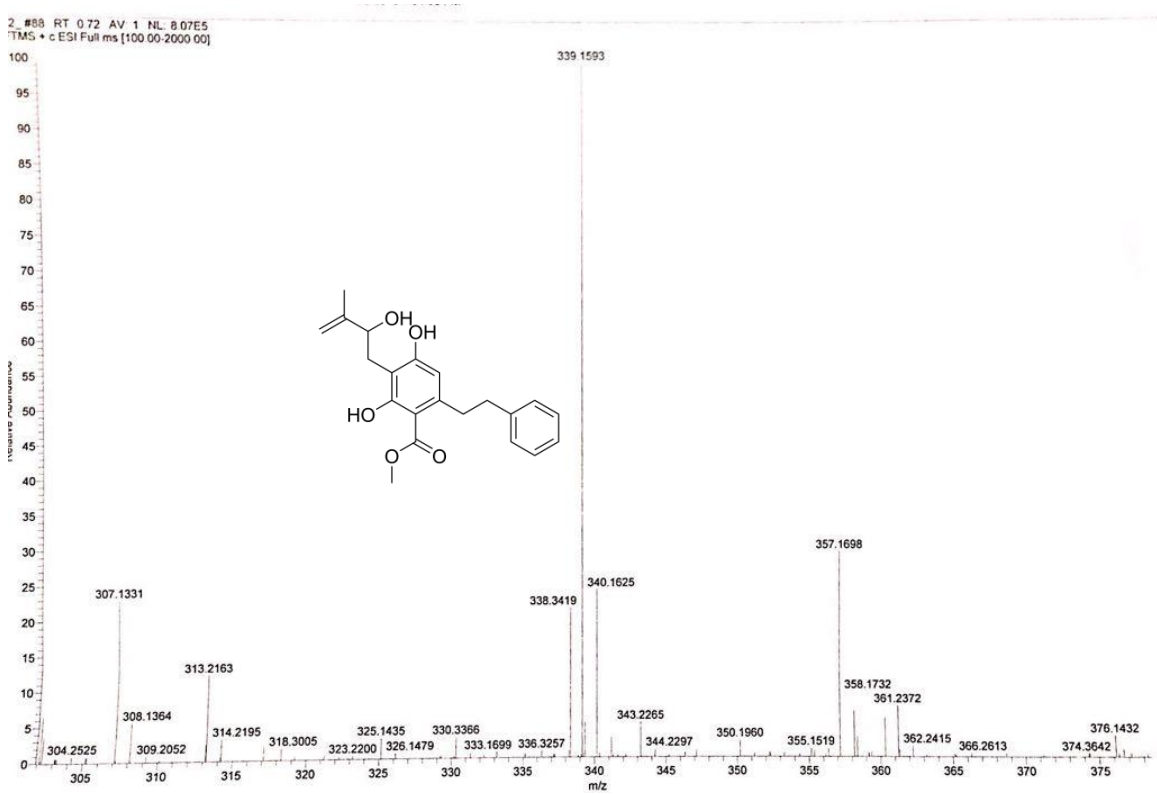

Figure S7. IR (KBr disc) spectrum of **1**.

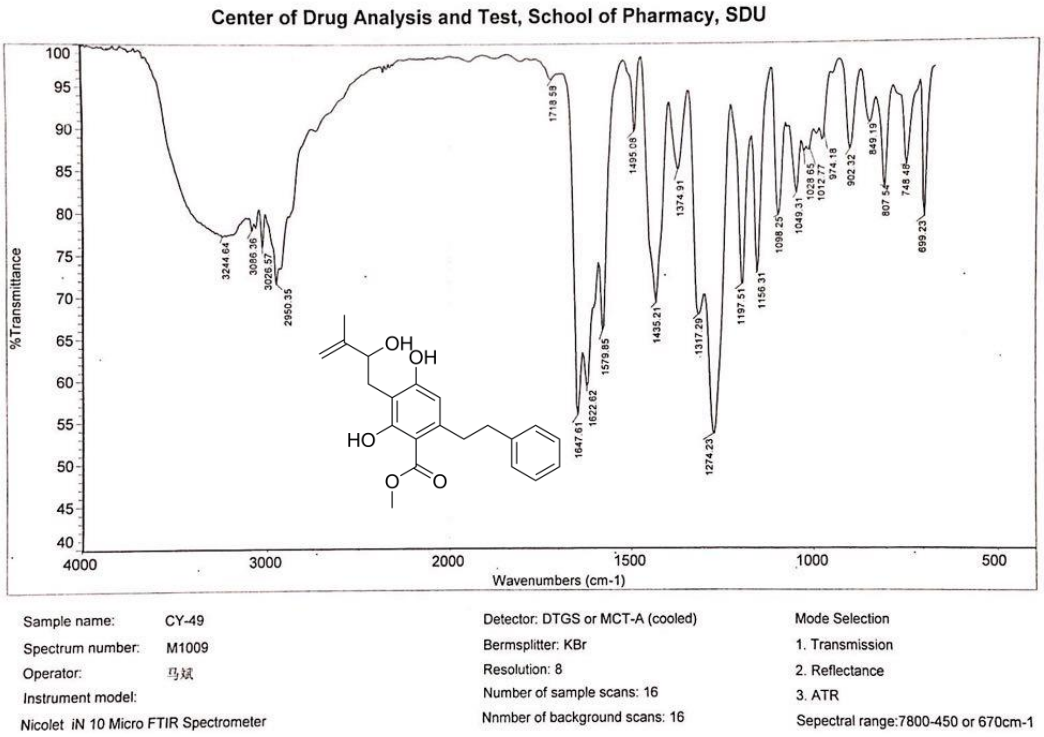

Figure S8. UV spectrum of **1**.

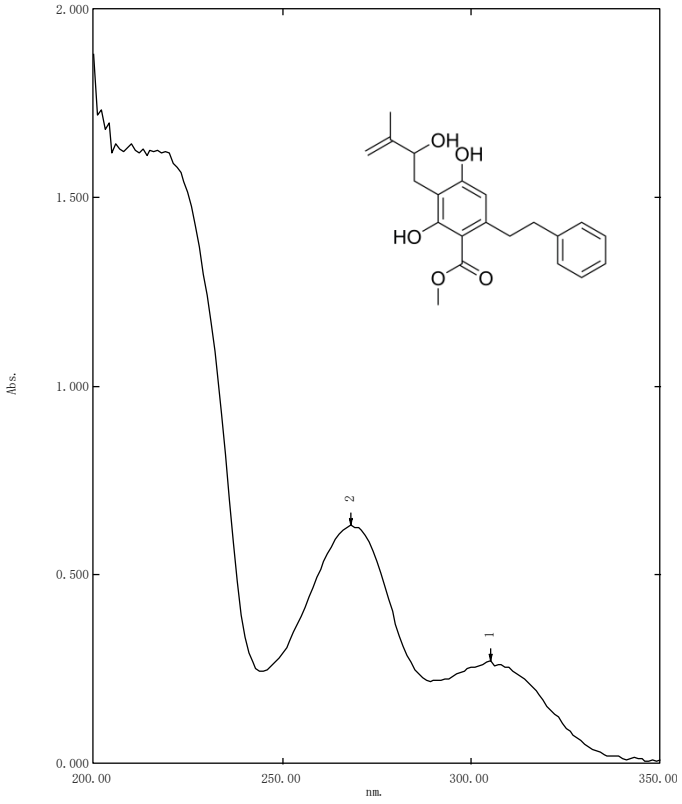

Figure S9. Chiral-phase HPLC analysis of **1**.

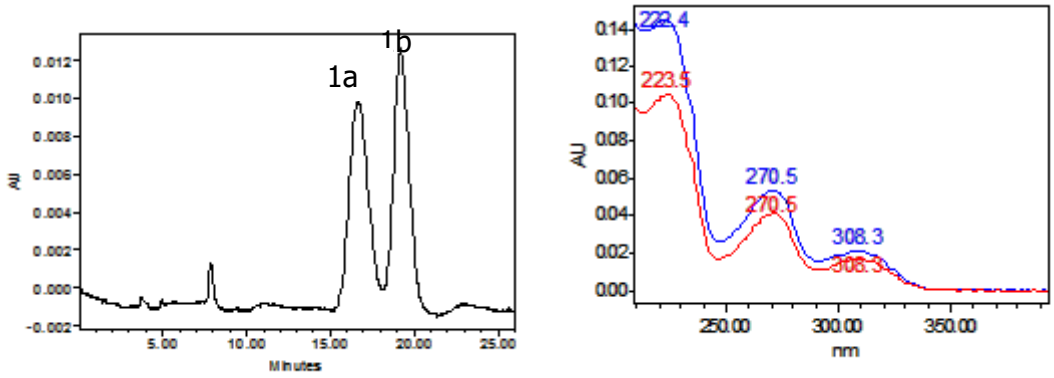

	Retention Time	Area	% Area	Height	Int Type
1	16.659	1035702	50.21	13865	bb
2	19.184	1026900	49.79	17068	bb

Figure S10. Experimental ECD spectra of **1a**/**1b** and calculated ECD spectrum of **1a**.

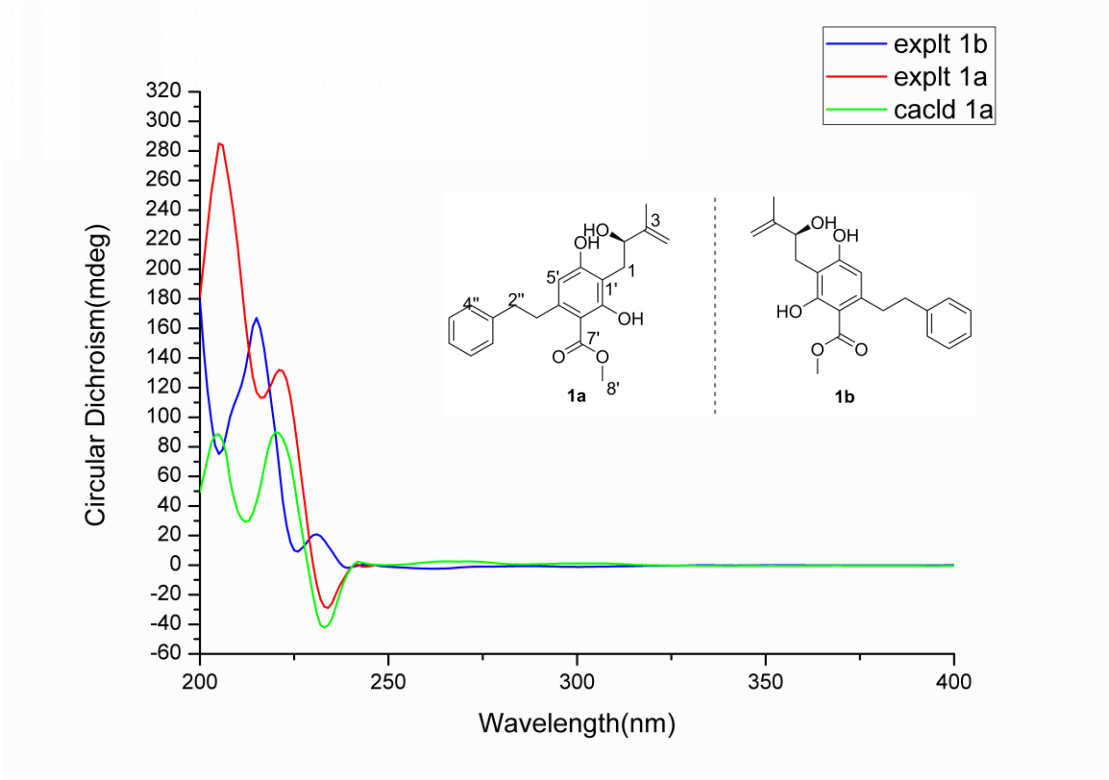

Figure S11. ^{1}H NMR spectrum (600 MHz) of **2** in $CDCl_3$.

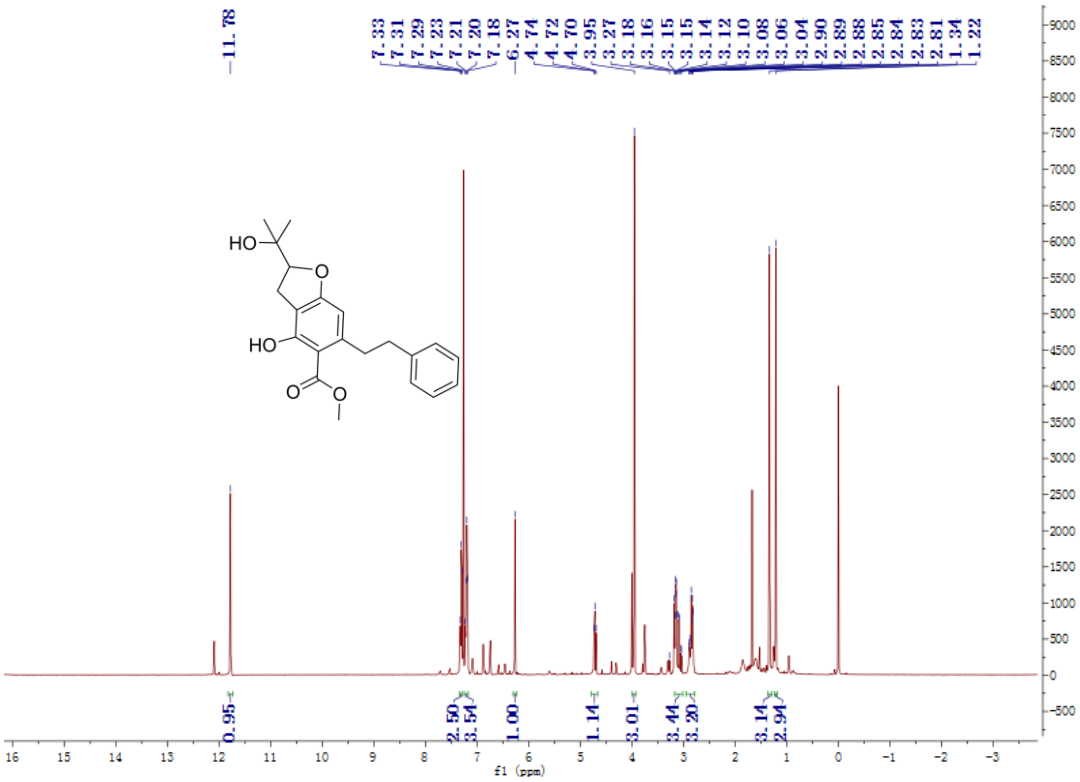

Figure S12. ^{13}C NMR spectrum (150 MHz) of **2** in $CDCl_3$..

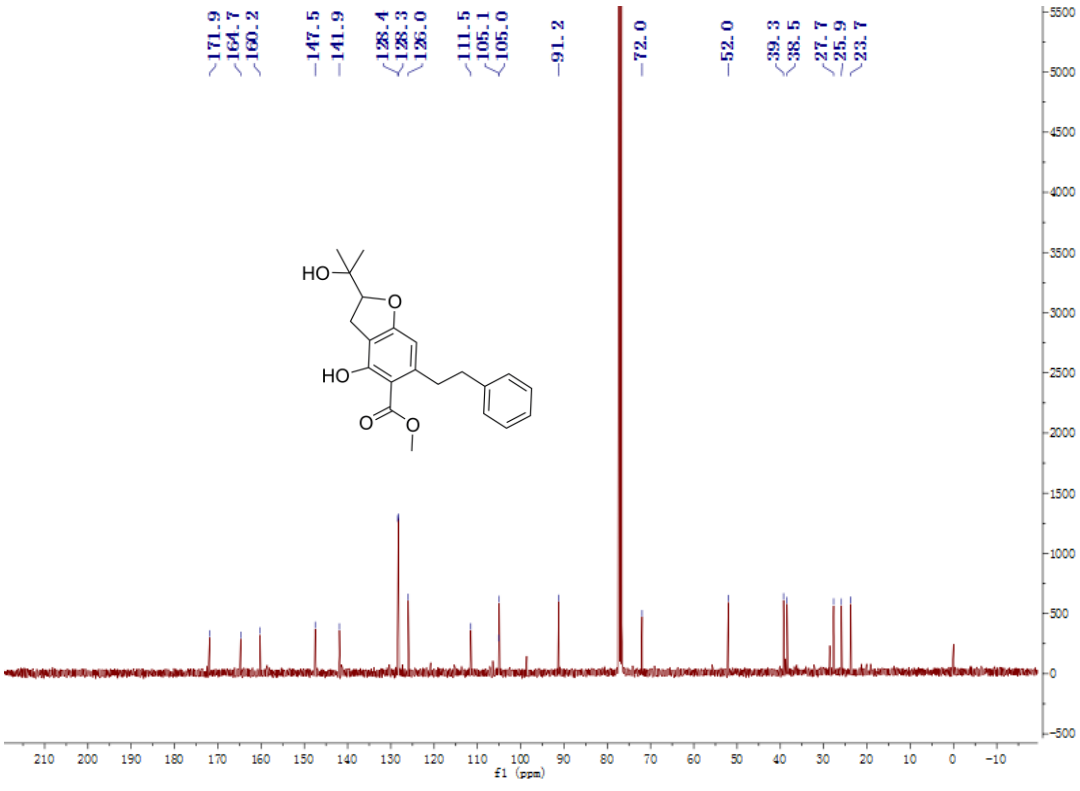

Figure S13. HSQC spectrum (600 MHz) of **2** in $CDCl_3$.

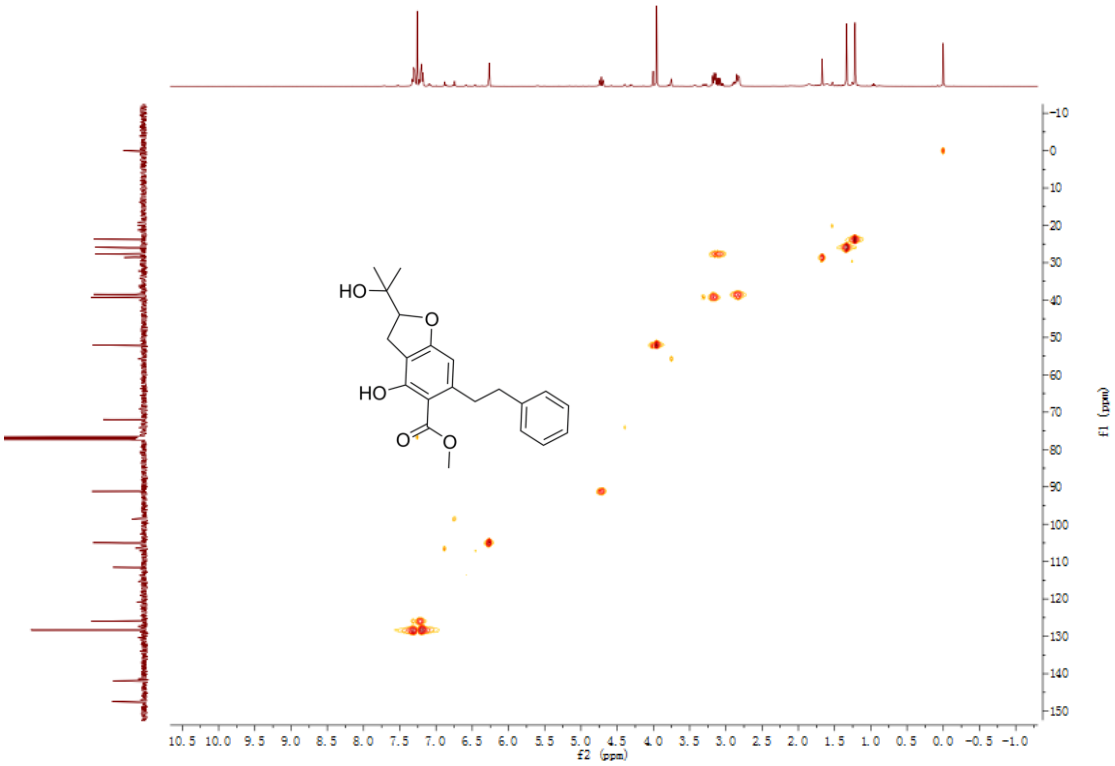

Figure S14. $^{1}H-^{1}H$ spectrum (600 MHz) of **2** in $CDCl_3$.

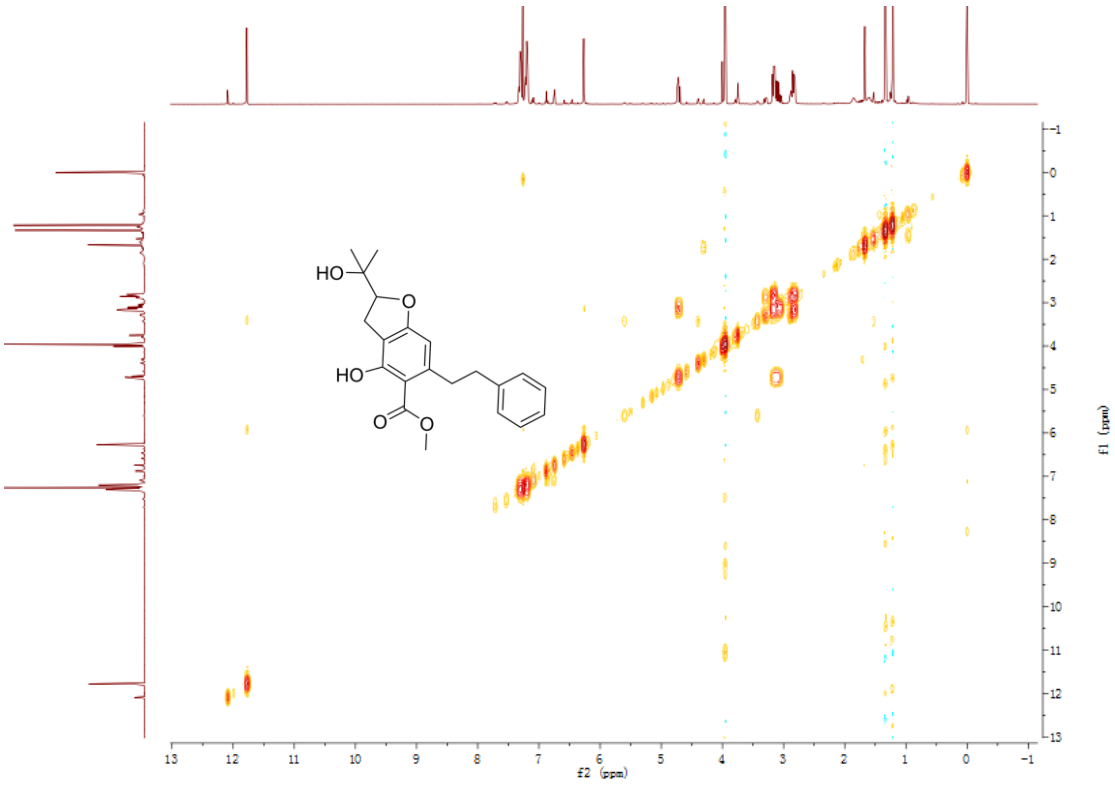

Figure S15. HMBC spectrum (600 MHz) of **2** in $CDCl_3$.

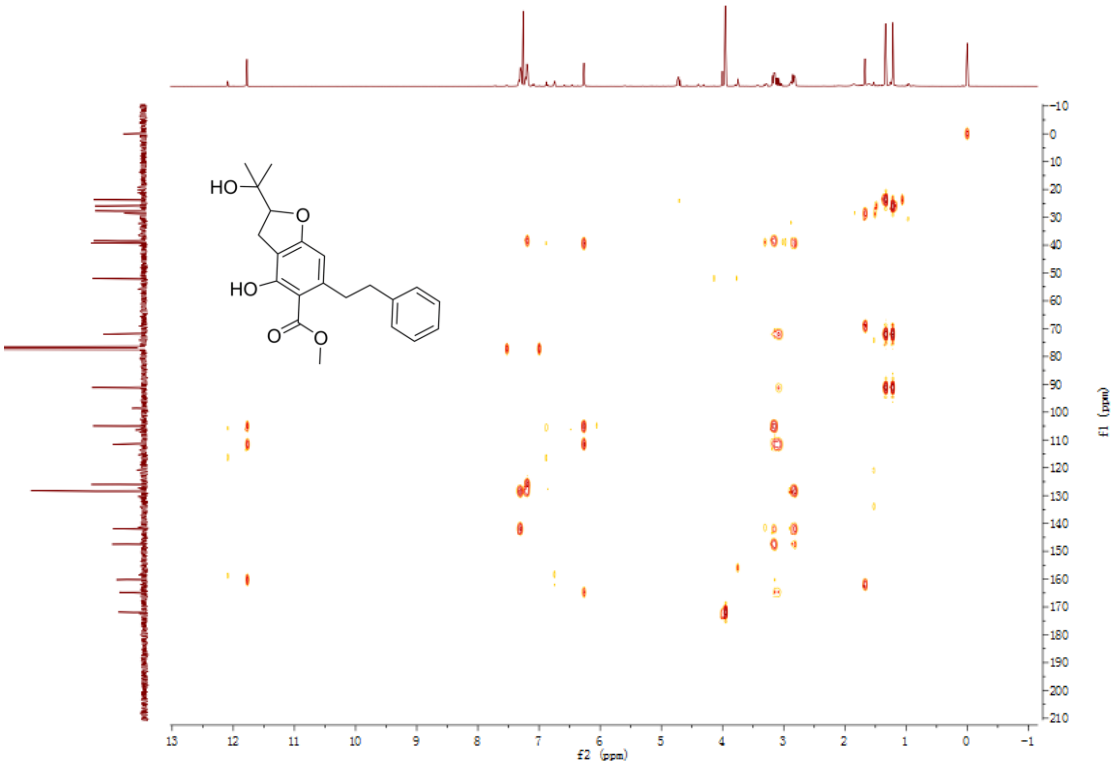

Figure S16. HRESIMS spectrum of **2**.

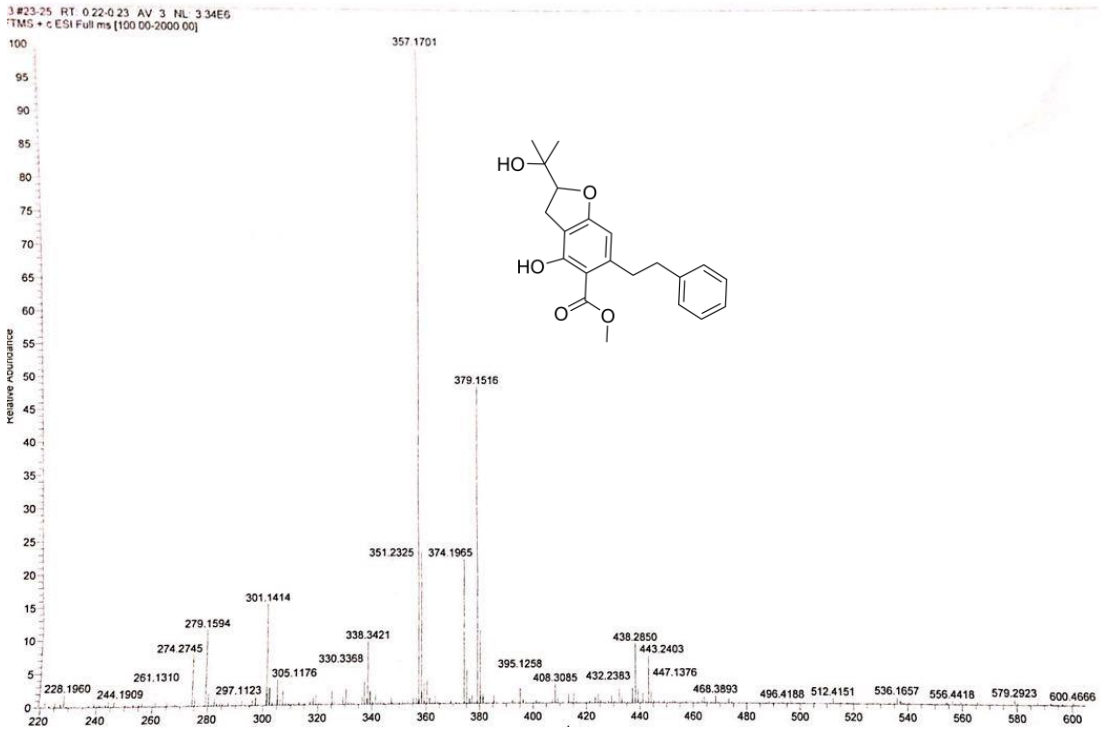

Figure S17. IR (KBr disc) spectrum of **2**.

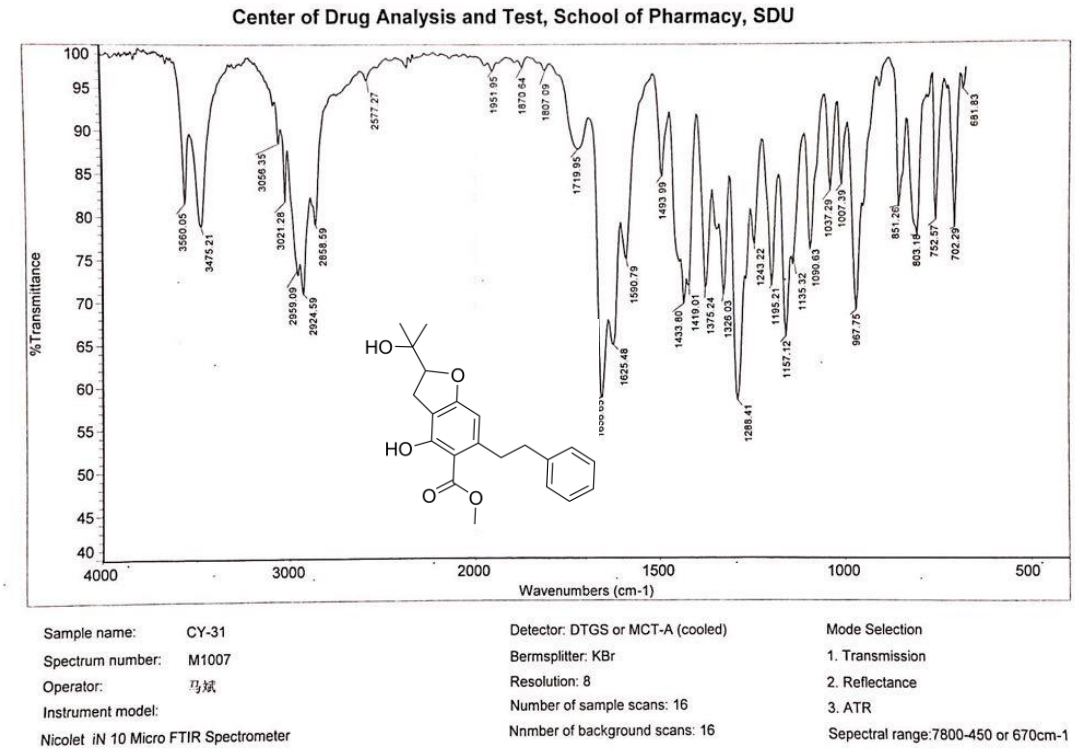

Figure S18. UV spectrum of **2**.

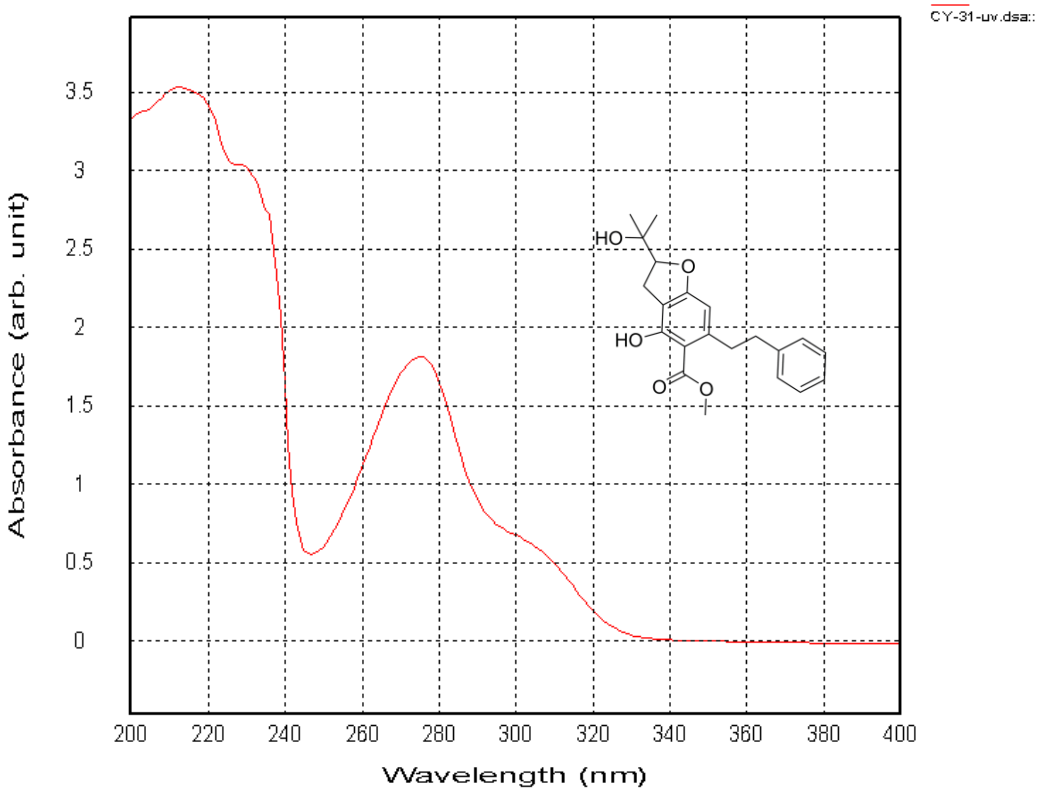

Figure S19. Chiral-phase HPLC analysis of **2**.

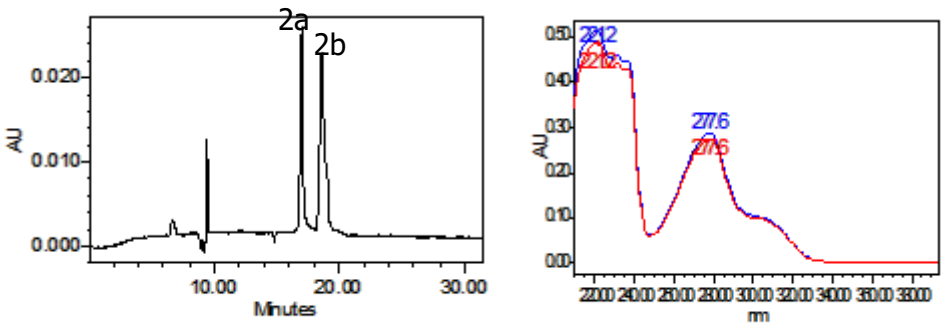

	Retention Time	Area	% Area	Height	Int Type
1	16.962	593724	52.91	19710	bb
2	18.613	528417	47.09	20630	bb

Figure S20. Experimental ECD spectra of **2a**/**2b** and calculated ECD spectrum of **2a**.

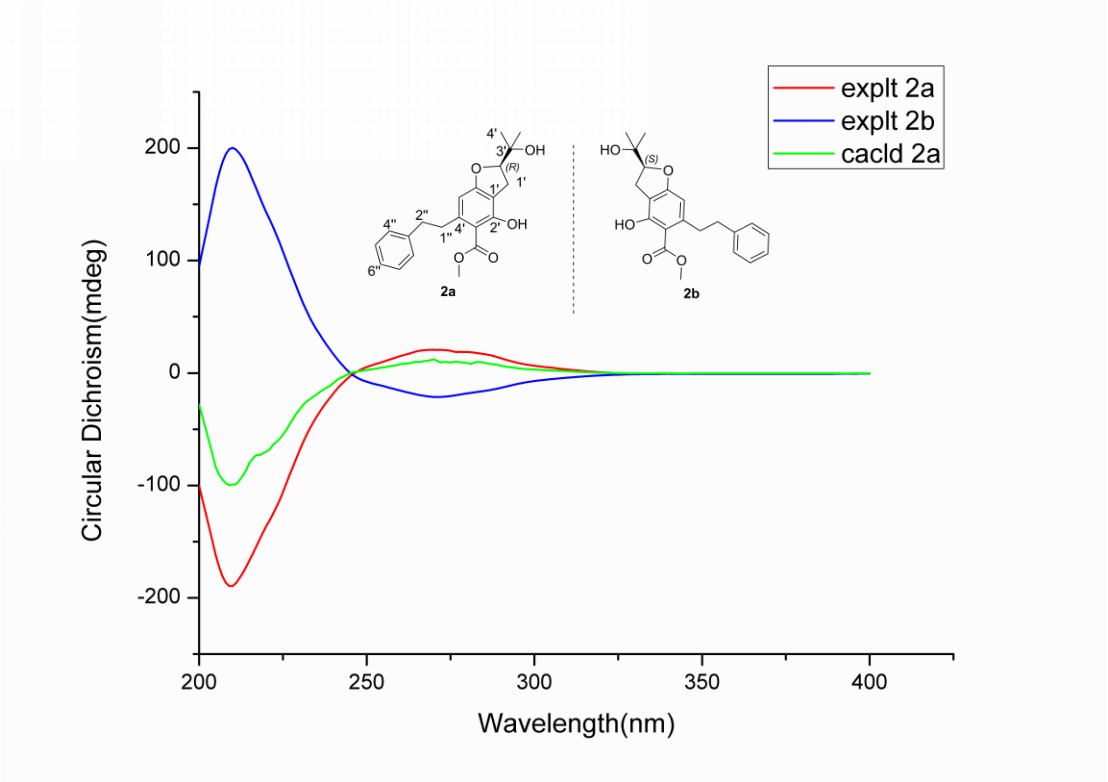

Figure S21. ^{1}H NMR spectrum (400 MHz) of **3** in $CDCl_3$.

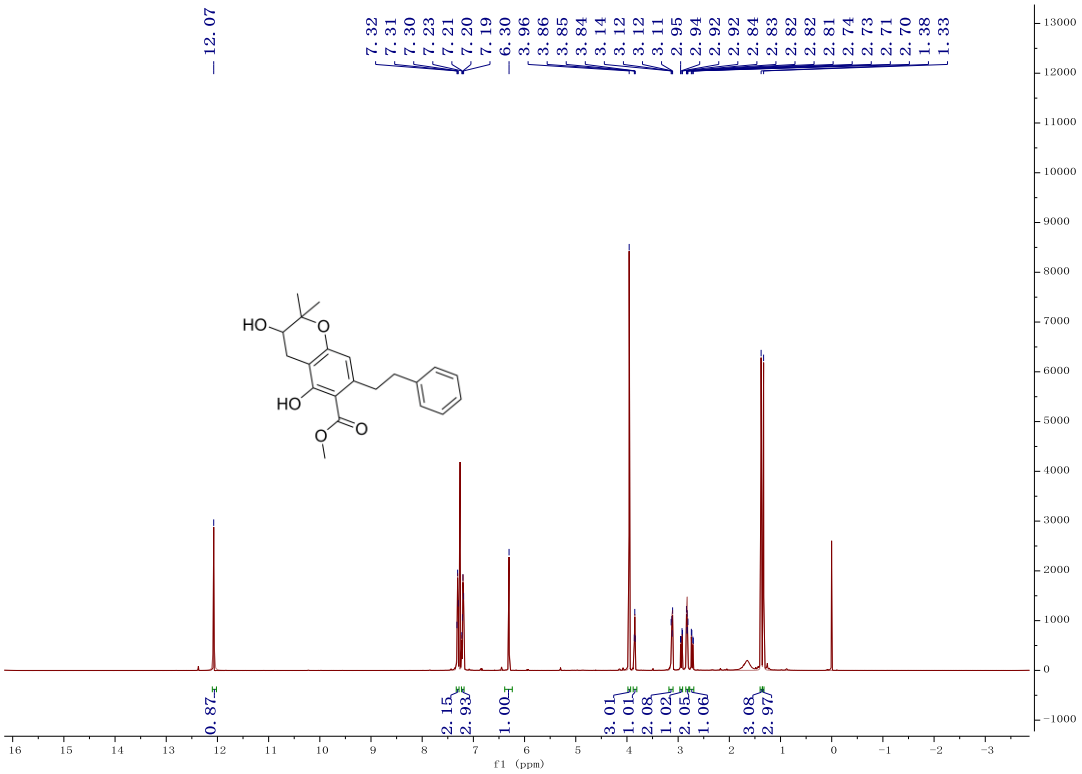

Figure S22. ^{13}C NMR spectrum (100 MHz) of **3** in $CDCl_3$.

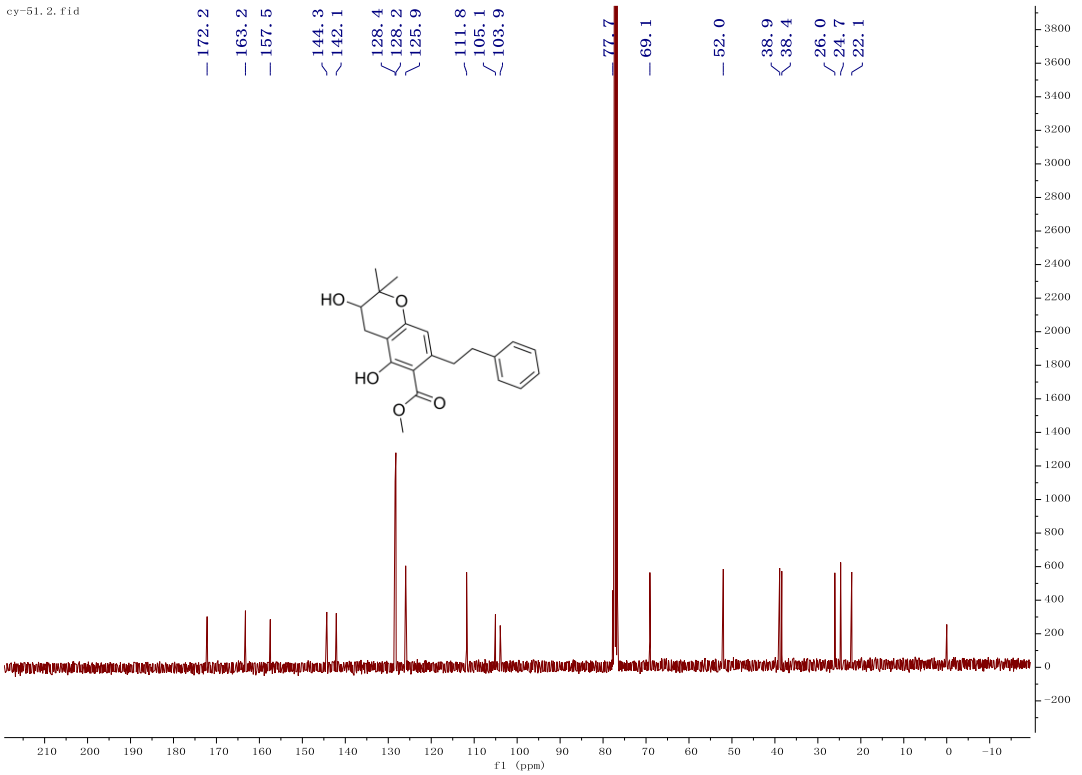

Figure S23. HMQC spectrum (400 MHz) of **3** in $CDCl_3$.

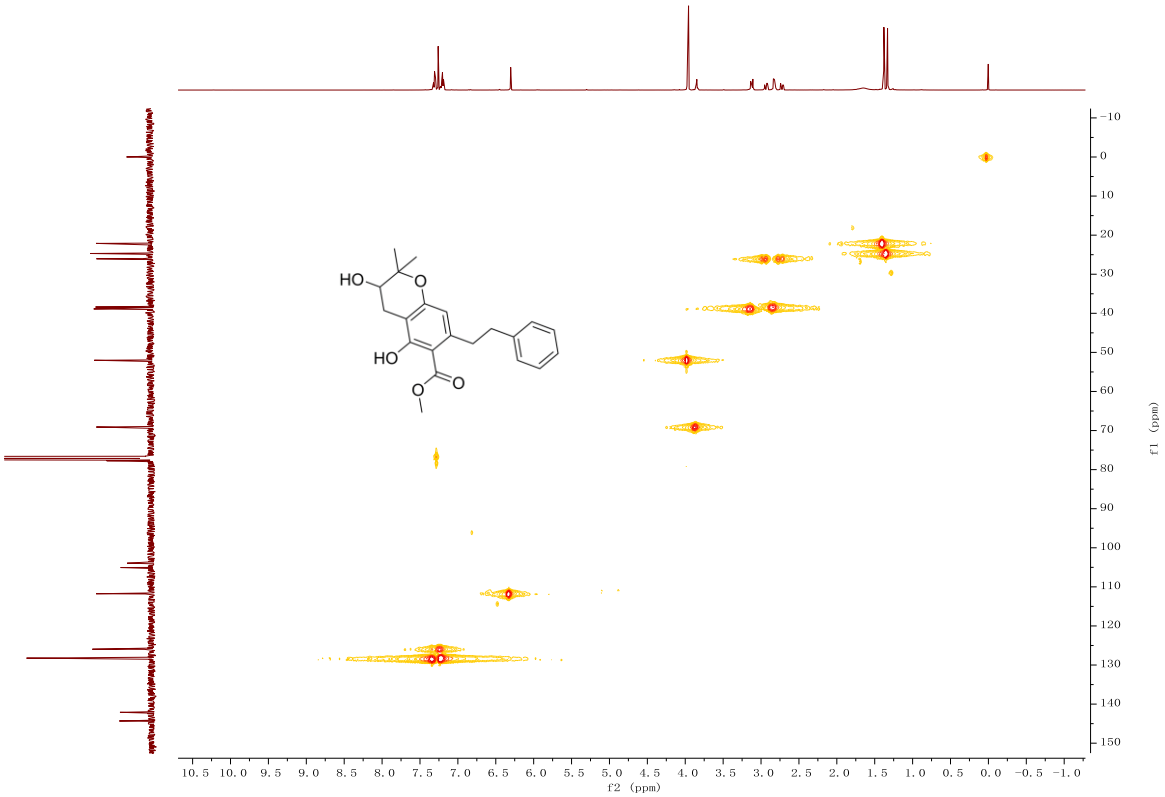

Figure S24. $^{1}H–^{1}H$ spectrum (400 MHz) of **3** in $CDCl_3$.

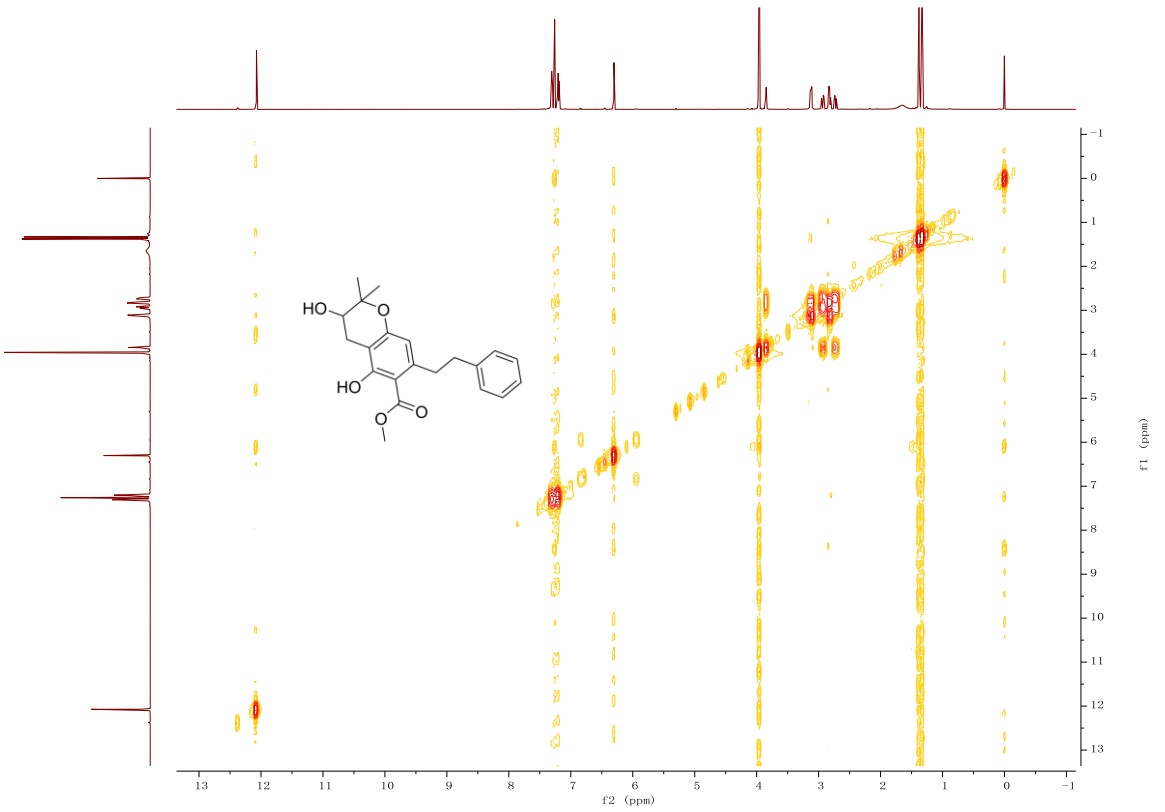

Figure S25. HMBC spectrum (400 MHz) of **3** in $CDCl_3$.

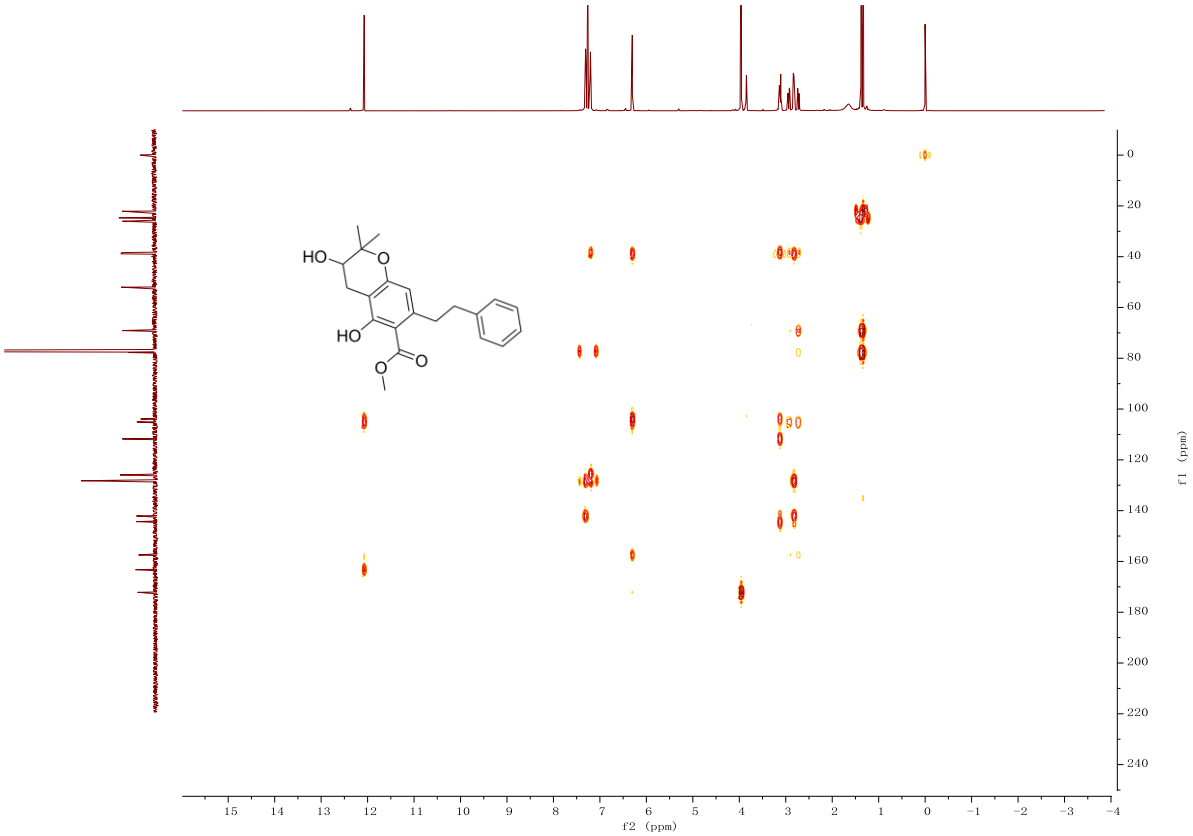

Figure S26. HRESIMS spectrum of **3**.

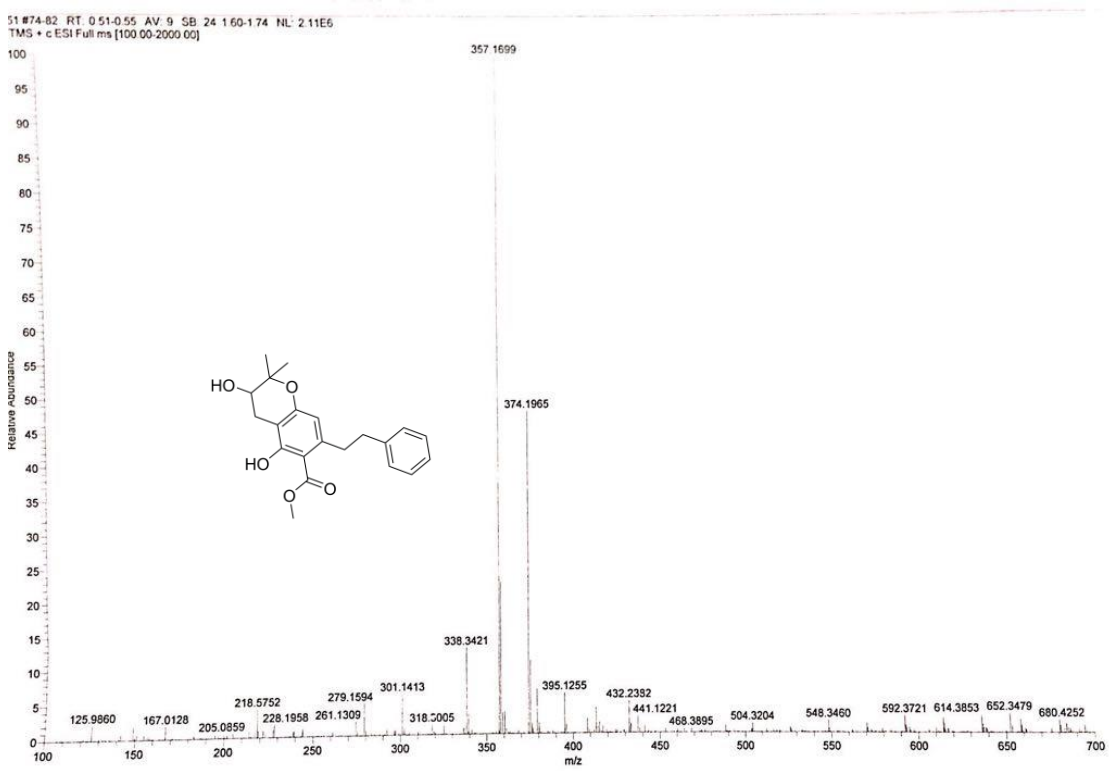

Figure S27. IR (KBr disc) spectrum of **3**.

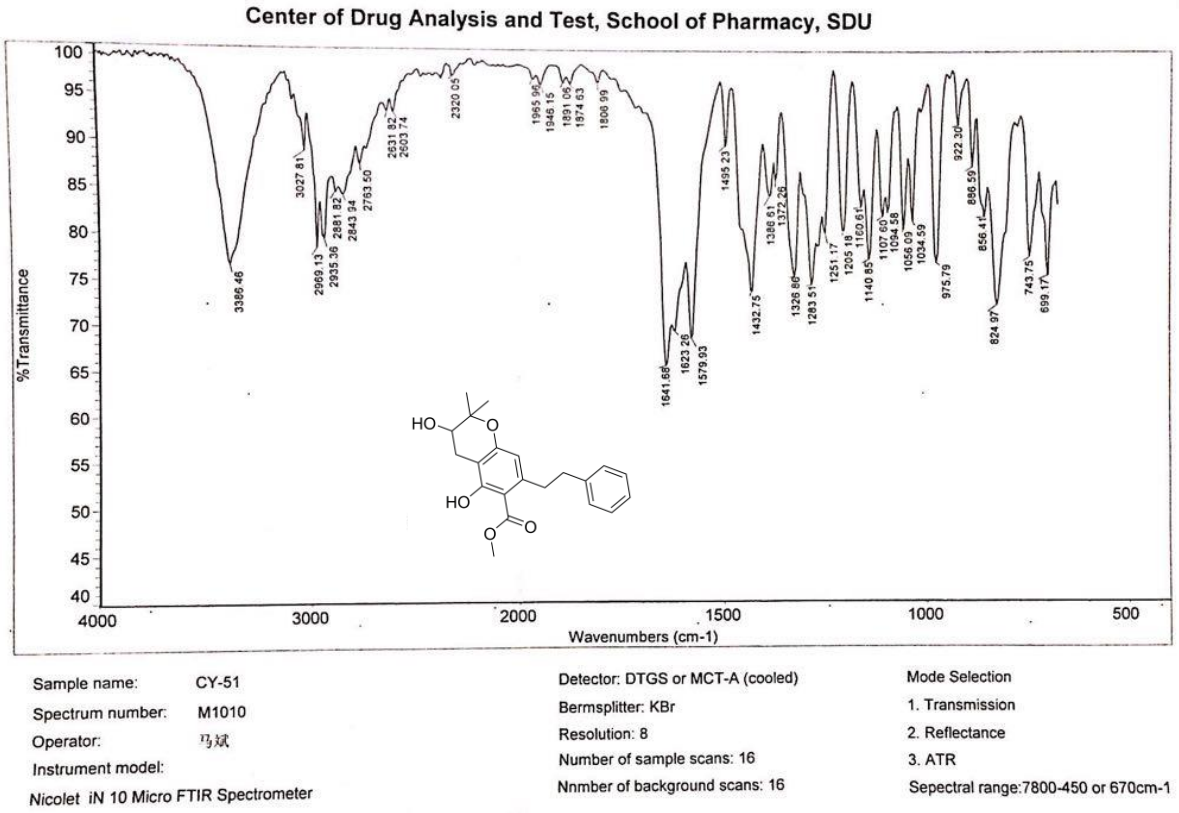

Figure S28. UV spectrum of **3**.

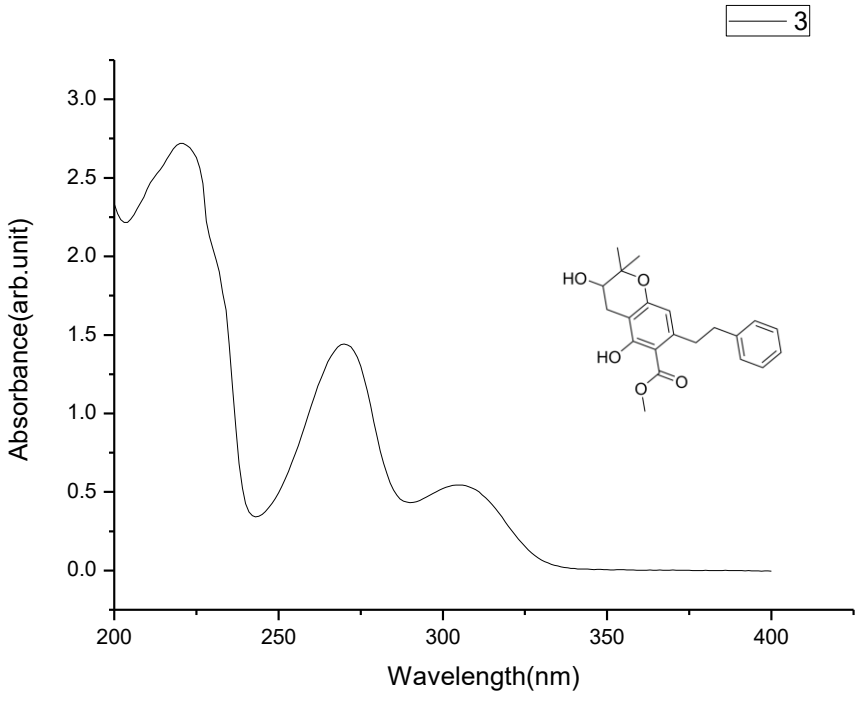

Figure S29. Chiral-phase HPLC analysis of **3**.

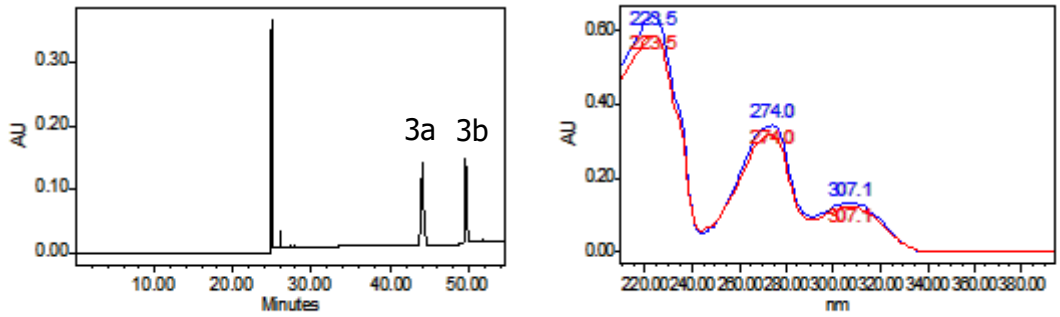

	Retention Time	Area	% Area	Height	Int Type
1	44.1	3061649	50.81	119265	bb
2	49.703	2964426	49.19	130699	bb

Figure S30. Experimental ECD spectra of **3a**/**3b** and calculated ECD spectrum of **3a**.

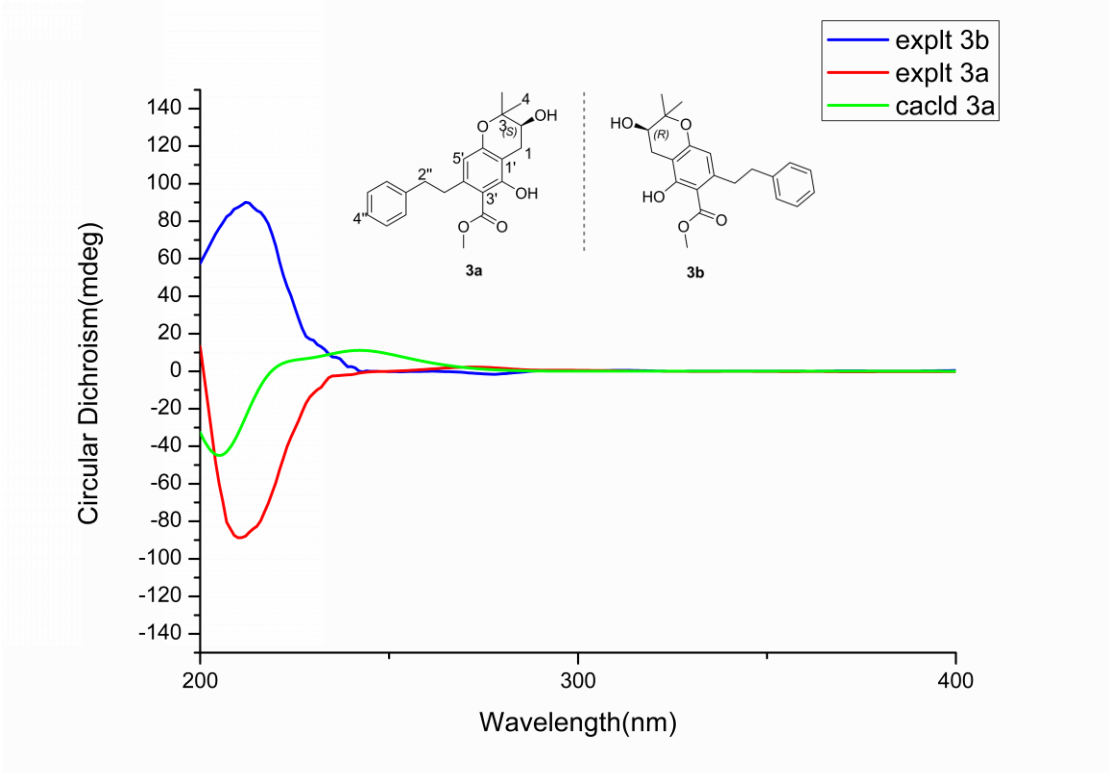

Figure S31. ^{1}H NMR spectrum (600 MHz) of **4** in $CDCl_3$.

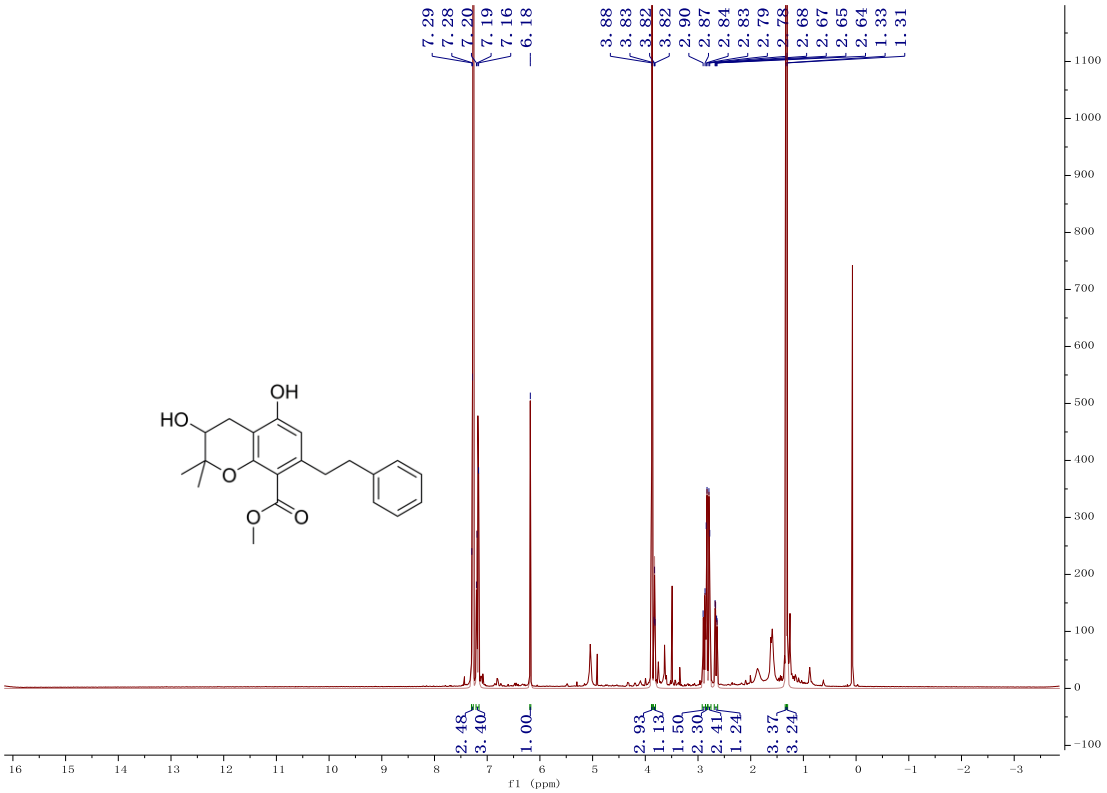

Figure S32. ^{13}C NMR spectrum (150 MHz) of **4** in $CDCl_3$.

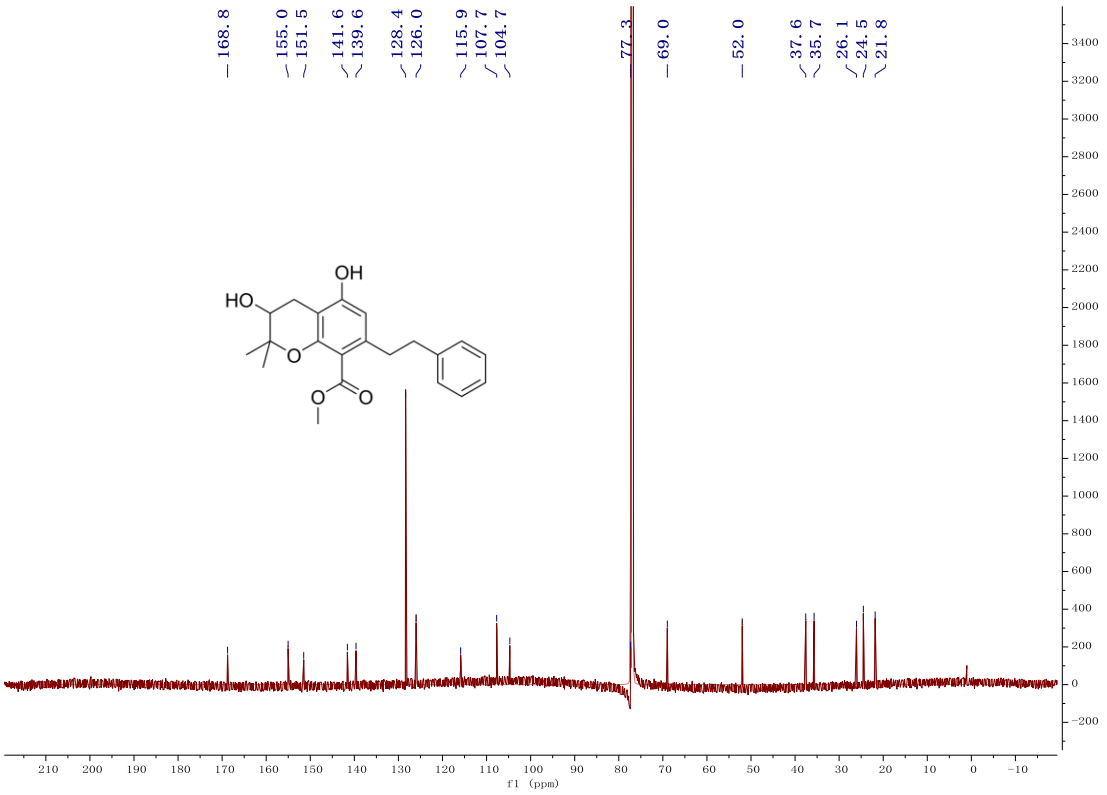

Figure S33. HSQC spectrum (600 MHz) of **4** in $CDCl_3$.

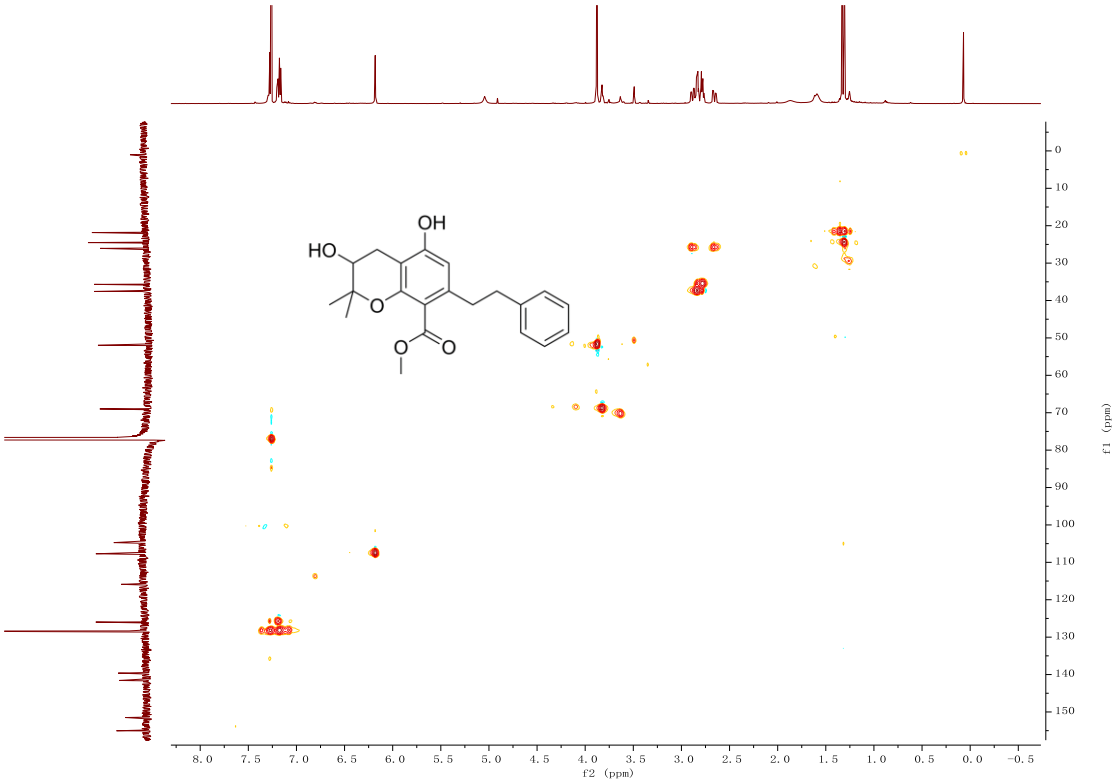

Figure S34. $^{1}H-^{1}H$ spectrum (600 MHz) of **4** in $CDCl_3$.

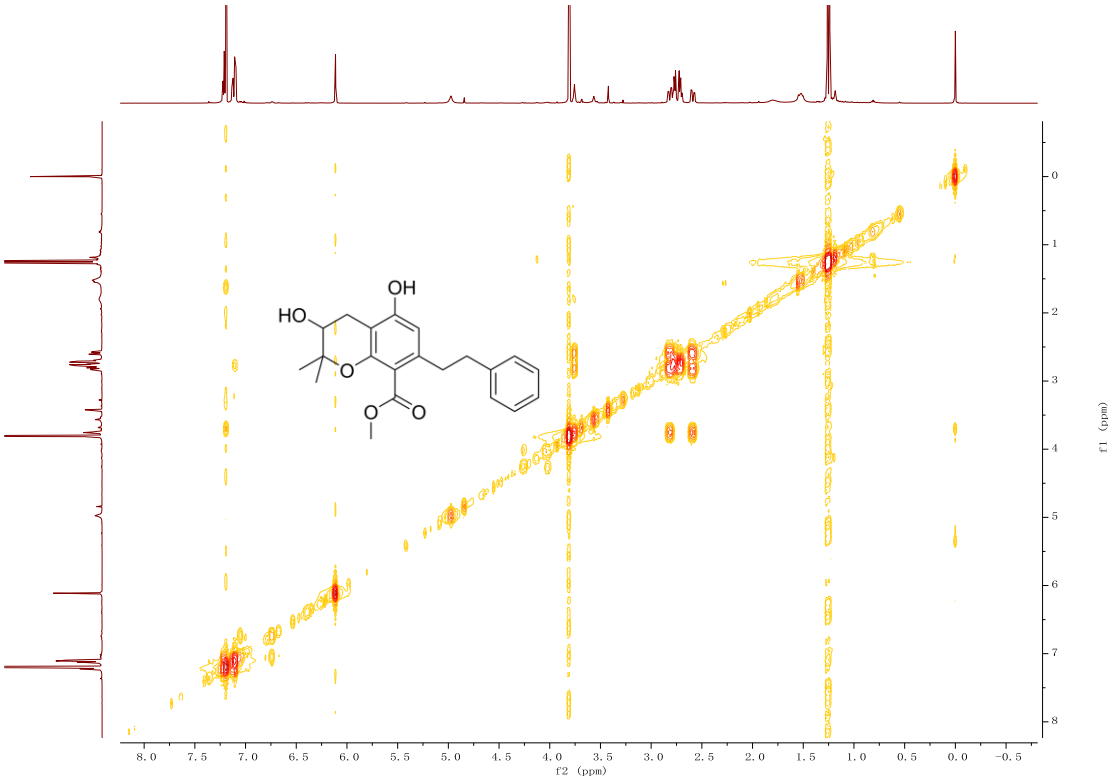

Figure S35. HMBC spectrum (600 MHz) of **4** in $CDCl_3$.

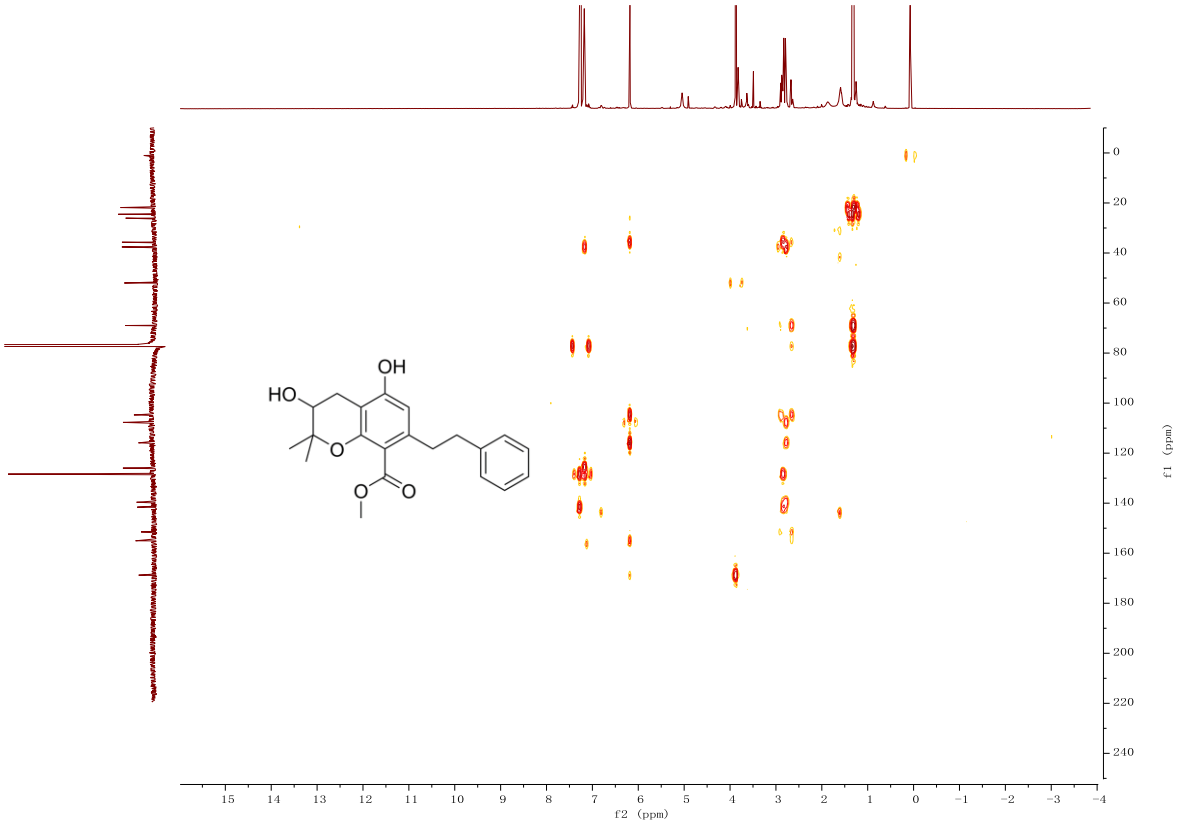

Figure S36. HRESIMS spectrum of **4**.

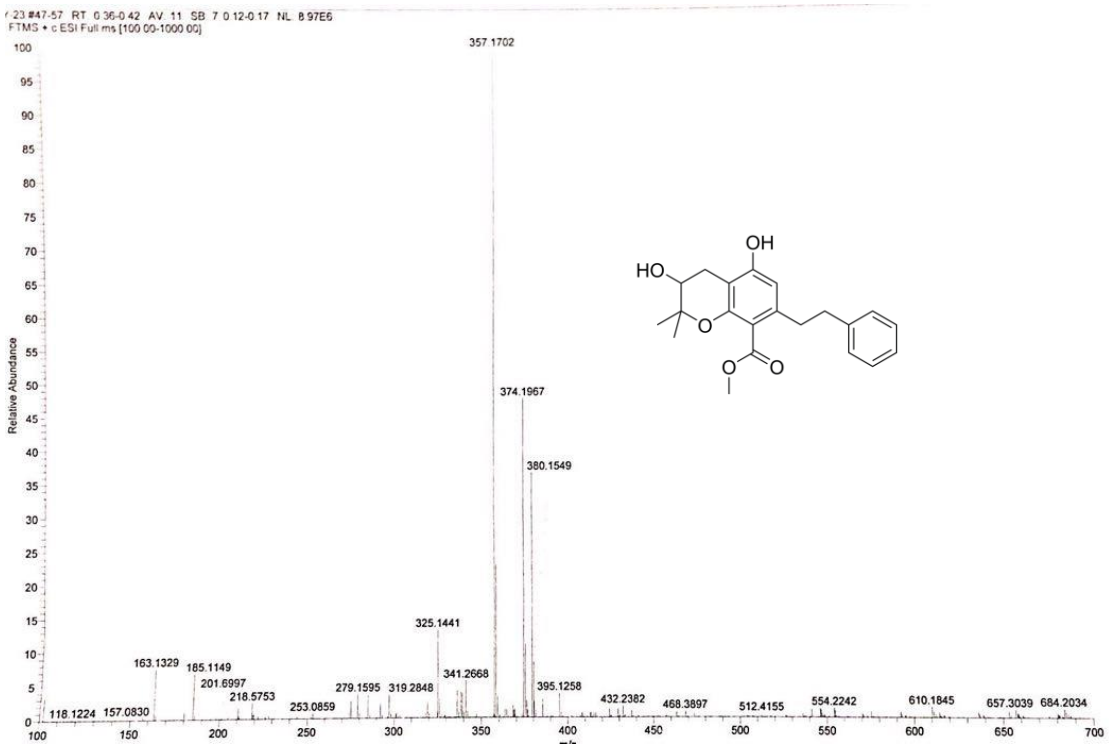

Figure S37. IR (KBr disc) spectrum of **4**.

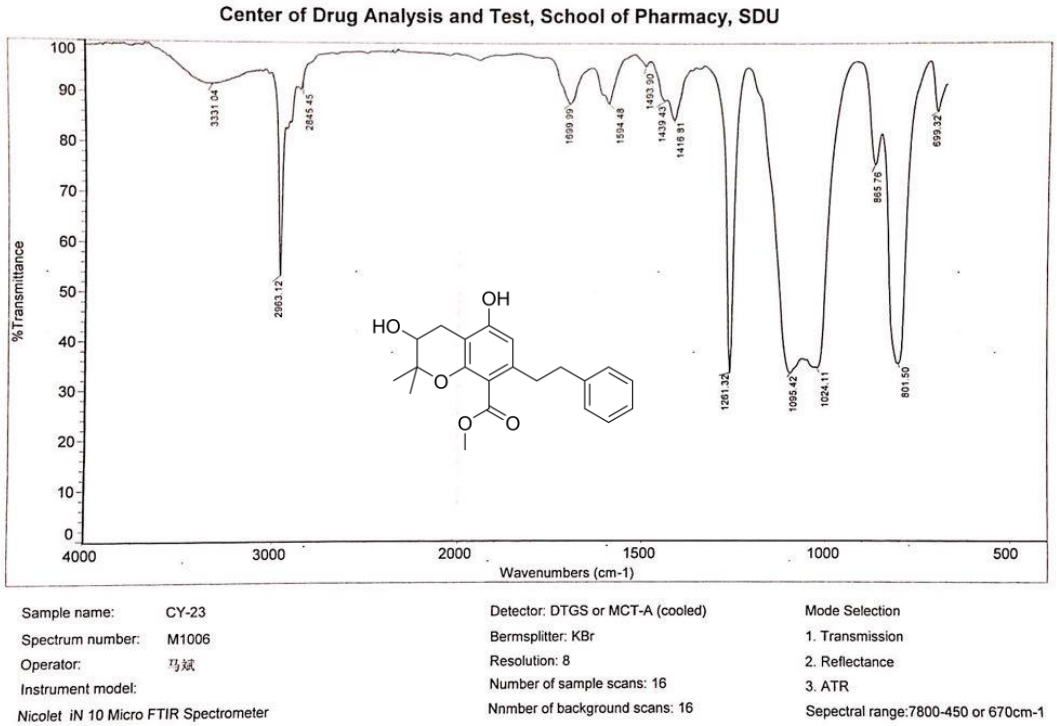

Figure S38. UV spectrum of **4**.

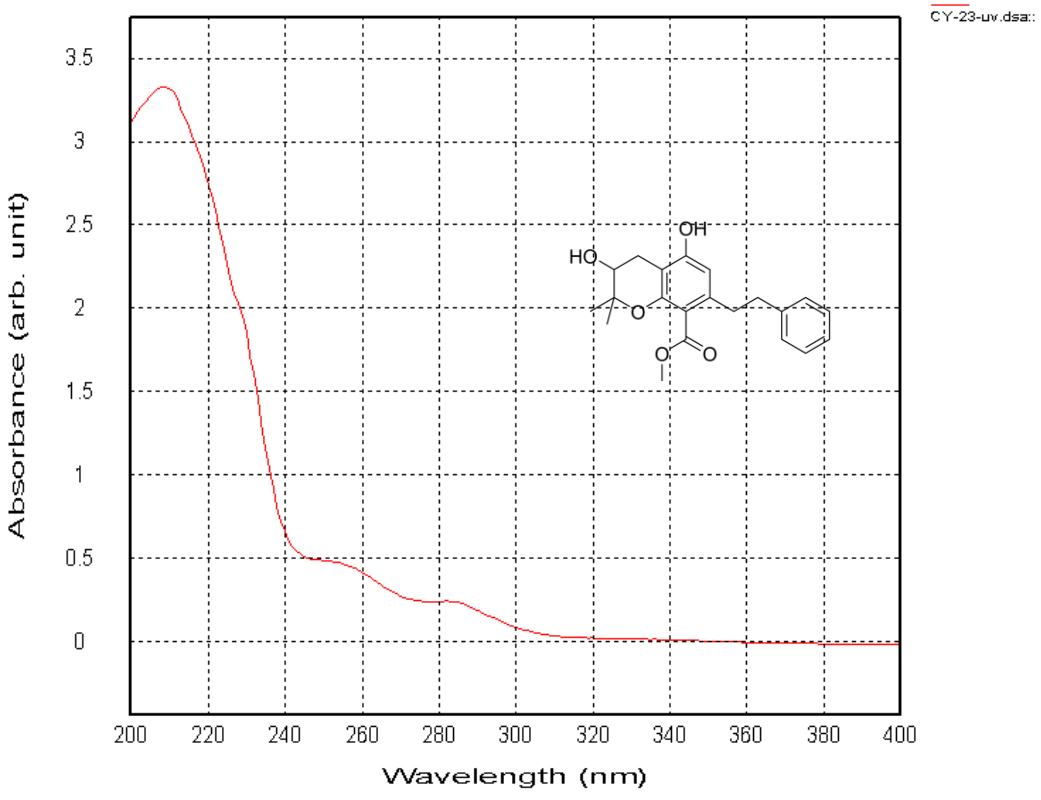

Figure S39. Chiral-phase HPLC analysis of **4**.

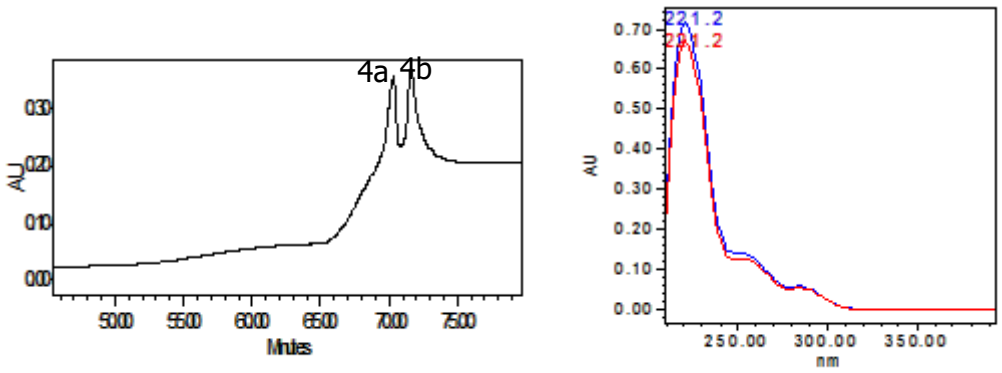

	Retention Time	Area	% Area	Height	Int Type
1	70.313	6350491	49.31	125887	bb
2	71.624	6527727	50.69	137766	bb

Figure S40. Experimental ECD spectra of **4a**/**4b** and calculated ECD spectrum of **4b**.

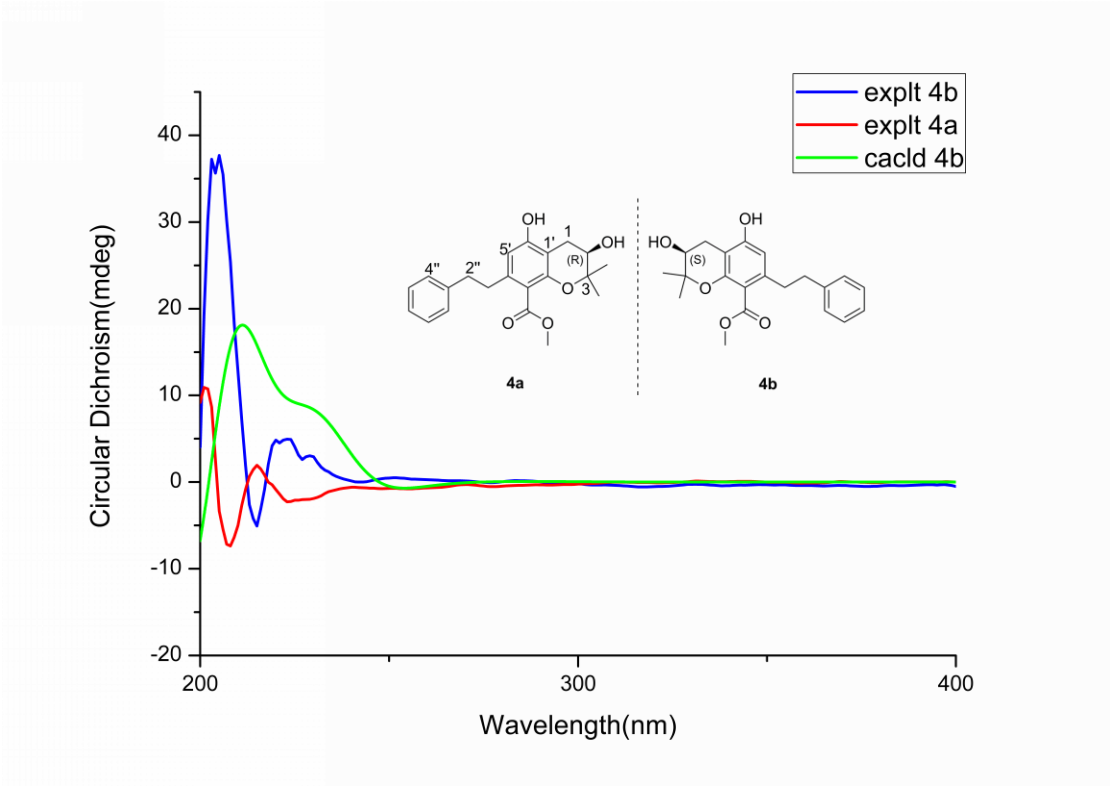

Figure S41. ^{1}H NMR spectrum (400 MHz) of **5** in $CDCl_3$.

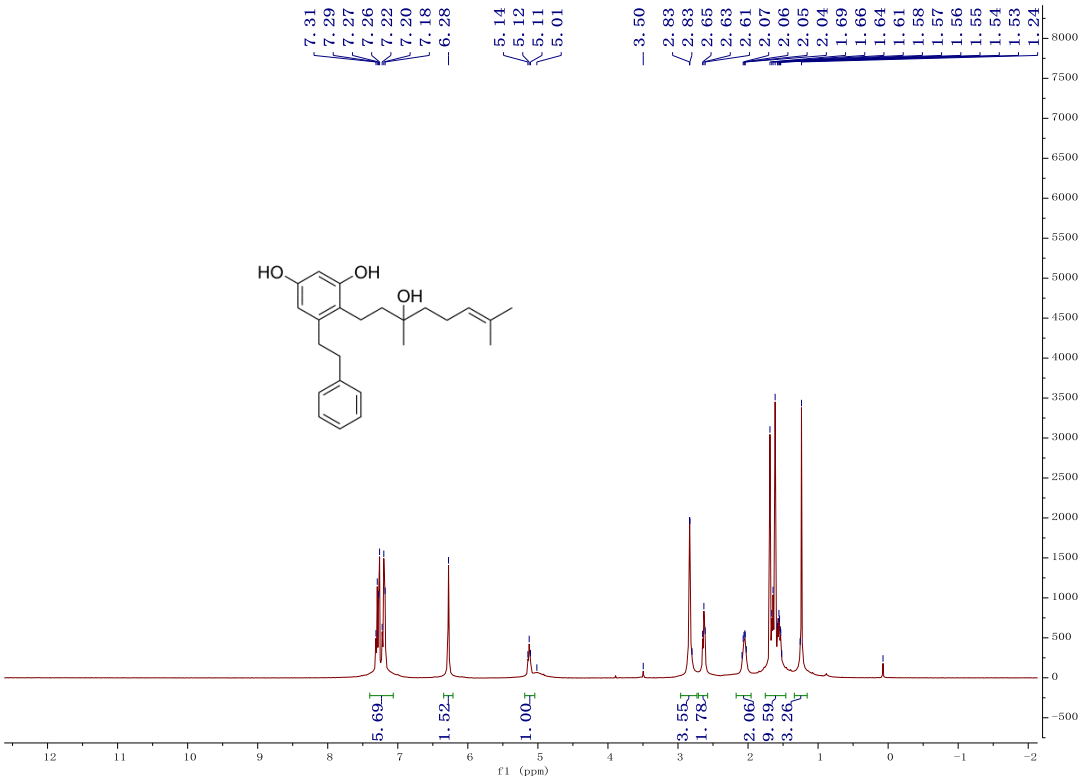

Figure S42. ^{13}C NMR spectrum (100 MHz) of **5** in $CDCl_3$.

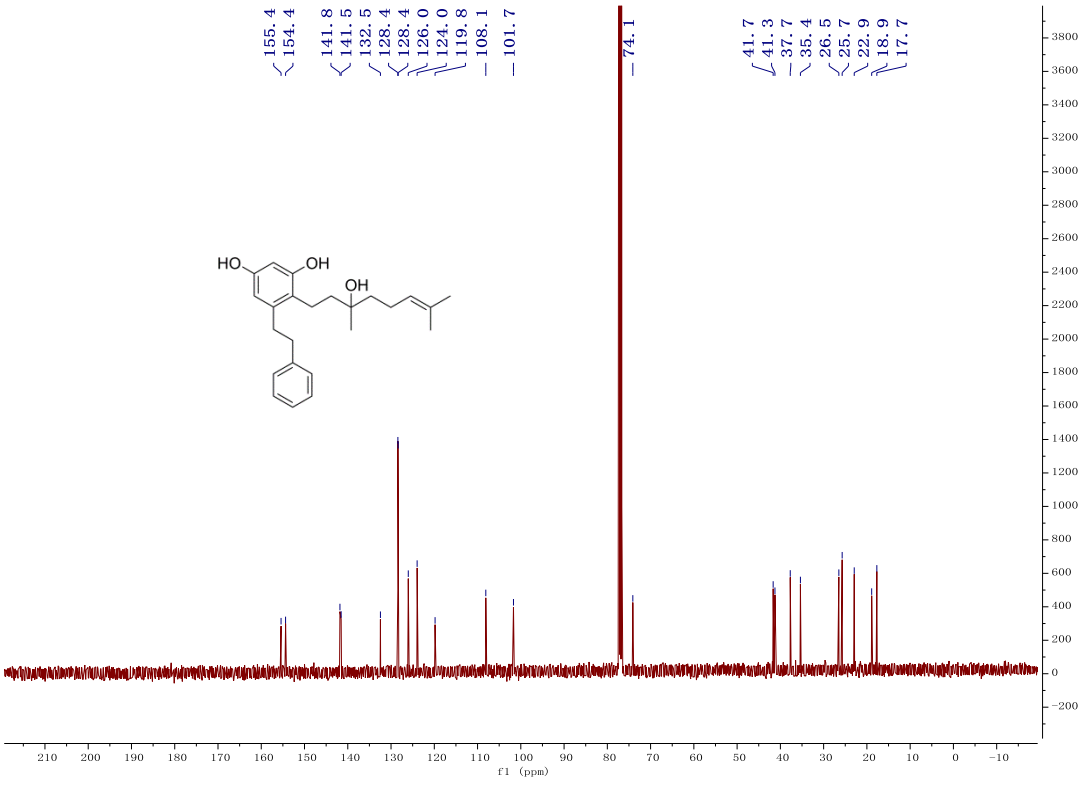

Figure S43. HSQC spectrum (400 MHz) of **5** in $CDCl_3$.

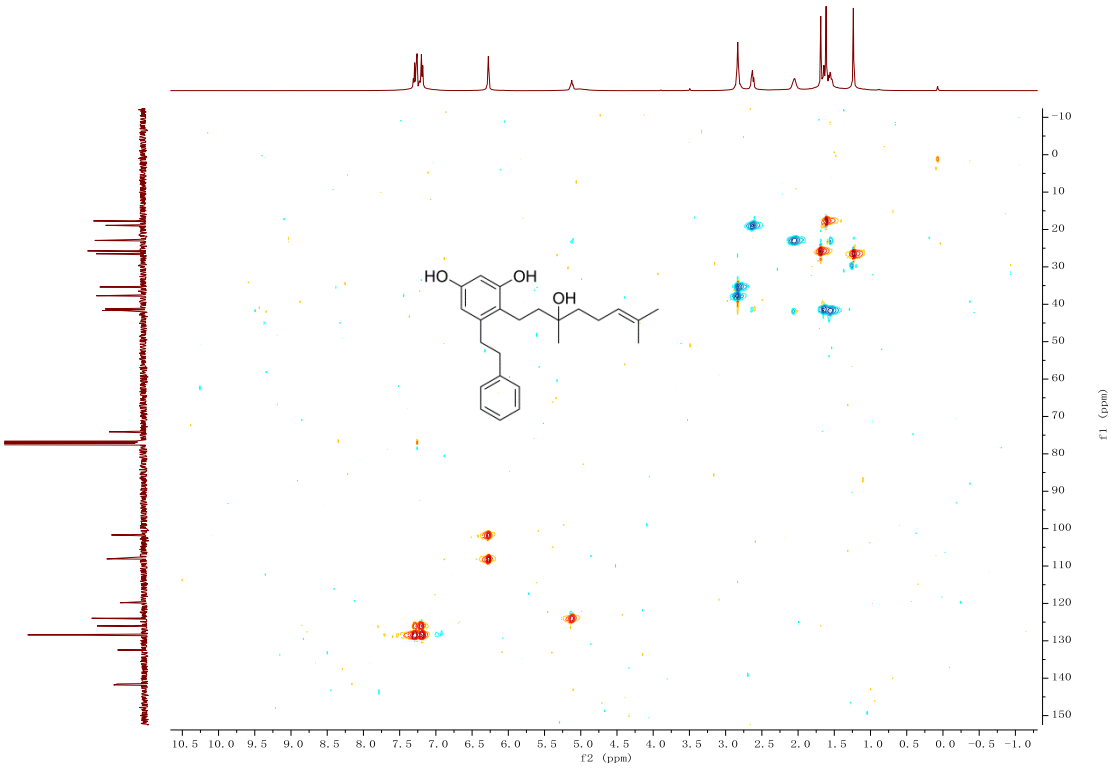

Figure S44. $^{1}H-^{1}H$ spectrum (400 MHz) of **5** in $CDCl_3$.

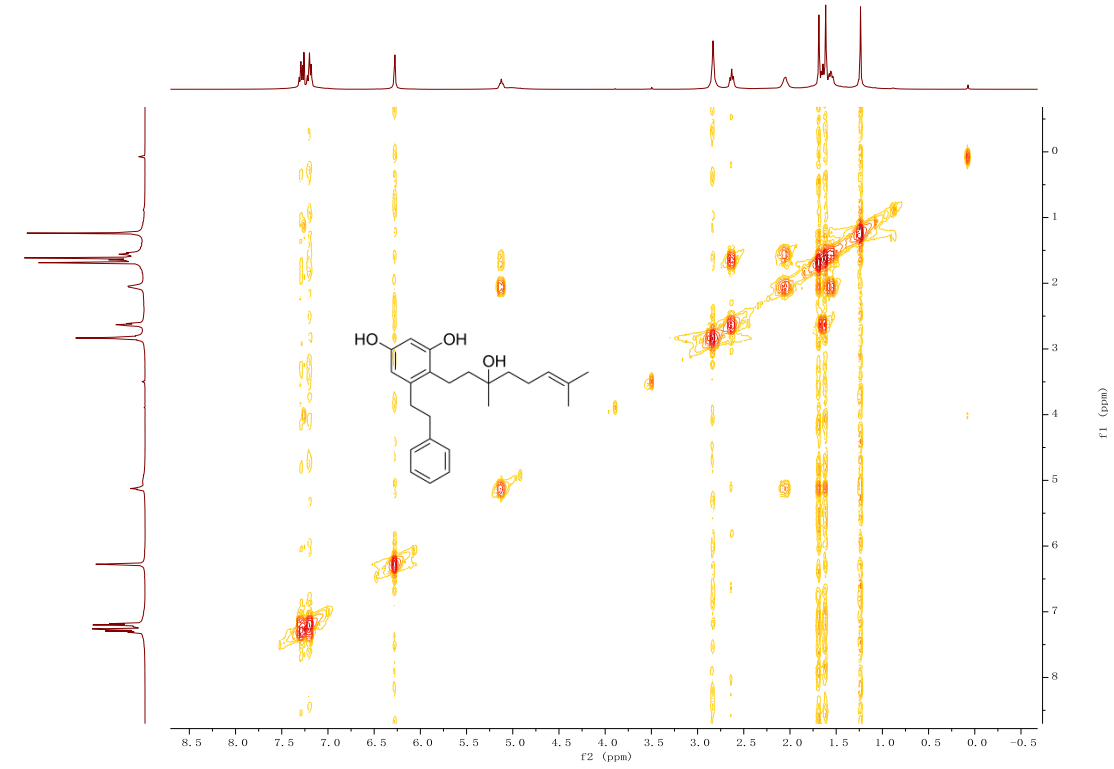

Figure S45. HMBC spectrum (400 MHz) of **5** in $CDCl_3$.

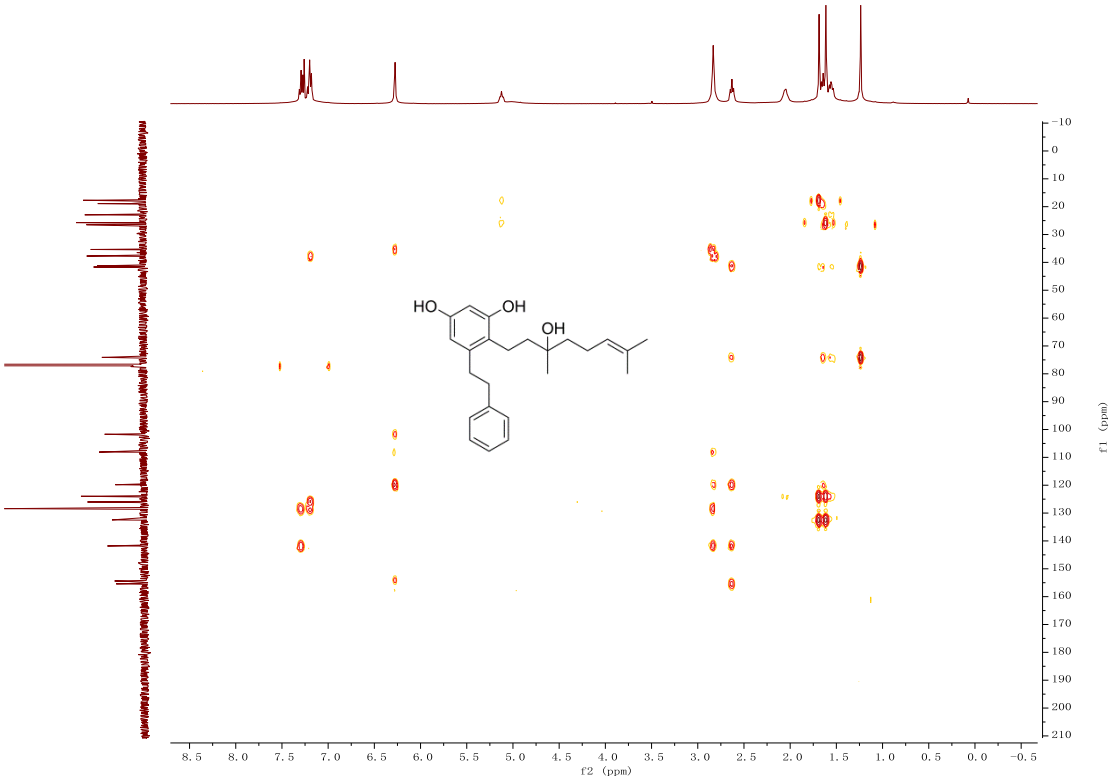

Figure S46. HRESIMS spectrum of **5.**

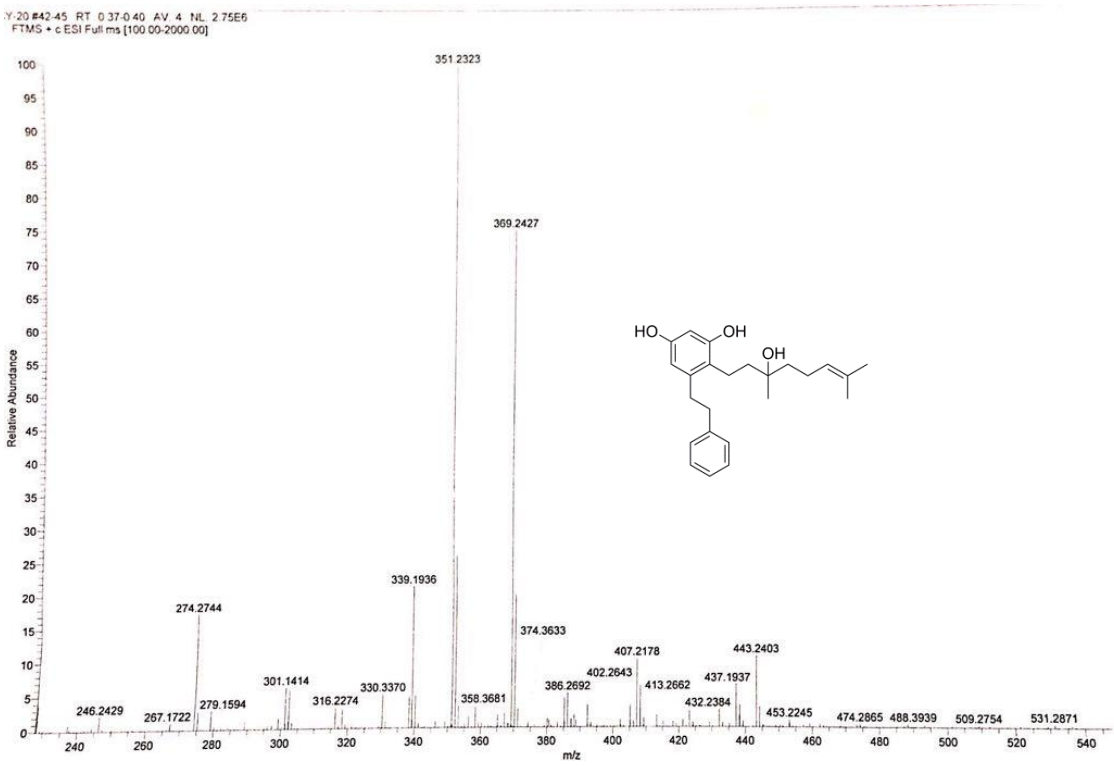

Figure S47. IR (KBr disc) spectrum of **5**.

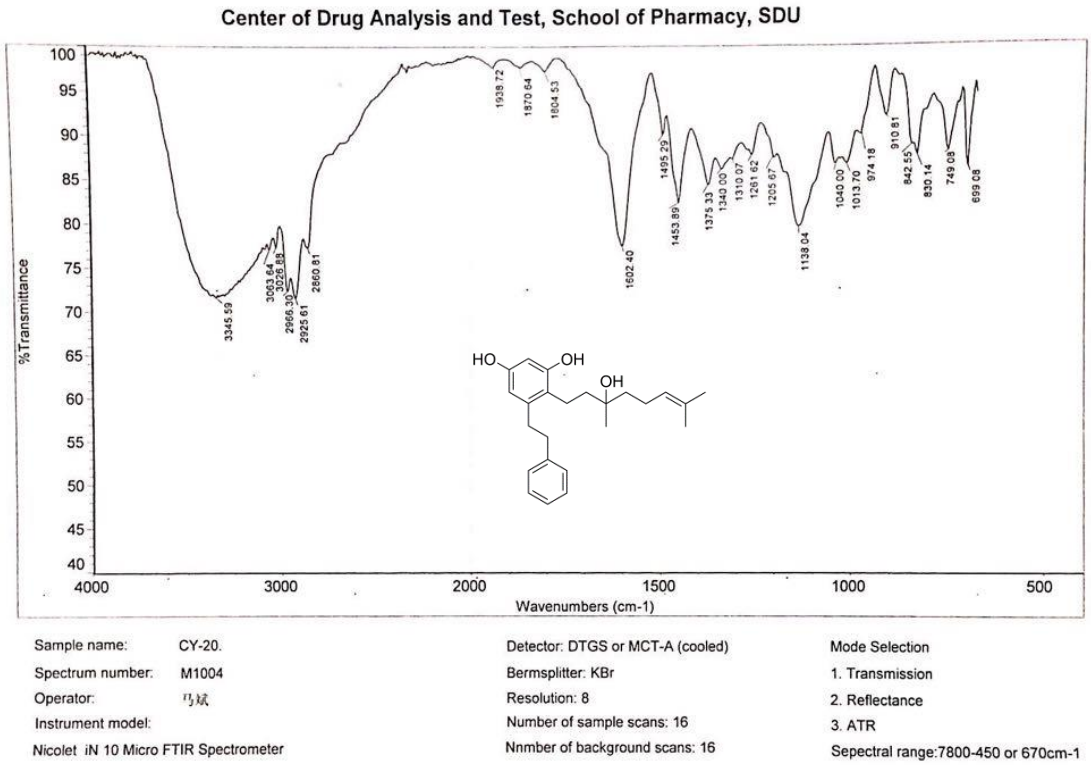

Figure S48. UV spectrum of **5**.

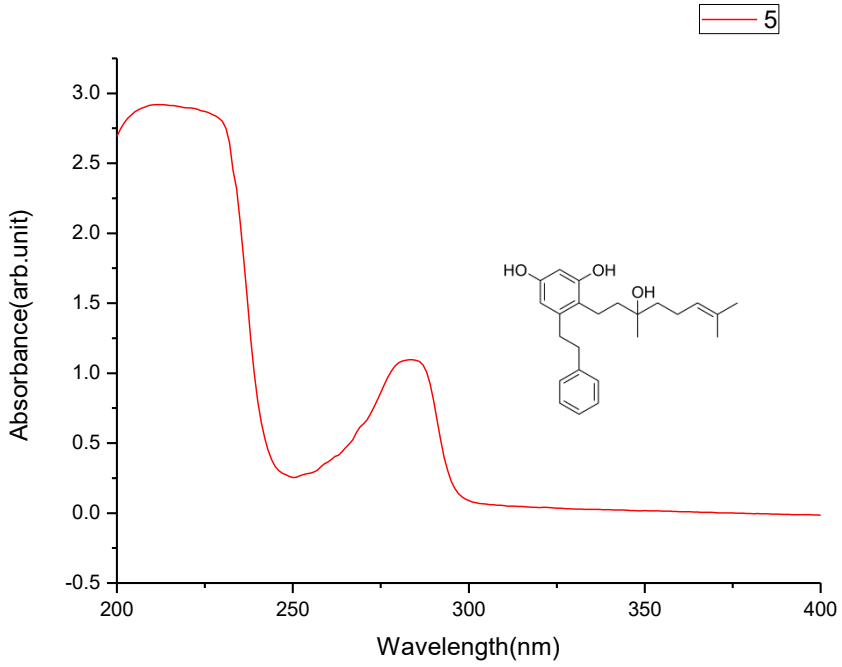

Figure S49. Chiral-phase HPLC analysis of **5**.

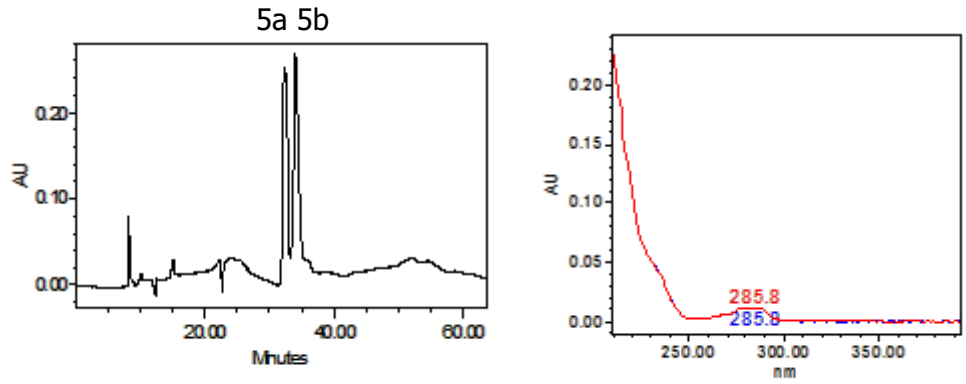

	Retention Time	Area	% Area	Height	Int Type
1	32.488	10759089	48.91	230645	bb
2	34.189	11237919	51.09	229510	bb

Figure S50. Experimental ECD spectra of **5a**/5**b** and calculated ECD spectrum of **5a.**

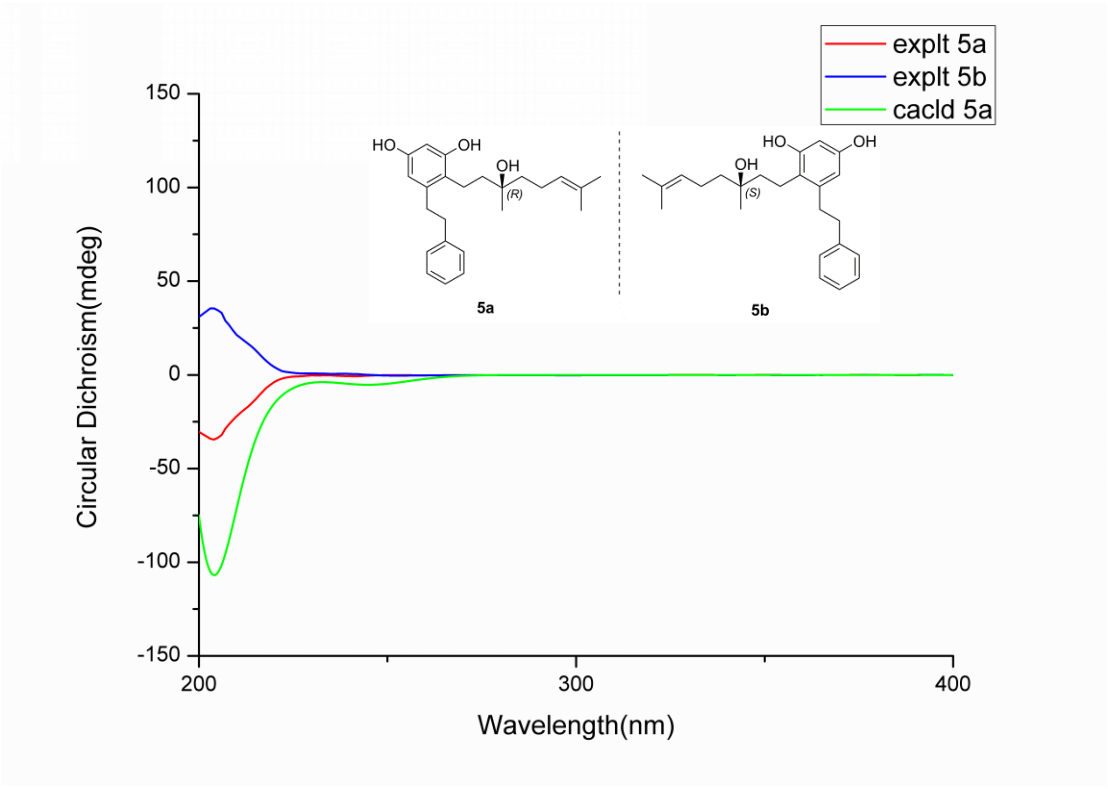

Figure S51. ^{1}H NMR spectrum (600 MHz) of **6** in $CDCl_3$.

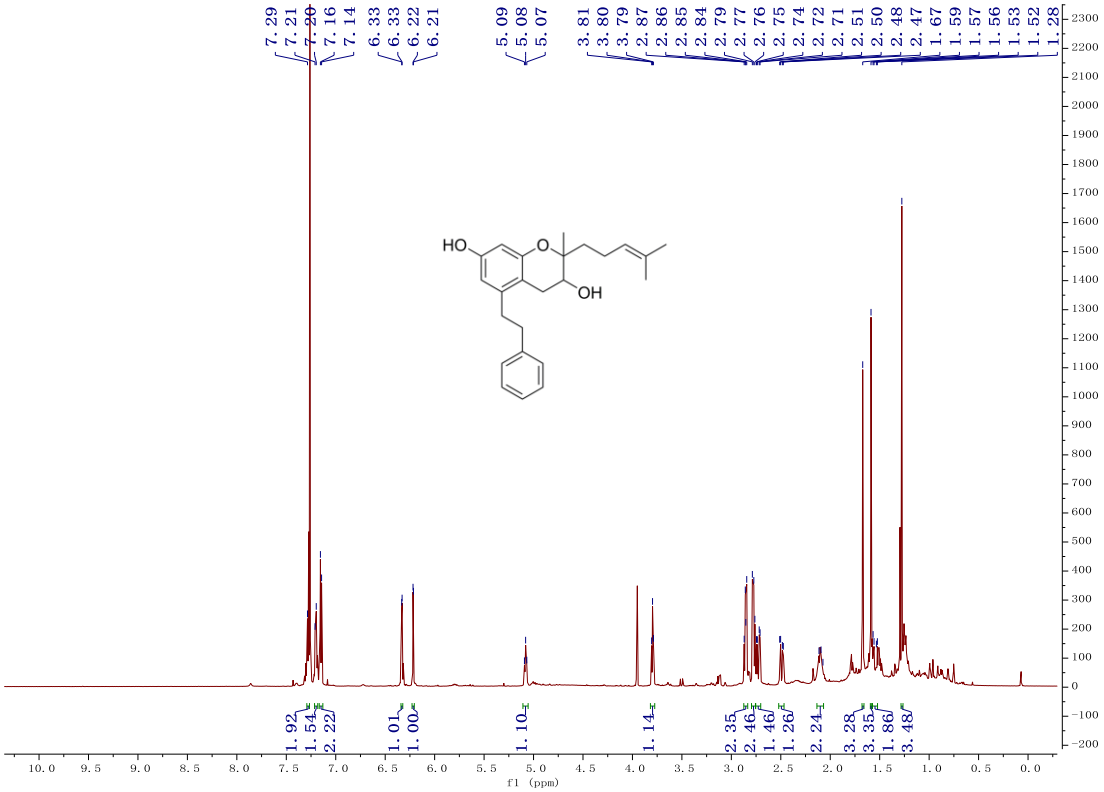

Figure S52. ^{13}C NMR spectrum (150 MHz) of **6** in $CDCl_3$.

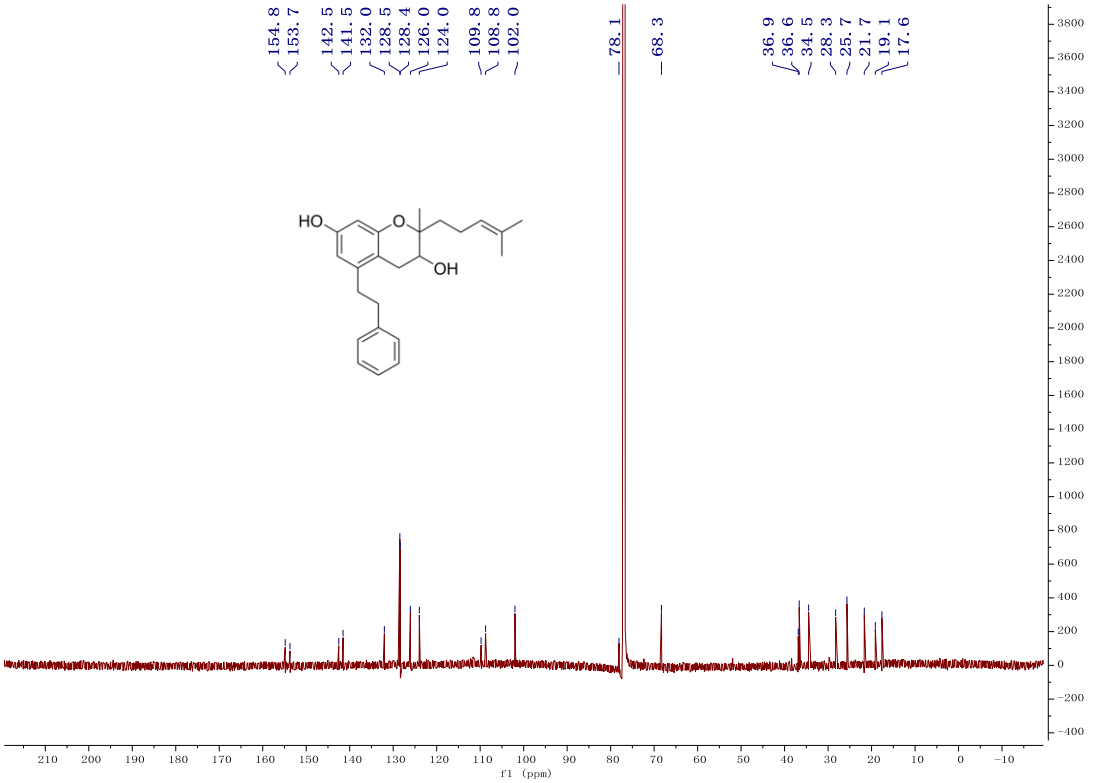

Figure S53. HSQC spectrum (600 MHz) of **6** in $CDCl_3$.

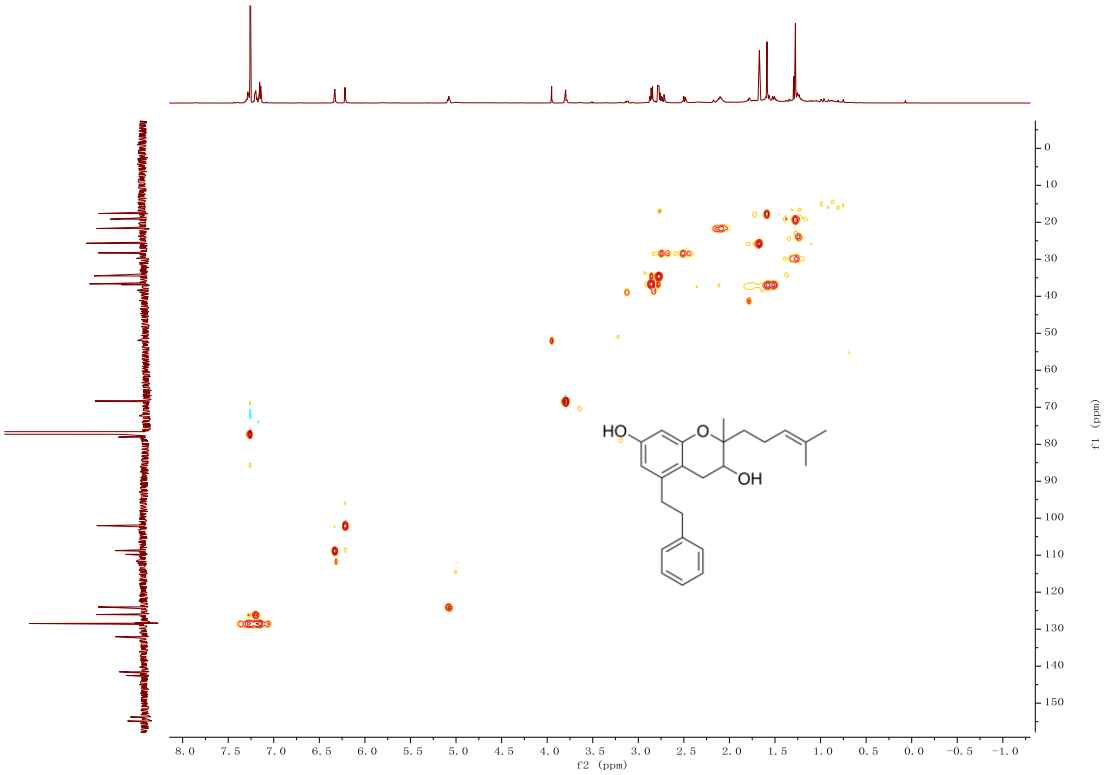

Figure S54. $^{1}H-^{1}H$ Spectrum (600 MHz) of **6** in $CDCl_3$.

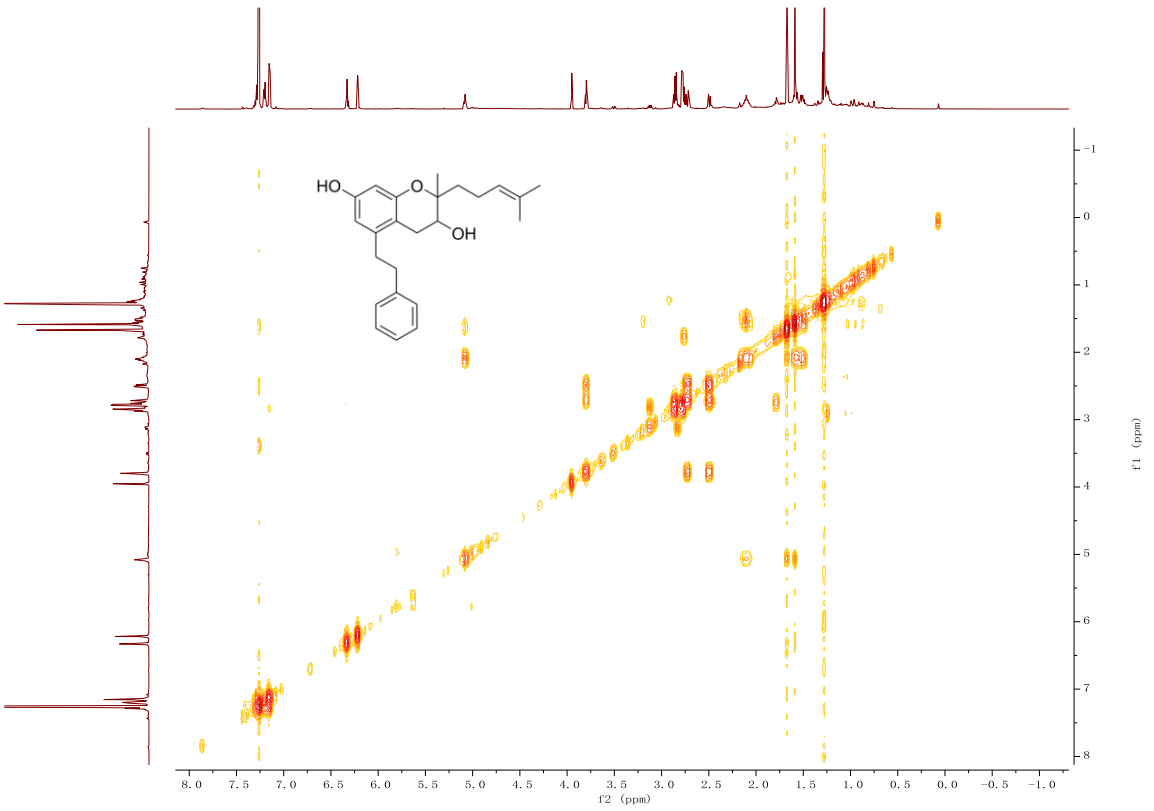

Figure S55. HMBC spectrum (600 MHz) of **6** in $CDCl_3$.

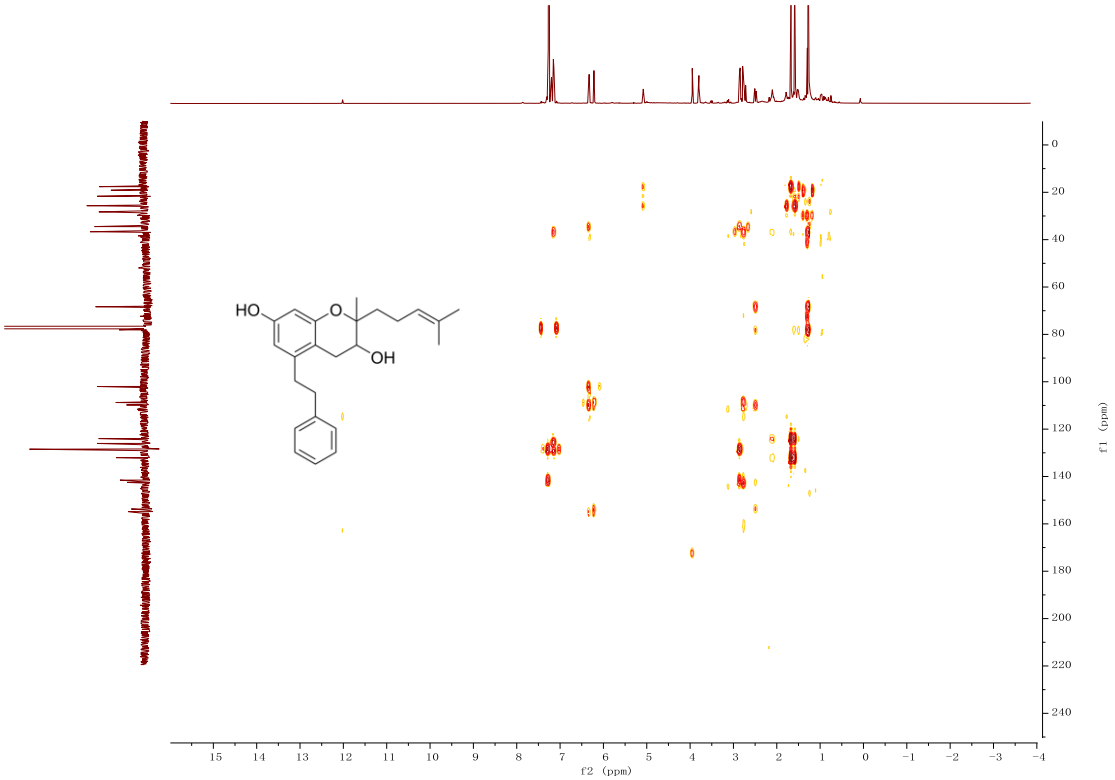

Figure S56. NOESY spectrum (600 MHz) of **6** in $CDCl_3$.

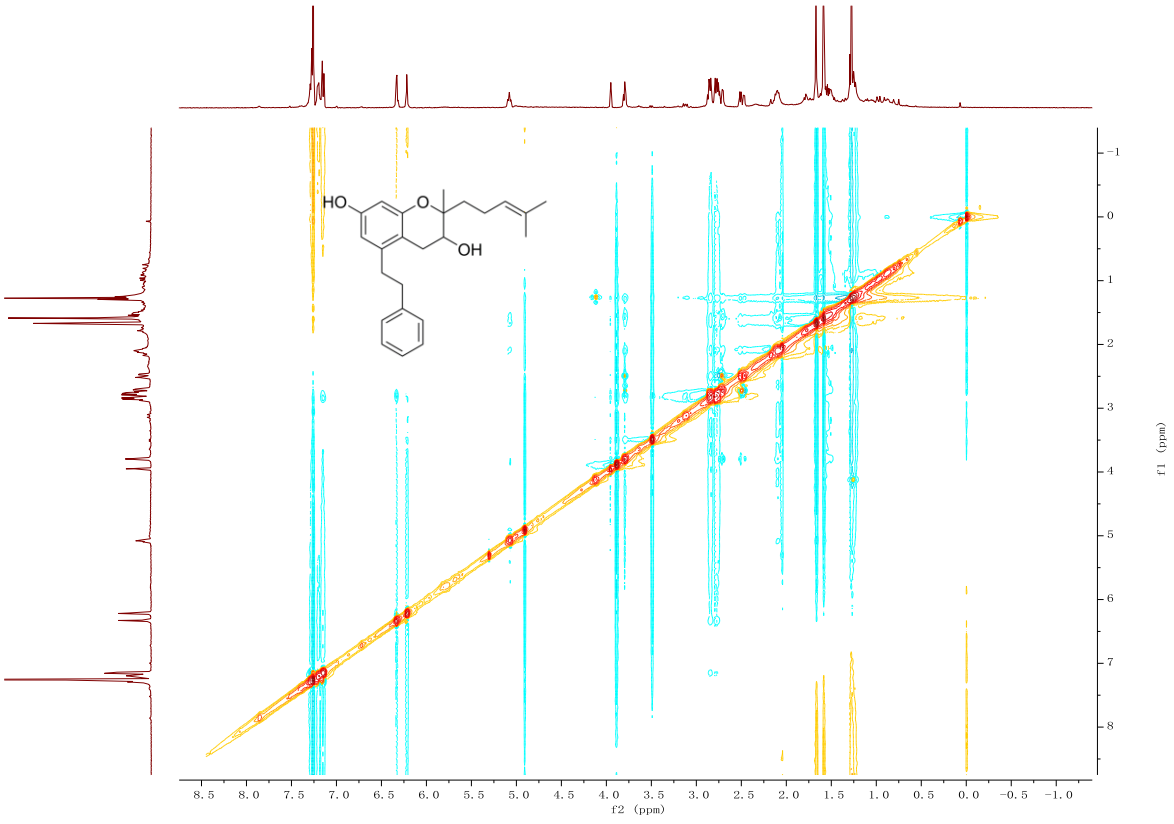

Figure S57. HRESIMS spectrum of **6**.

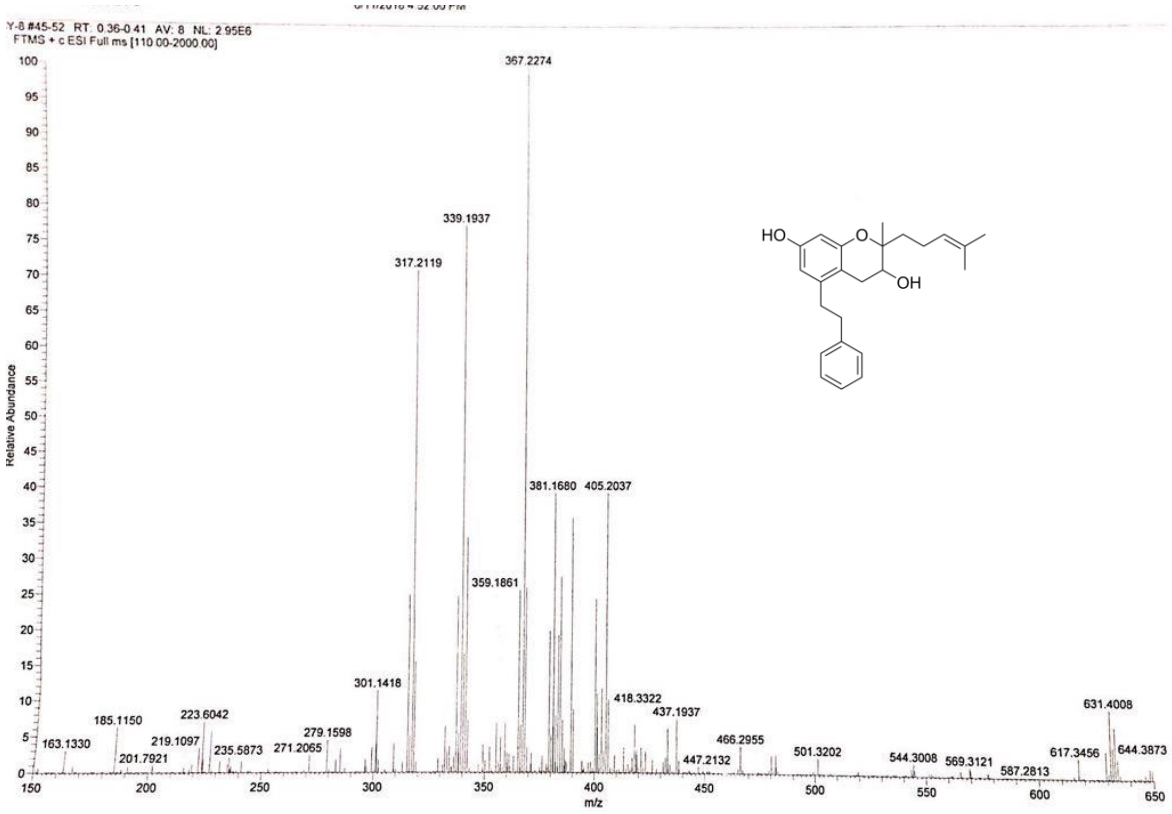

Figure S58. IR (KBr disc) spectrum of **6**.

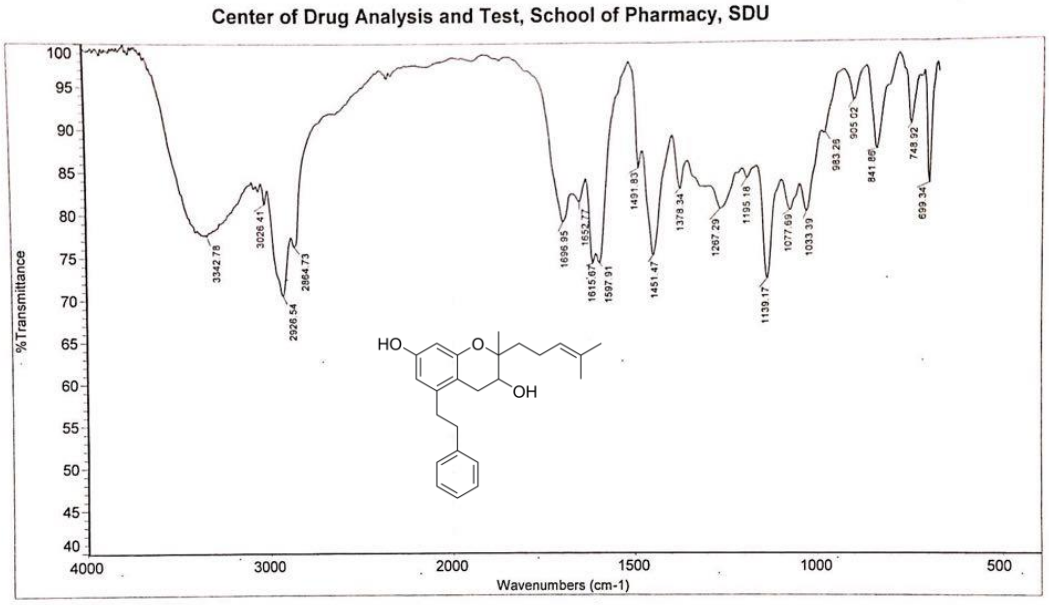

Sample name: CY-8
Spectrum number: M1002
Operator: 马斌
Instrument model:
Nicolet iN 10 Micro FTIR Spectrometer

Detector: DTGS or MCT-A (cooled)
Bermsplitter: KBr
Resolution: 8
Number of sample scans: 16
Nnmber of background scans: 16

Mode Selection
1. Transmission
2. Reflectance
3. ATR
Sepectral range:7800-450 or 670cm-1

Figure S59. UV spectrum of **6**.

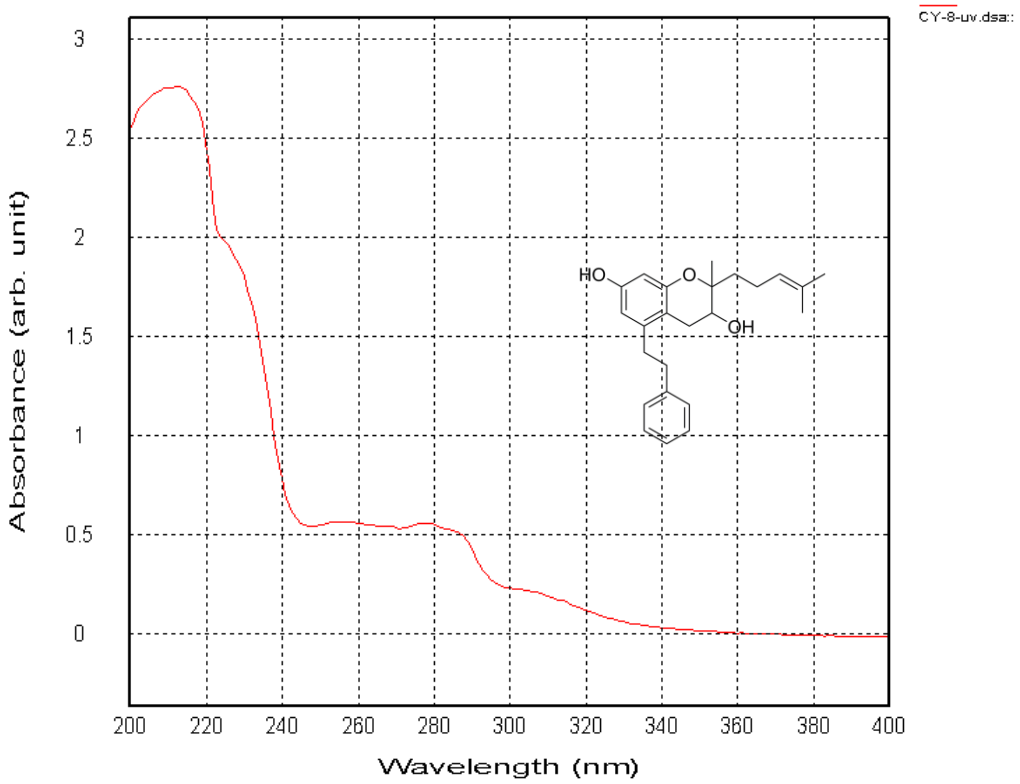

Figure S60. Chiral-phase HPLC analysis of **6**.

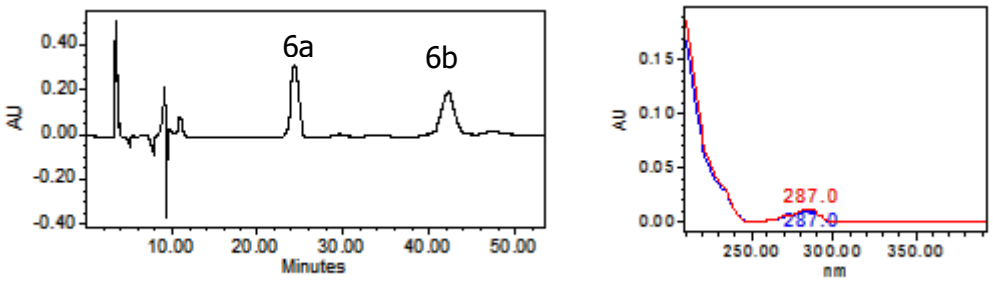

	Retention Time	Area	% Area	Height	Int Type
1	24.314	15129104	49.12	272278	bb
2	42.167	15673025	50.88	164819	bb

Figure S61. Experimental ECD spectra of **6a**/**6b** and calculated ECD spectrum of **6a**.

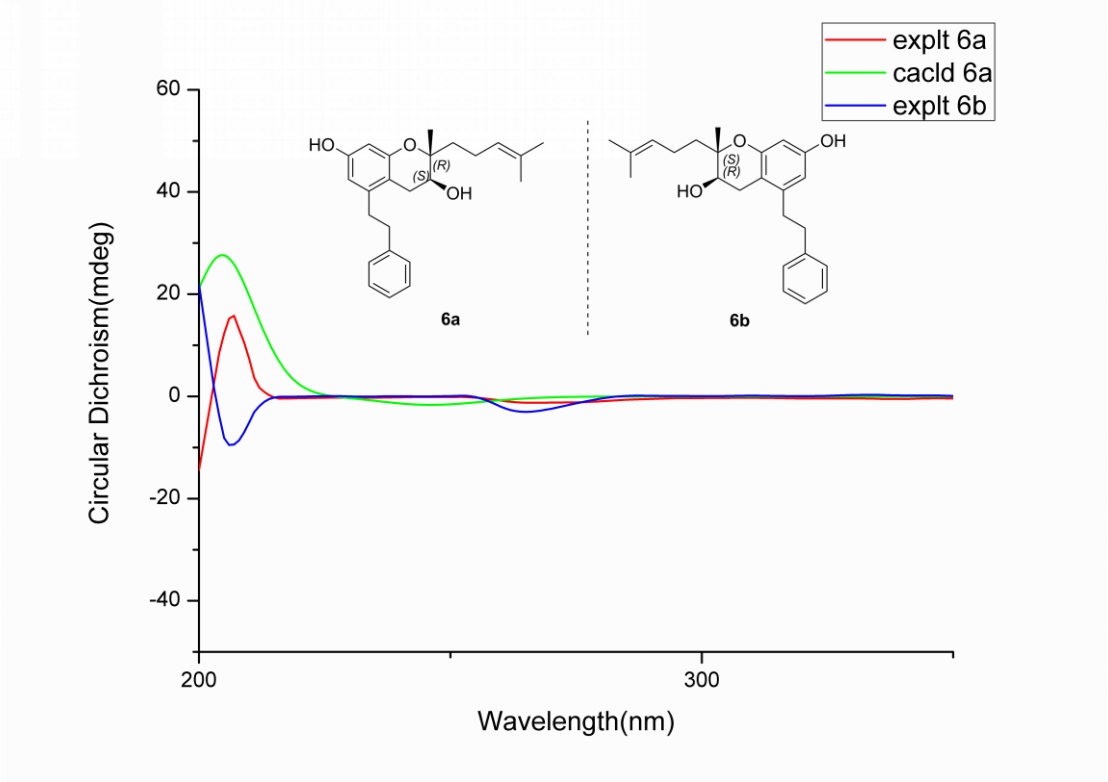

Figure S62. ^{1}H NMR spectrum (600 MHz) of **7** in $CDCl_3$.

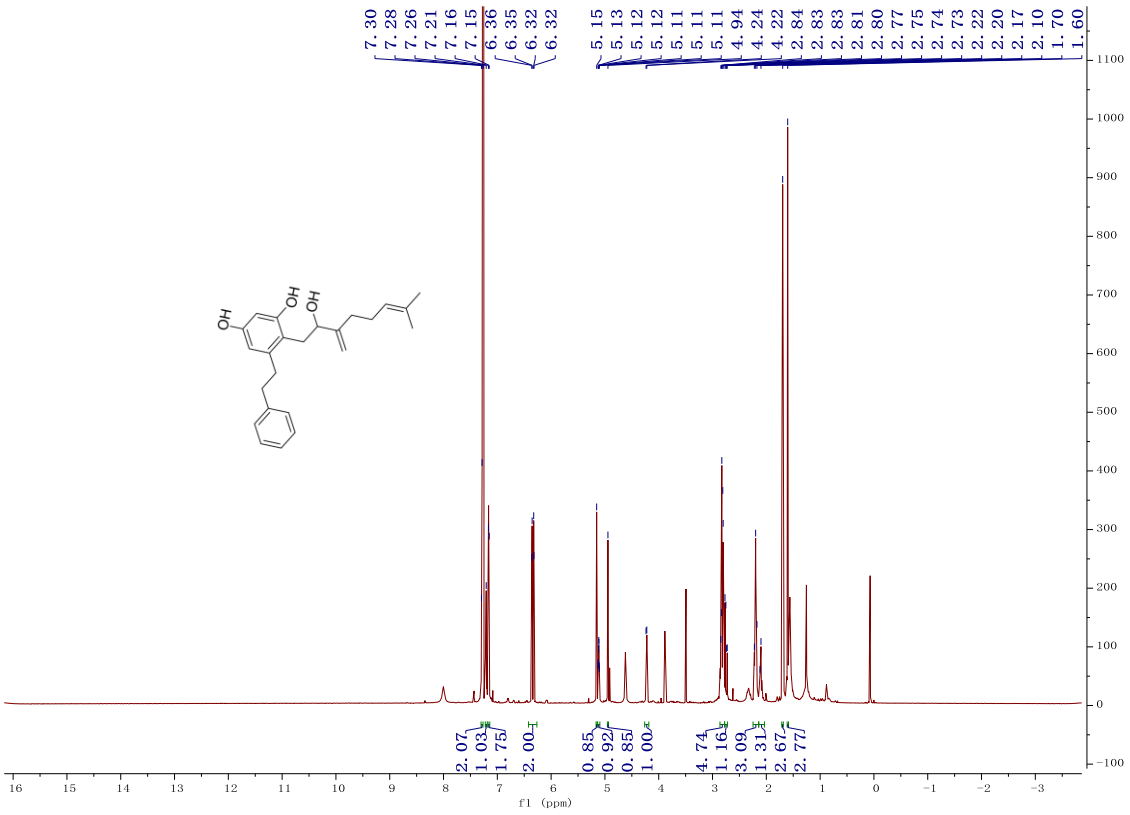

Figure S63. ^{13}C NMR spectrum (150 MHz) of **7** in $CDCl_3$.

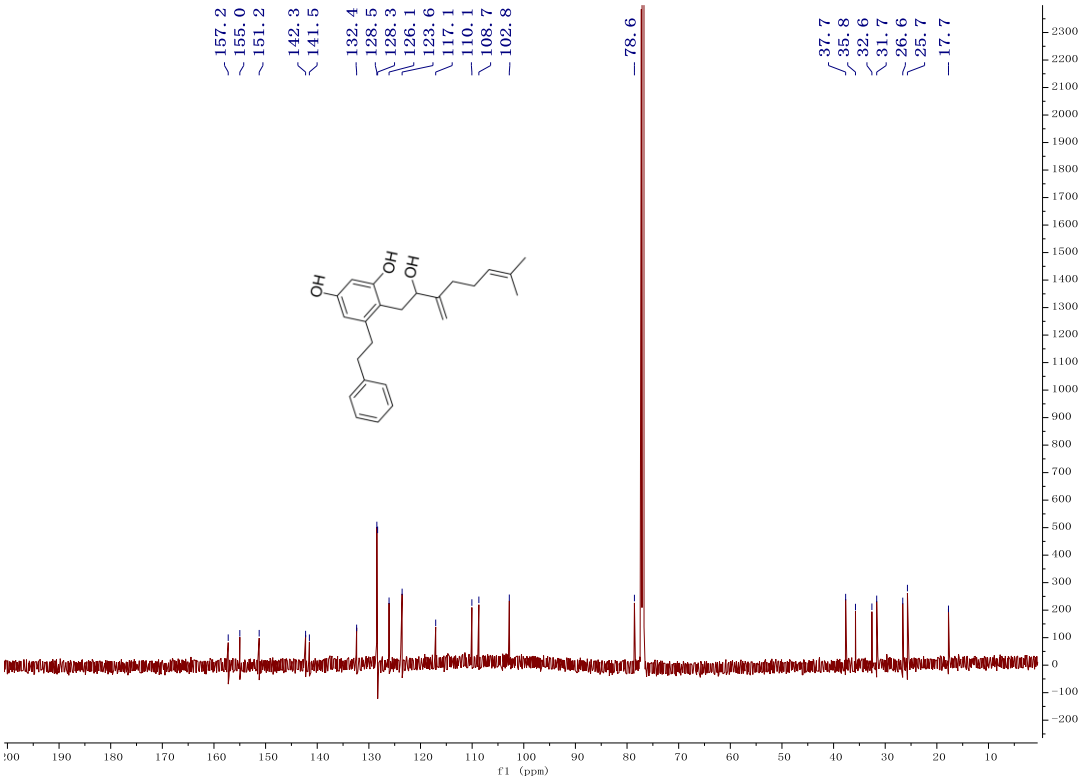

Figure S64. HSQC spectrum (600 MHz) of **7** in $CDCl_3$.

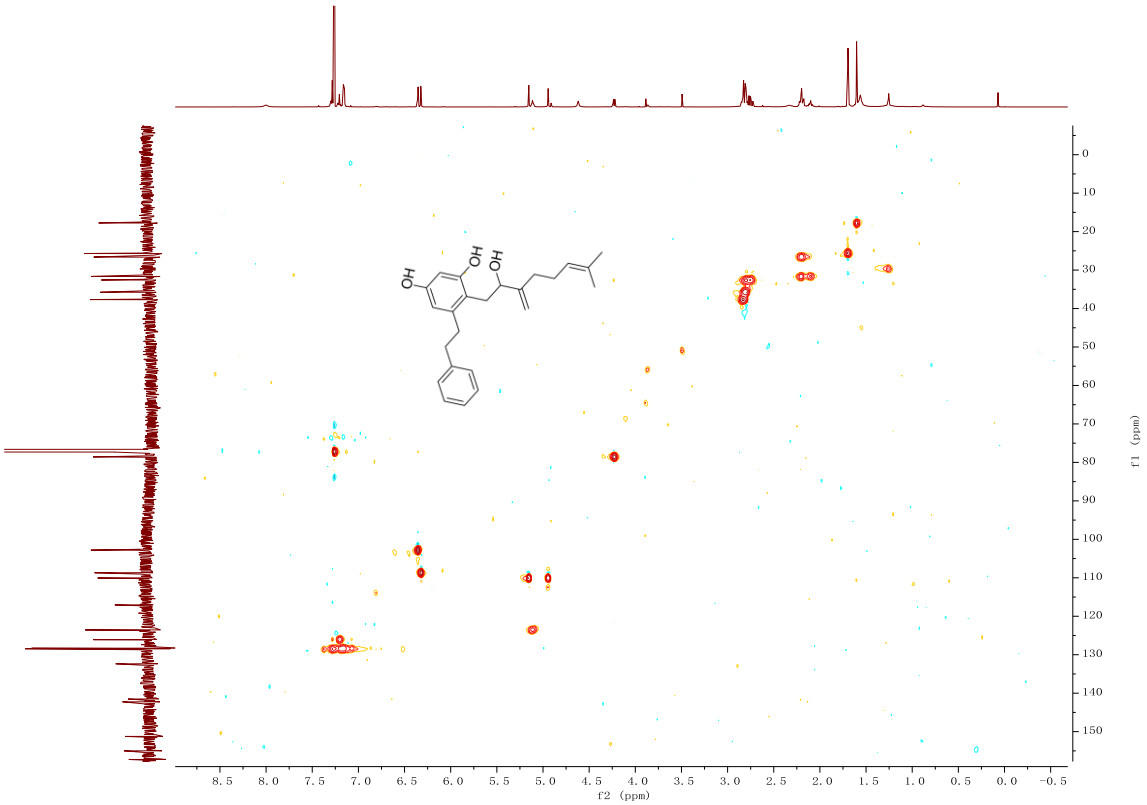

Figure S65. $^{1}H-^{1}H$ spectrum (600 MHz) of **7** in $CDCl_3$.

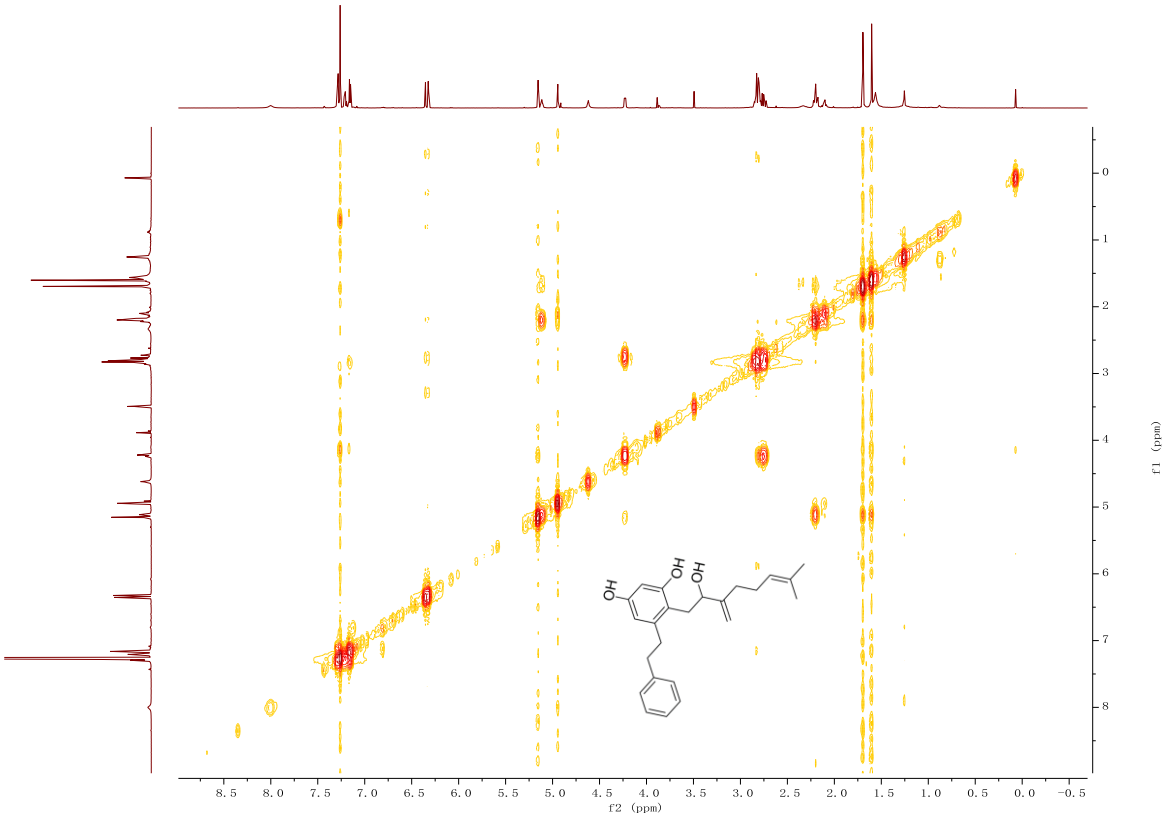

Figure S66. HMBC spectrum (600 MHz) of **7** in $CDCl_3$.

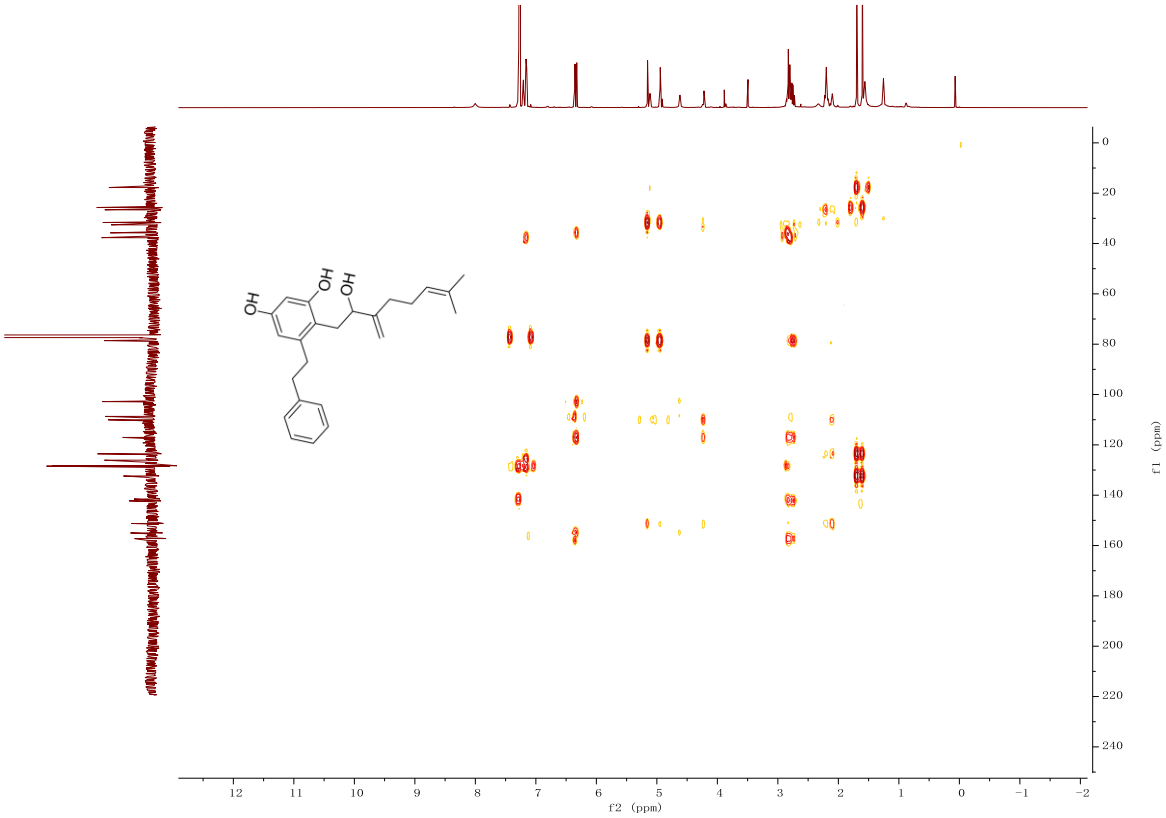

Figure S67. HRESIMS spectrum of **7**.

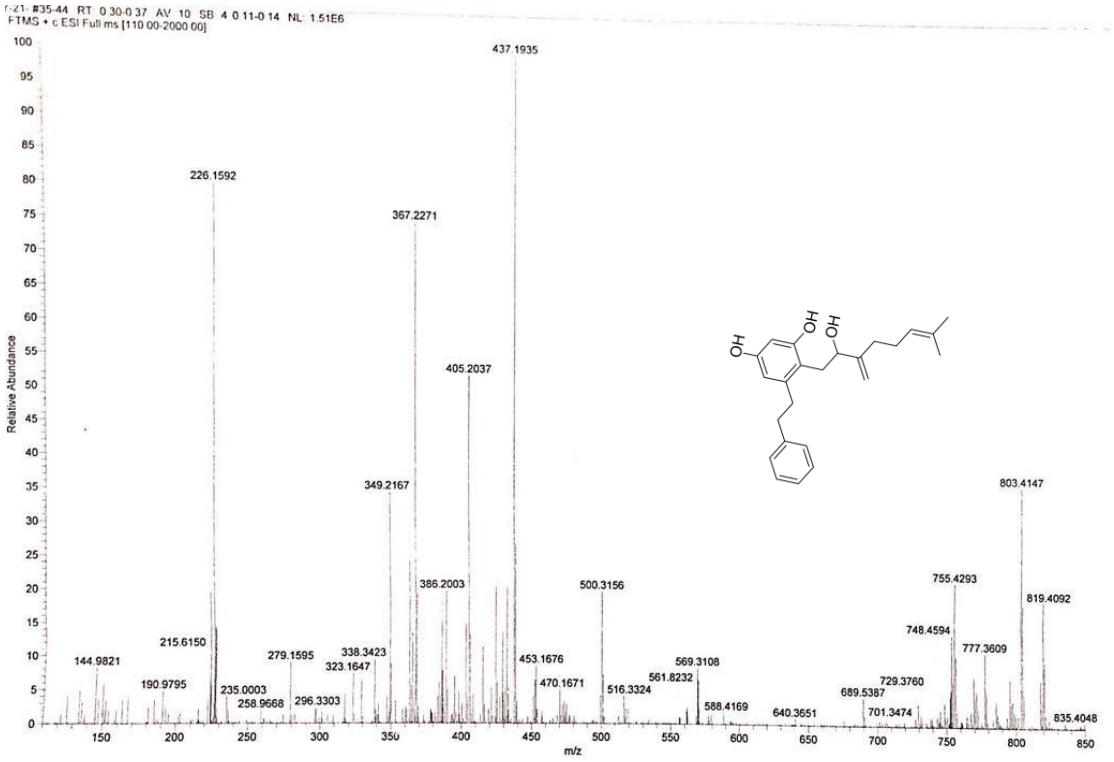

Figure S68. IR (KBr disc) spectrum of **7**.

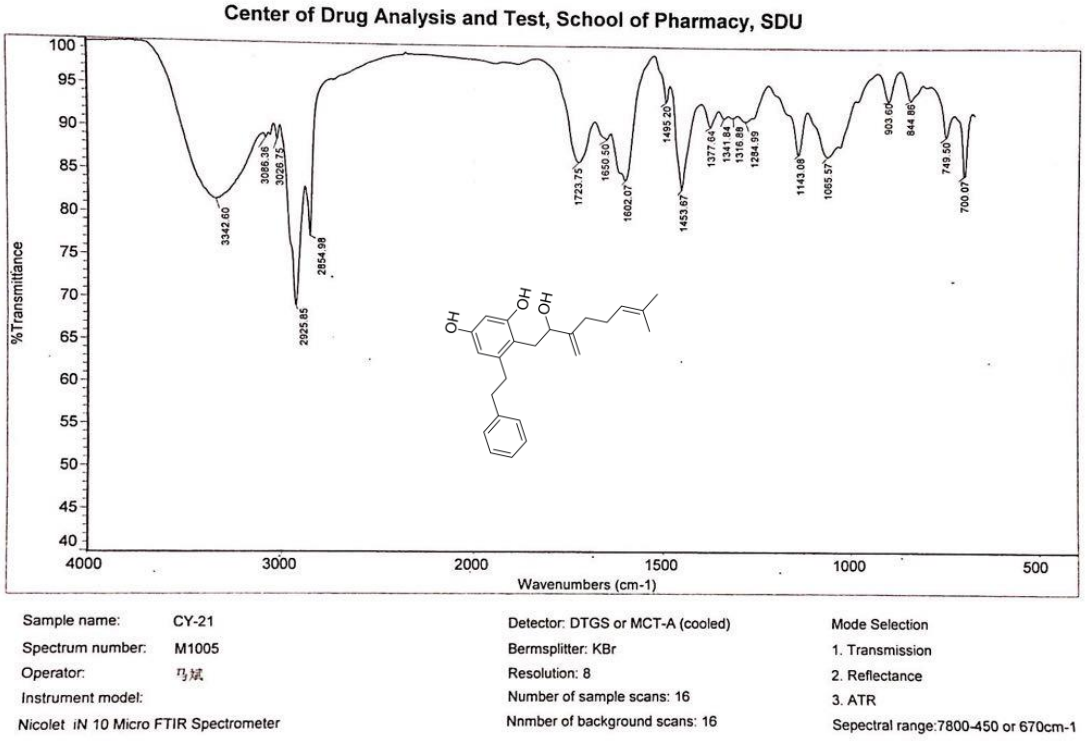

Figure S69. UV spectrum of **7**.

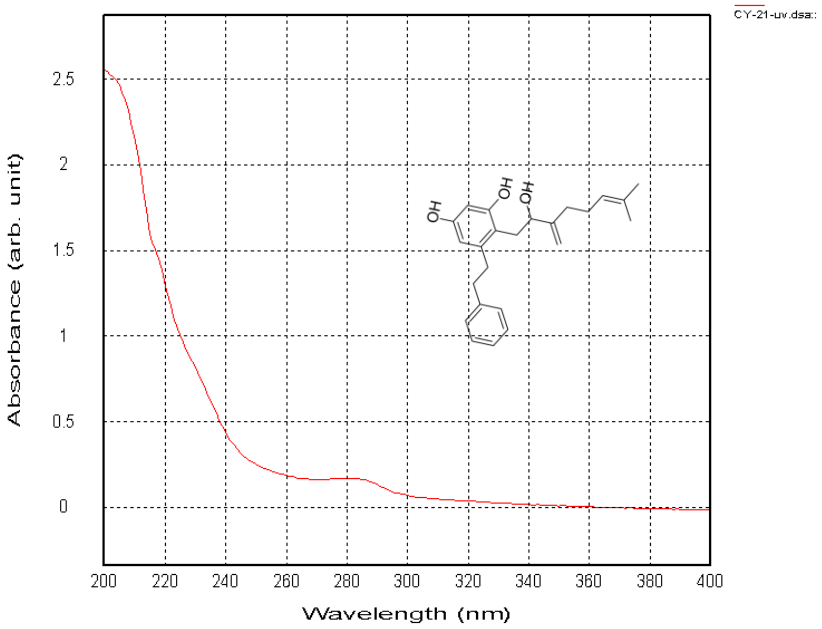

Figure S70. Chiral-phase HPLC analysis of **7**.

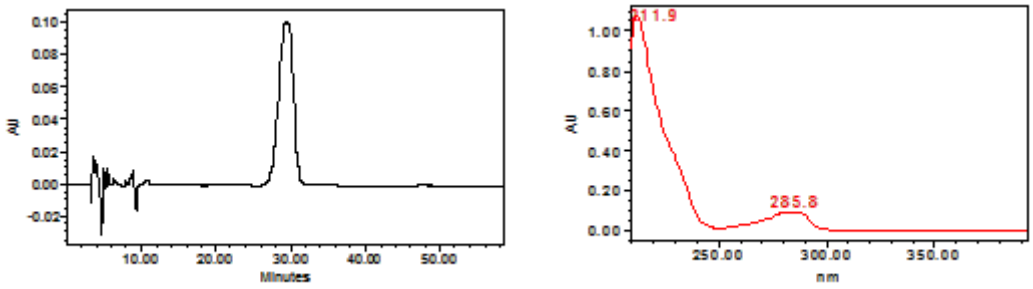

Figure S71. Experimental ECD spectra of **7.**

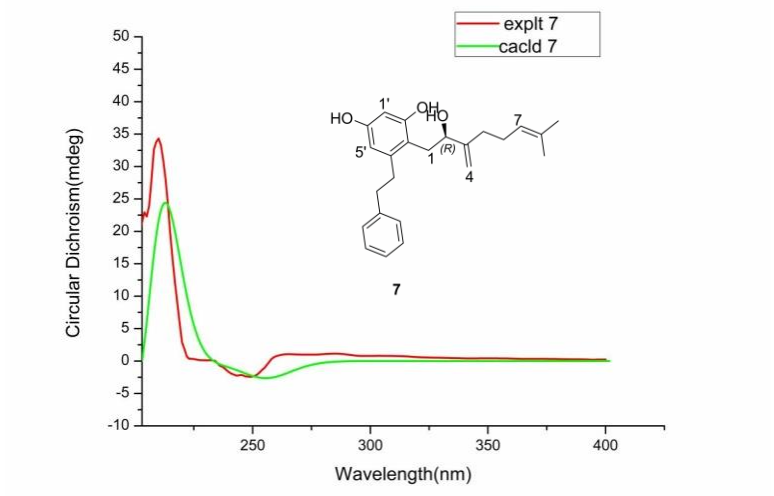

Figure S72. ^{1}H NMR spectrum (600 MHz) of **8** in $CDCl_3$.

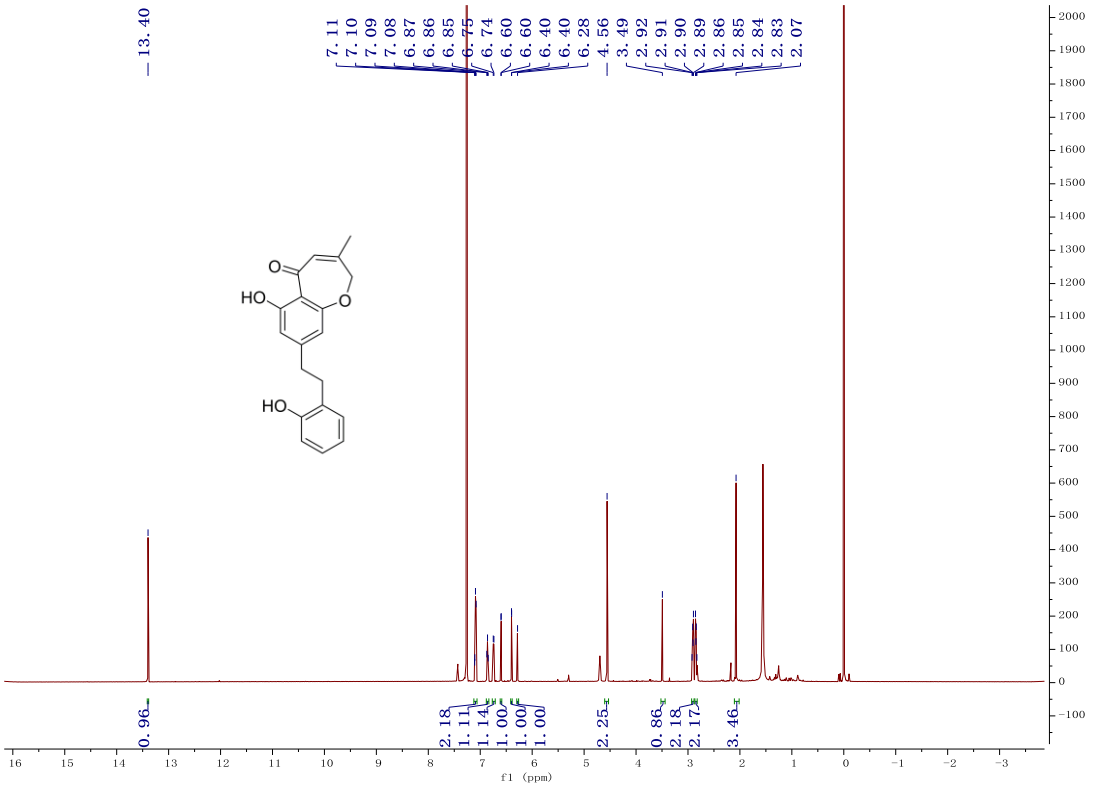

Figure S73. ^{13}C NMR spectrum (150 MHz) of **8** in $CDCl_3$.

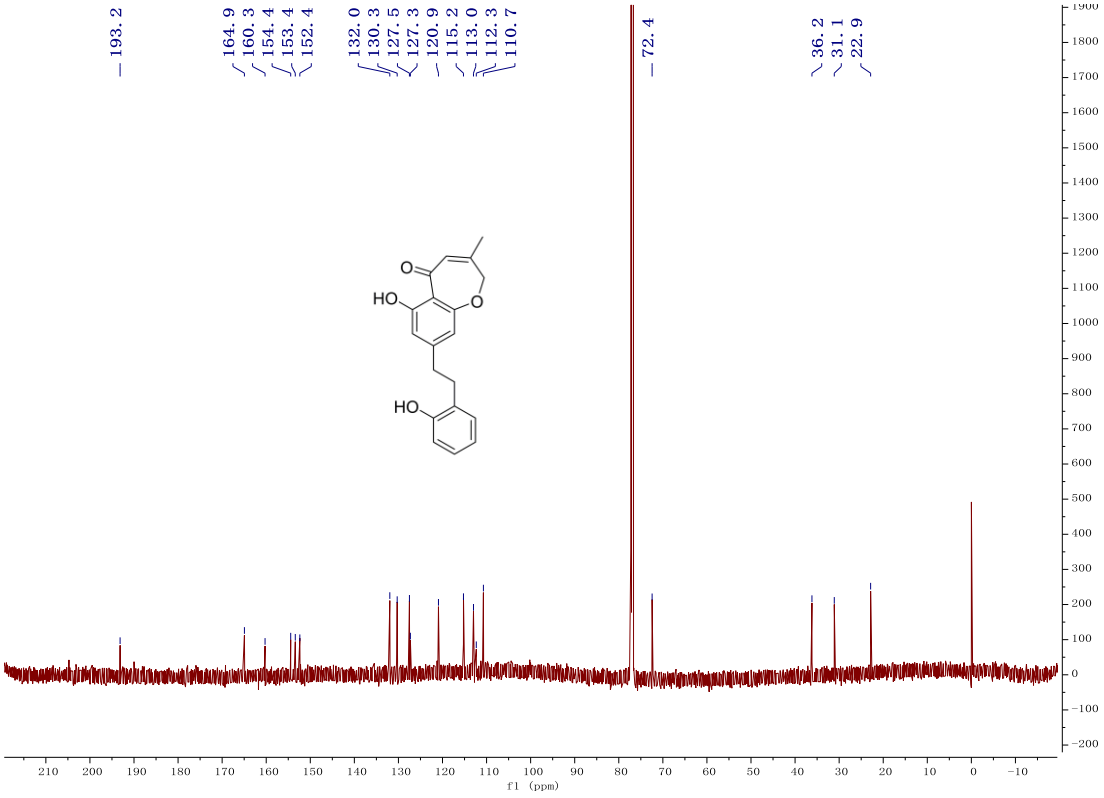

Figure S74. HSQC spectrum (600 MHz) of **8** in $CDCl_3$.

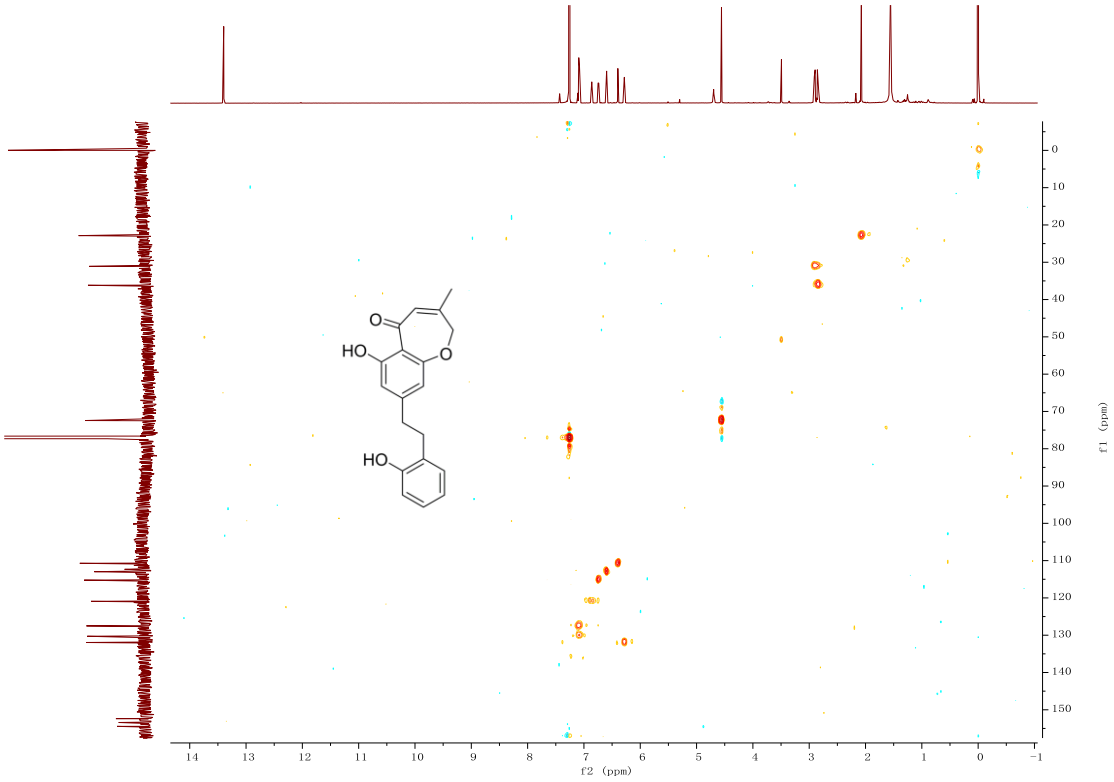

Figure S75. $^{1}H-^{1}H$ spectrum (600 MHz) of **8** in $CDCl_3$.

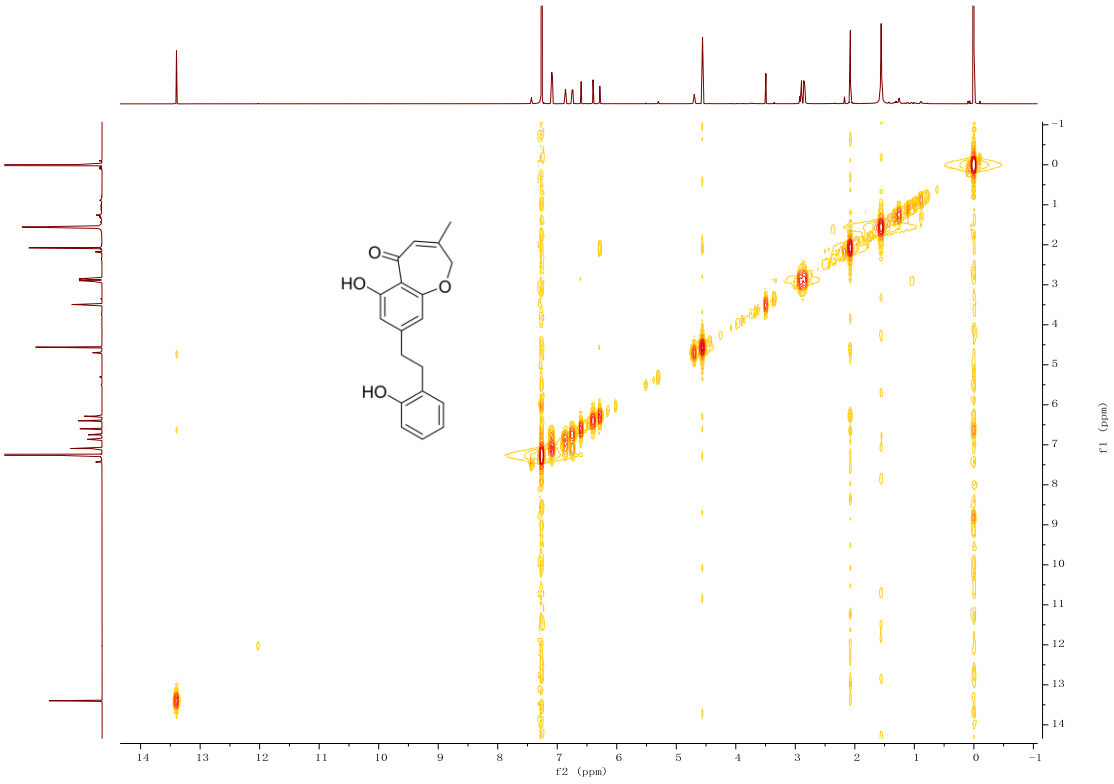

Figure S76. HMBC spectrum (600 MHz) of **8** in $CDCl_3$.

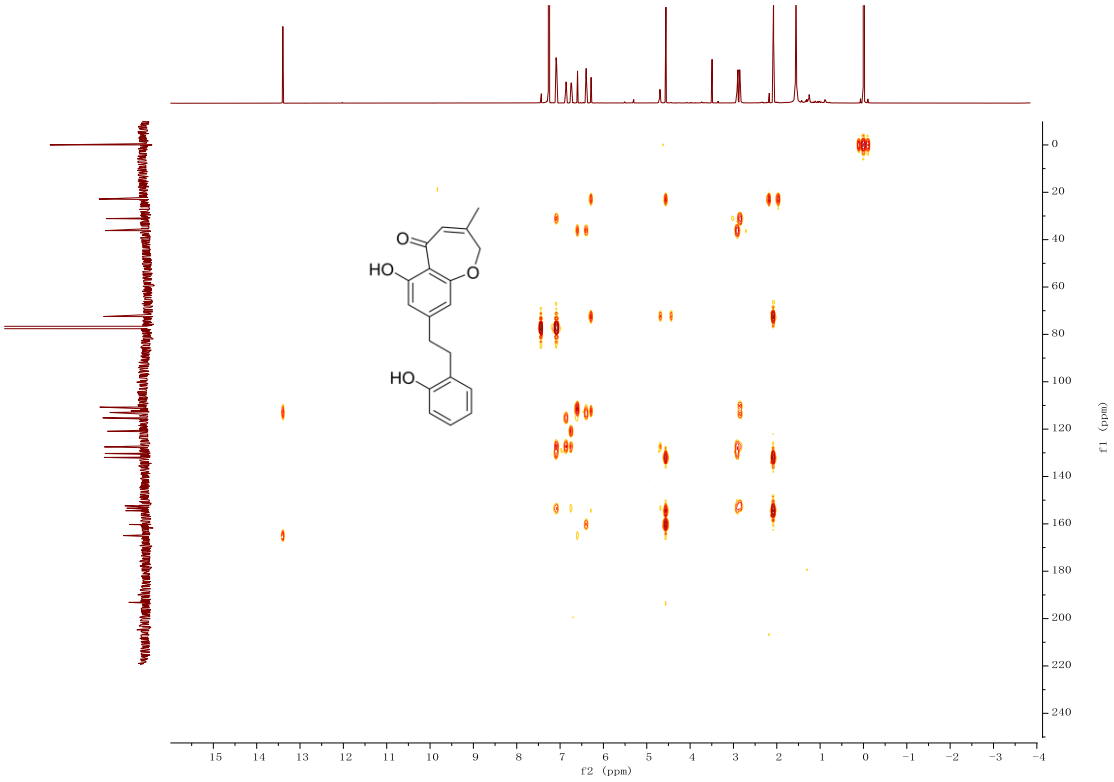

Figure S77. HRESIMS spectrum of **8**.

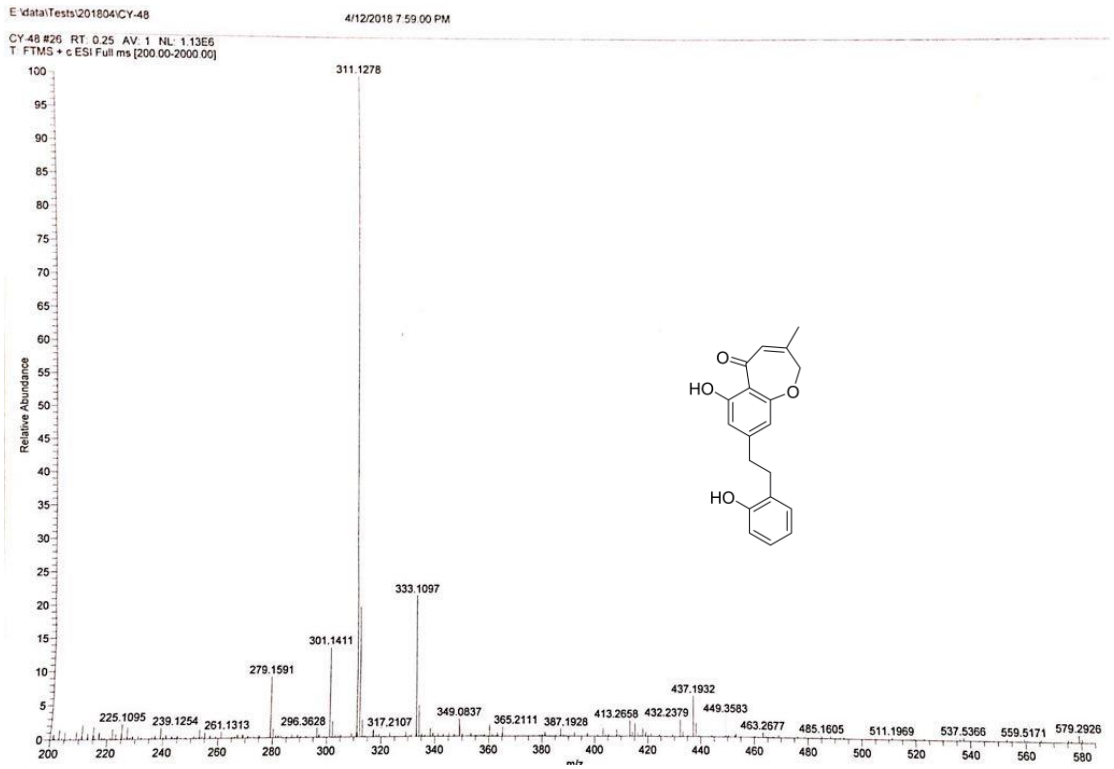

Figure S78. IR (KBr disc) spectrum of **8**.

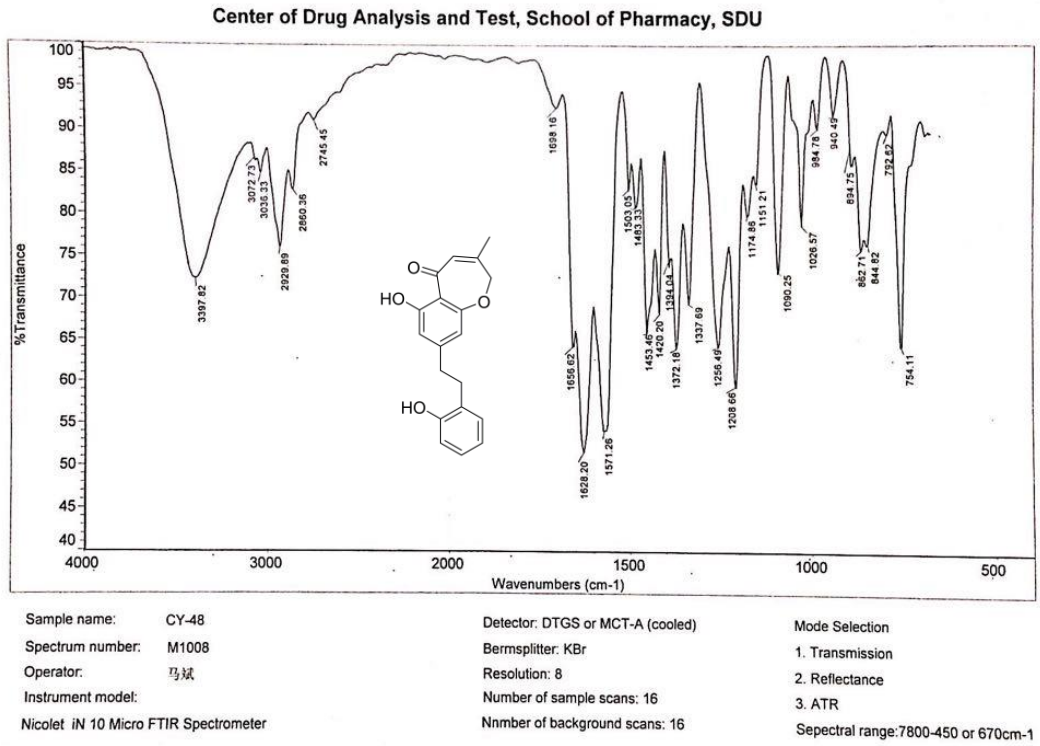

Figure S79. UV spectrum of **8**.

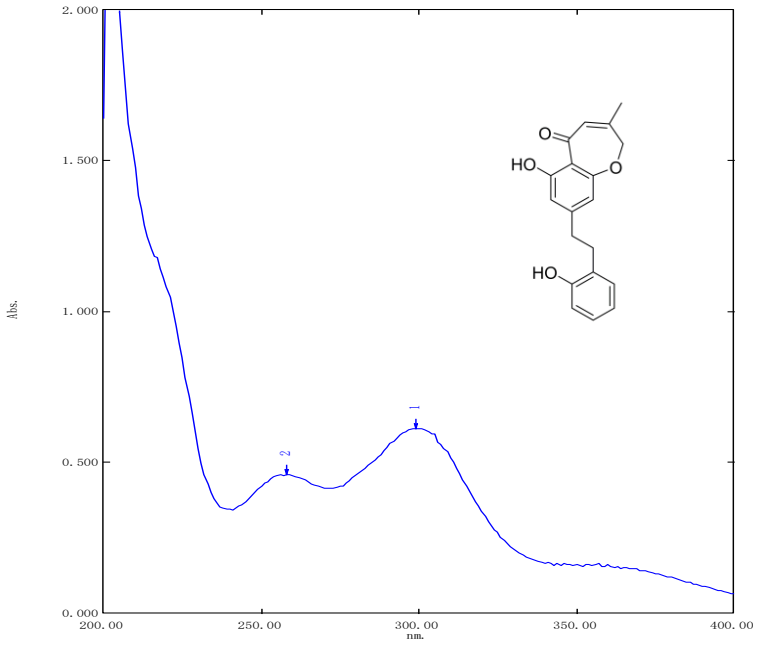

Figure S80. ^{1}H NMR spectrum (400 MHz) of **9** in CD_3OD.

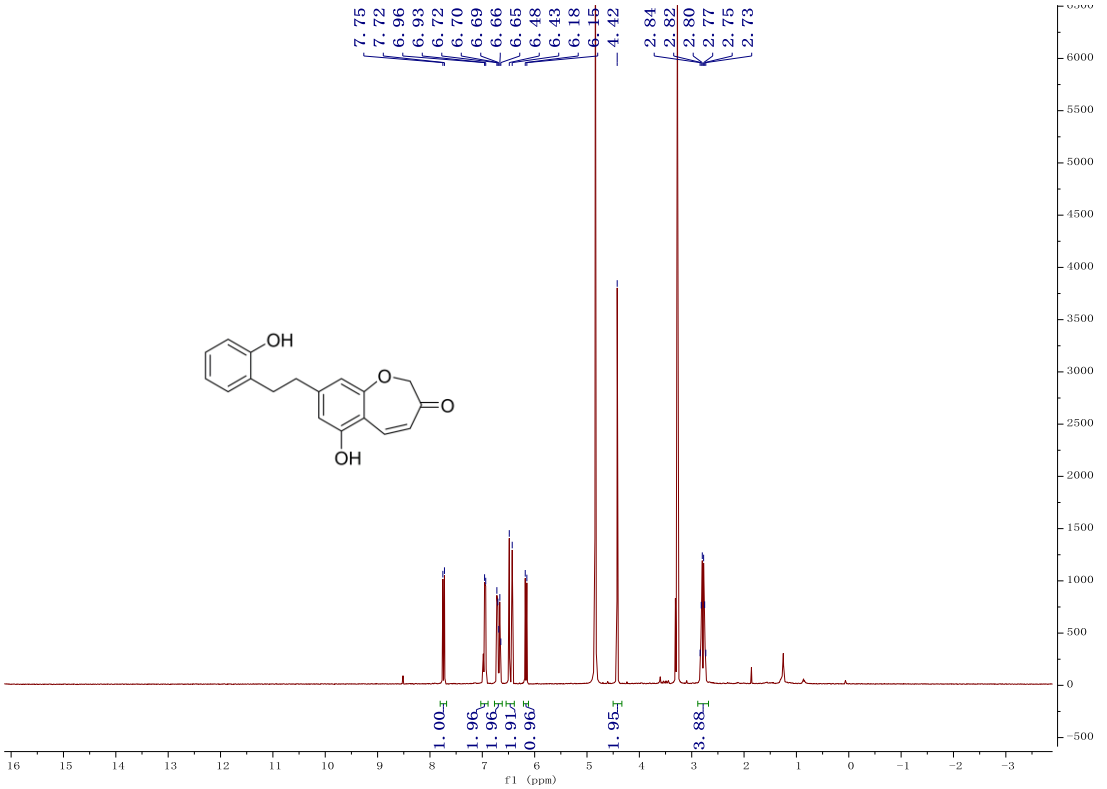

Figure S81. ^{13}C NMR spectrum (100 MHz) of **9** in CD_3OD.

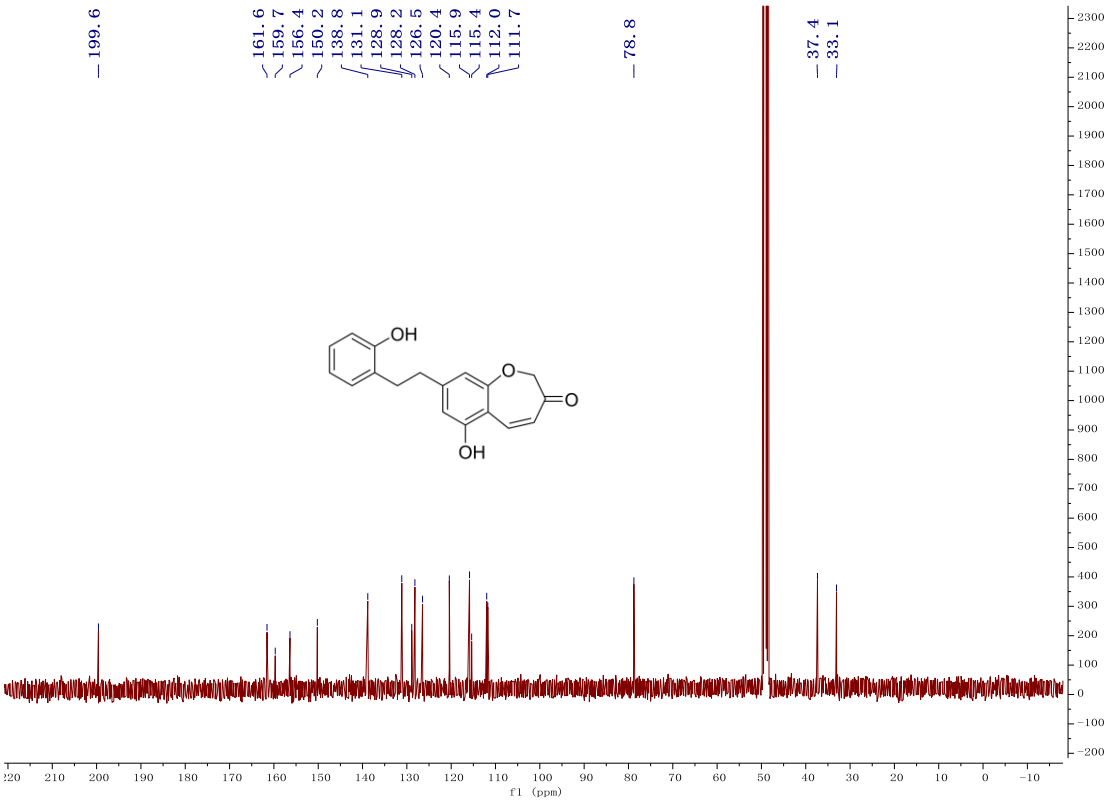

Figure S82. HSQC spectrum (400 MHz) of **9** in CD_3OD.

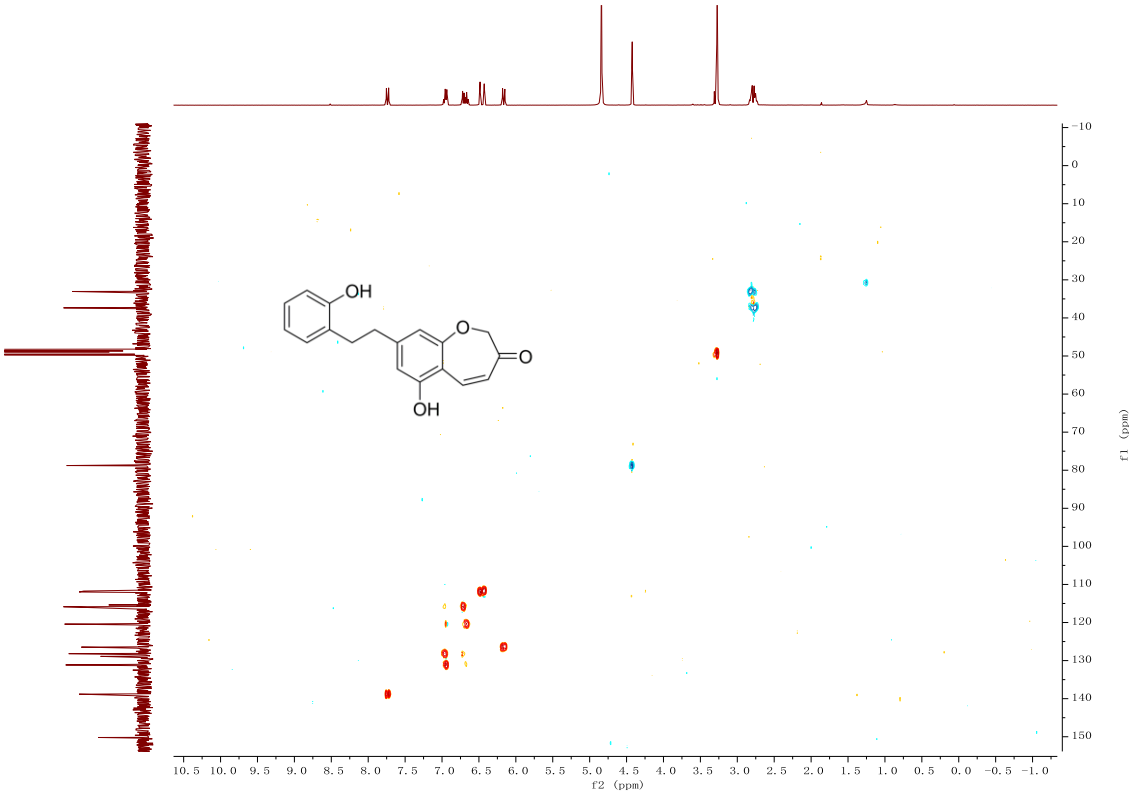

Figure S83. $^{1}H-^{1}H$ spectrum (400 MHz) of **9** in CD_3OD.

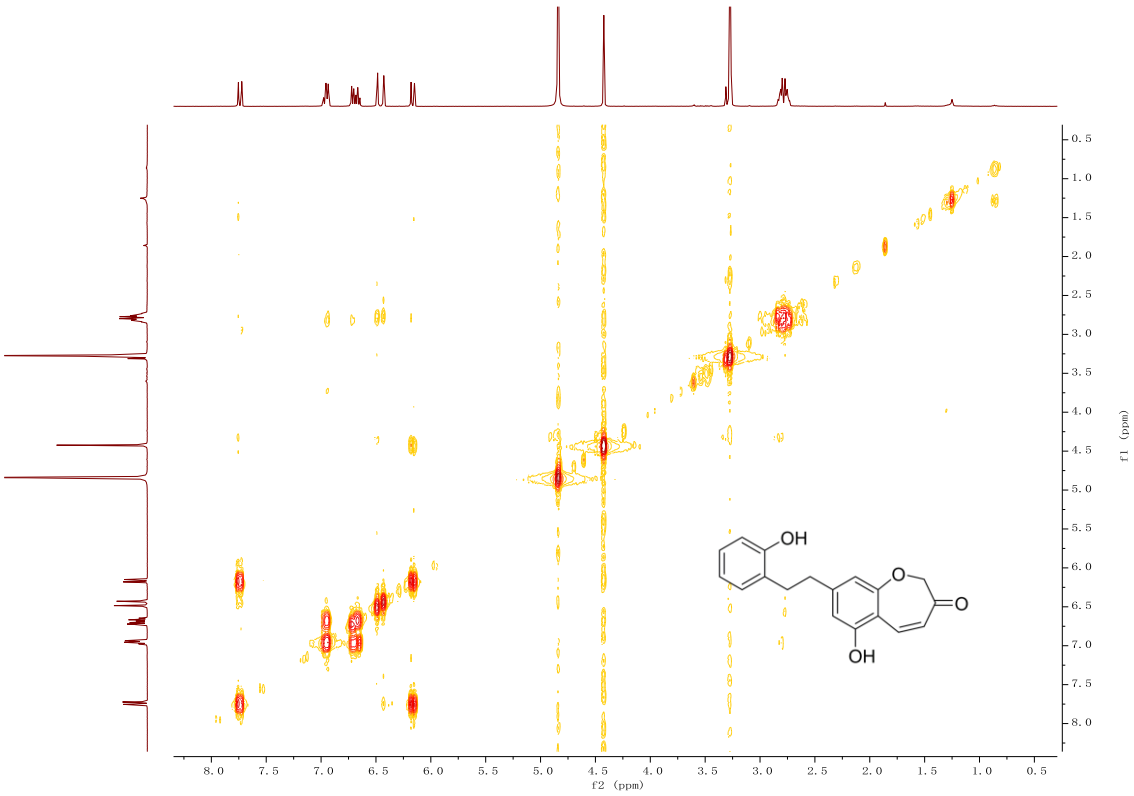

Figure S84. HMBC spectrum (400 MHz) of **9** in CD_3OD.

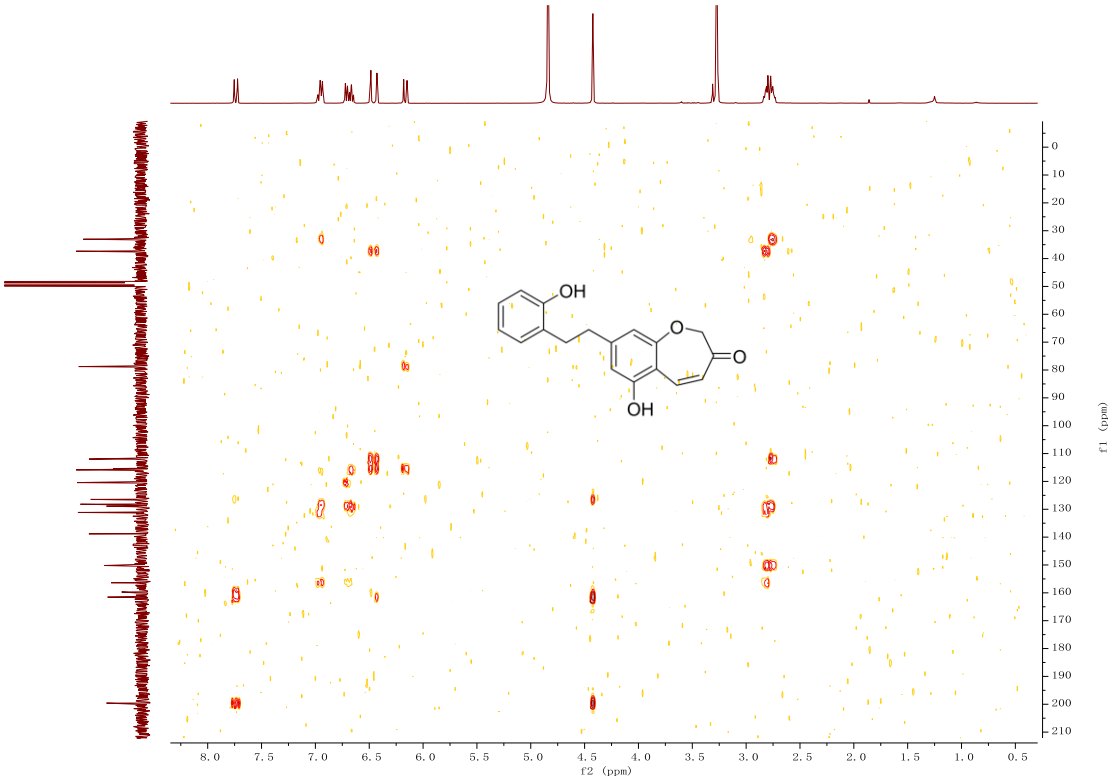

Figure S85. HRESIMS spectrum of **9**.

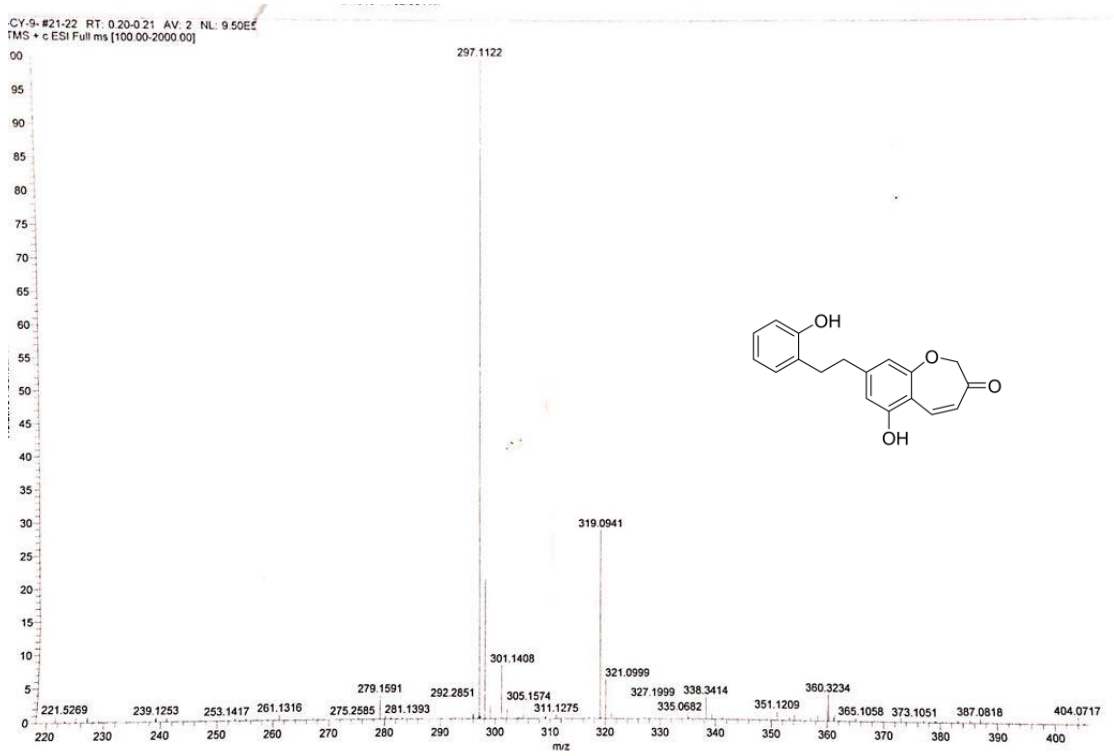

Figure S86. IR (KBr disc) spectrum of **9**.

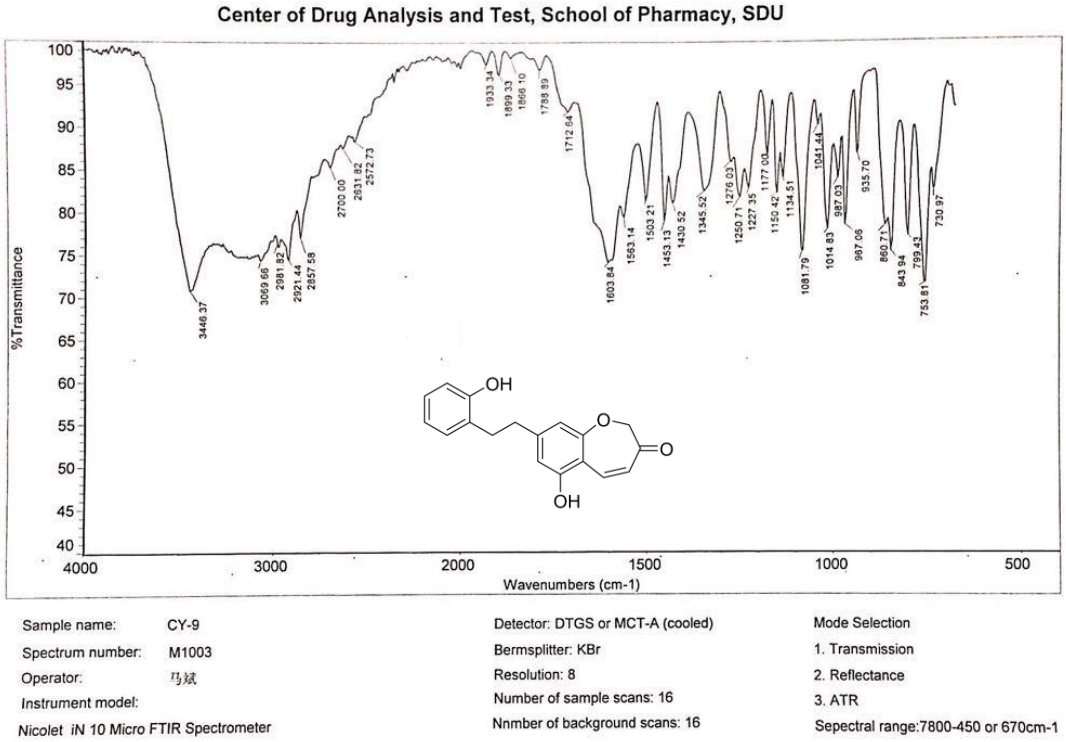

Figure S87. UV spectrum of **9**.

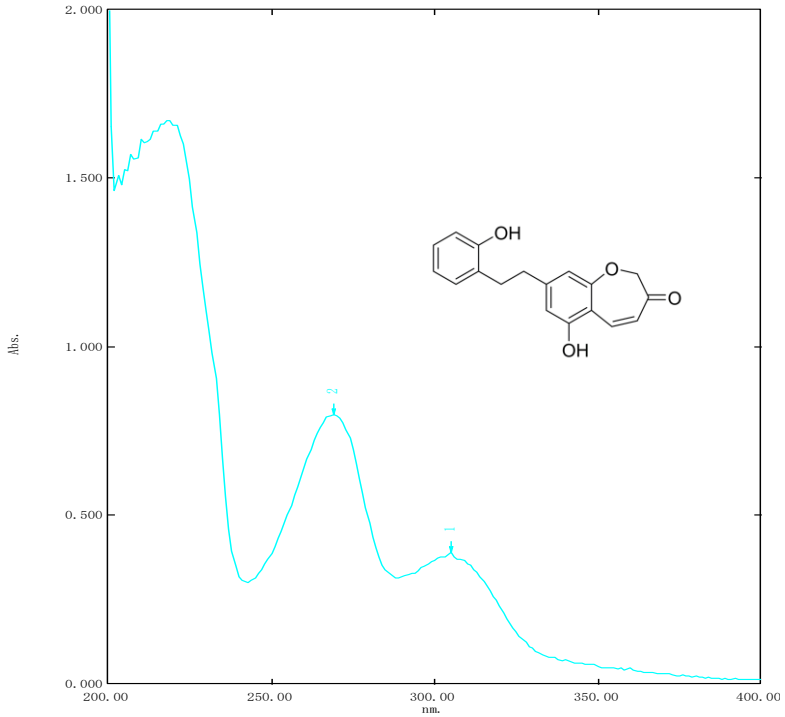

Figure S88. Compounds Induces Vacuolization.

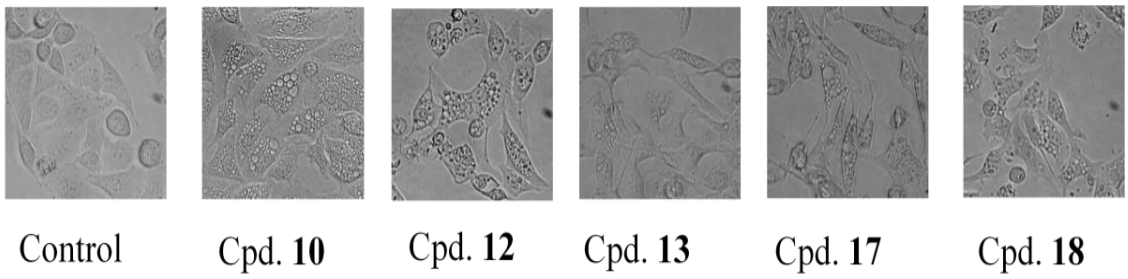

Figure S89. The Histogram of Annexin V and PI Staining in A549 and NCI-H1299 Cells (A549 and NCI-H1299 Cells were Treated with the 10 μM of Compound **10** for 24 h).

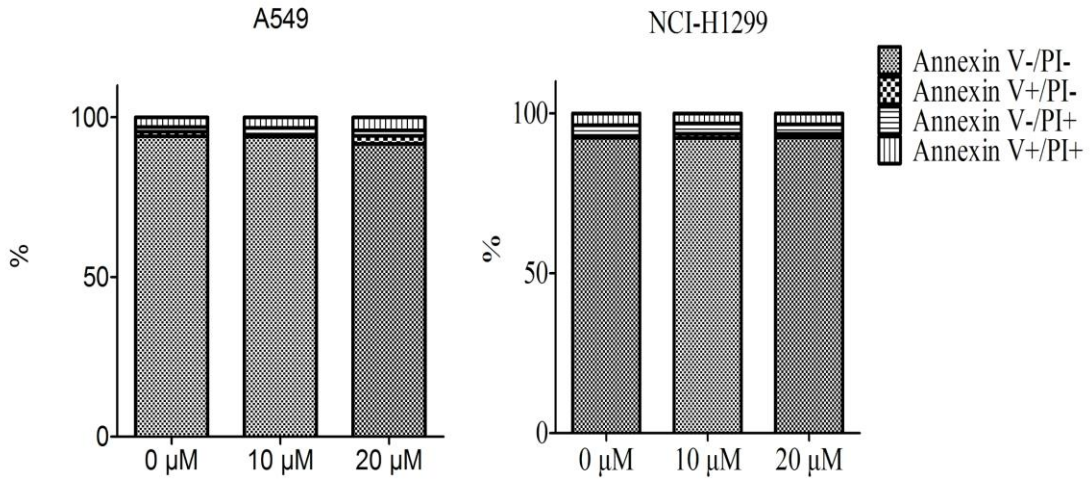

Table S1. Cytotoxicity of Compounds and Adriamycin in Several Human Cancer Cell Lines.

Compound[a]	NCI-H1299	A549	HepG-2	SMMC-7721	MCF-7	U251	Sw620	HT29	KB
1	> 40	36.6 ± 0.1	34.9 ± 0.2	9.0 ±1.0	37.9 ± 0.8	8.7 ± 0.6	22.2 ± 0.8	29.6 ± 0.2	> 40
2	> 40	> 40	> 40	> 40	> 40	> 40	> 40	> 40	> 40
3	> 40	> 40	> 40	> 40	> 40	> 40	> 40	> 40	> 40
4	> 40	> 40	> 40	> 40	> 40	> 40	> 40	> 40	> 40
5	> 40	> 40	> 40	38.7 ± 0.7	> 40	36.7 ± 0.7	> 40	> 40	29.6 ± 0.6
6	> 40	> 40	> 40	> 40	> 40	> 40	> 40	> 40	> 40
7	> 40	26.0 ± 0.4	20.4 ± 0.7	15.8 ± 0.5	18.7 ± 0.5	9.1 ± 0.9	15.2 ± 2.0	19.8 ± 1.0	16.8 ± 1.9
8	> 40	> 40	> 40	> 40	> 40	> 40	> 40	> 40	> 40
9	> 40	> 40	> 40	14.7 ± 2.0	33.2 ± 2.5	21.7 ± 1.0	13.8 ± 1.1	> 40	> 40
10	5.8 ± 0.3	6.0 ± 0.1	6.3 ± 0.2	8.6 ± 1.3	10.2 ± 0.7	9.0 ± 0.2	6.3 ± 1.4	5.0 ± 0.5	6.7 ± 1.6
11	> 40	> 40	> 40	> 40	> 40	> 40	> 40	> 40	> 40
12	> 40	28.9 ± 1.9	28.2 ± 2.7	40	> 40	38.6 ± 0.6	> 40	24.3 ± 1.8	> 40
13	> 40	> 40	> 40	> 40	> 40	> 40	> 40	> 40	> 40
14	> 40	> 40	> 40	> 40	> 40	26.1 ± 1.3	> 40	> 40	> 40
15	> 40	> 40	35.0 ± 2.0	24.8 ± 1.3	> 40	8.9 ± 2.0	18.5 ± 0.9	> 40	28.1 ± 0.7
16	> 40	> 40	36.0 ± 1.9	24.5 ± 2.0	> 40	9.3 ± 1.0	25.6 ± 0.1	> 40	25.7 ± 2.1
17	> 40	25.5 ± 1.0	22.2 ± 1.6	29.5 ± 2.7	28.9 ± 1.0	> 40	19.7 ± 1.7	29.0 ± 0.4	17.2 ± 0.2
18	15.0 ± 0.5	9.8 ± 0.2	13.1 ± 0.7	13.5 ± 2.5	20.0 ± 0.4	25.6 ± 2.5	10.4 ± 2.5	10.0 ± 0.7	16.0 ± 1.7
19	> 40	28.0 ± 1.2	31.6 ± 2.4	28.4 ± 2.6	37.0 ± 1.8	14.6 ± 1.9	21.3 ± 2.3	35.3 ± 2.2	38.0 ± 1.3
20	> 40	> 40	> 40	> 40	> 40	> 40	> 40	> 40	> 40
Adriamycin	0.8 ± 0.4	1.8 ± 0.3	1.5 ±1.5	0.8 ± 1.6	1.0 ± 0.9	2.8 ± 1.6	1.2 ± 0.4	3.8 ± 0.7	3.2 ± 0.3

[a]Cytotoxicity of compounds and adriamycin (used as a positive control) were examined in NCI-H1299, A549, HepG-2, SMMC-7721, MCF-7, U251, Sw620, HT29, and KB cell lines by MTT assay. The cells were treated with various concentrations of compounds for 48 h. Data are mean ± SD (n = 3)